Mathematical Modelling, Vol. 7, pp. 1513–1577, 1986
Printed in the U.S.A.

0270–0255/86 $3.00 + .00

REVIEW ARTICLE

COMPUTER MODELS AND AUTOMATA THEORY IN BIOLOGY AND MEDICINE

ION C. BAIANU

University of Illinois at Urbana
Physical Chemistry and NMR Laboratories
567 Bevier Hall, 905 S. Goodwin Ave.
Urbana, Illinois 61801

(*Received* 27 *February* 1985; *revised* 12 *September* 1985)

1. INTRODUCTION

The applications of computers to biological and biomedical problem solving goes back to the very beginnings of computer science, automata theory[1], and mathematical biology[2]. With the advent of more versatile and powerful computers, biological and biomedical applications of computers have proliferated so rapidly that it would be virtually impossible to compile a comprehensive review of all developments in this field.

Limitations of computer simulations in biology have also come under close scrutiny, and claims have been made that biological systems have limited information processing power[3]. Such general conjectures do not, however, deter biologists and biomedical researchers from developing new computer applications in biology and medicine.

Microprocessors are being widely employed in biological laboratories both for automatic data acquisition/processing and modelling; one particular area, which is of great biomedical interest, involves fast digital image processing and is already established for routine clinical examinations in radiological and nuclear medicine centers. Powerful techniques for biological research are routinely employing dedicated, on-line microprocessors or array processors; among such techniques are: Fourier-transform nuclear magnetic resonance (NMR), NMR imaging (or tomography), x-ray tomography, x-ray diffraction, high performance liquid chromatography, differential scanning calorimetry and mass spectrometry. Networking of laboratory microprocessors linked to a central, large memory computer is the next logical step in laboratory automation. Previously unapproachable problems, such as molecular dynamics of solutions, many-body interaction calculations and statistical mechanics of biological processes are all likely to benefit from the increasing access to the new generation of "supercomputers".

In view of the large number, diversity and complexity of computer applications in biology and medicine, we could not review in any degree of detail all computer applications in these fields; instead, we shall be selective and focus our discussion on suggestive computer models of biological systems and those fundamental aspects of computer applications that are likely to continue to make an impact on biological and biomedical research. Thus, we shall consider unifying trends in mathematics, mathematical logics and computer science that are relevant to computer modelling of biological and biomedical systems. The latter are pitched at a more formal, abstract level than the applications and, therefore, encompass a number of concepts drawn from the abstract theory of sets and relations, network theory, automata theory, Boolean and n-valued logics, abstract algebra, topology and category theory. The purpose of these theoretical sections is to provide the

means for approaching a number of basic biological questions:

(1) What are the essential characteristics of a biological organism as opposed to an automaton?
(2) Are biological systems recursively computable?
(3) What is the structure of the simplest (primordial) organism?
(4) What are the basic structures of neural and genetic networks?
(5) What are the common properties of classes of biological organisms?
(6) Which system representations are adequate for biodynamics?
(7) What is the optimal strategy for modifying an organism through genetic engineering?
(8) What is the optimal simulation of a biological system with a digital or analog computer?
(9) What is life?

The present analysis of relational theories in biology and computer simulation has also inspired a number of new results which are presented as "conjectures" since their proofs are too lengthy and too technical to be included in this review. In order to maintain a self-contained presentation definitions of the main concepts are given, with the exception of a minimum of simple mathematical concepts.

2. COMPUTER MODELS OF BRANCHING PROCESSES AND TREELIKE MORPHOLOGY

One of the simplest but nontrivial applications of computers in biology and medicine has been the generation of "trees" or patterns of branching. Such patterns of branching are common to arteries, bronchi, trees and rivers, and have attracted considerable attention[4–22]. Computer simulation of the geometry of trees, based on branching angles, length ratio of branches and differential rates of growth, has been quite successful in producing models which are closely resembling the morphology of biological systems[7, 17–19]. In such models of trees, the branching ratio was found to be variable and, therefore, of little descriptive value. A computer program that generates dichotomously various branching trees was recently described[22] and it was employed to investigate if the human bronchial tree could be adequately modelled.

A. *Generation of trees by the computer*

According to Horsfield and Thurlbeck[22], each branch is encoded in the computer by providing the three-dimensional (3D) coordinates of the branch ends. Horsfield and Cumming[5] order the branches by starting at the peripheral ones, which are assigned "order 1", and the order is increased by 1 unit at each junction [Fig. 1(a)] after Horsfield and Thurlbeck[22]). The asymmetry of the branching is represented by an asymmetry parameter δ which is the difference in order between the two daughter branches. An example of asymmetry of branching which was given by Horsfield and Thurlbeck is reproduced in Fig. 1(b). A stem branch is generated by inputing its coordinates and stating its Horsfield order; the stem bifurcates in the x-y plane, the order of the major daughter branch being one digit less than the parent branch by definition, while the order of the minor branch is defined by using a value of δ. By defining the angles of branching and the lengths, the coordinates of the ends of the daughter branches can also be calculated. The daughter branches bifurcate in turn until an order 1 branch is generated recursively and then bifurcation stops on that selected pathway. The value of δ for a given bifurcation is determined by a pseudorandom number generated by a digital computer, and takes values between 0 and 9. The probability for a given value of δ to be realized in a given tree from the pseudorandom string of numbers is defined on input; for example if $\delta = 0$, the prob-

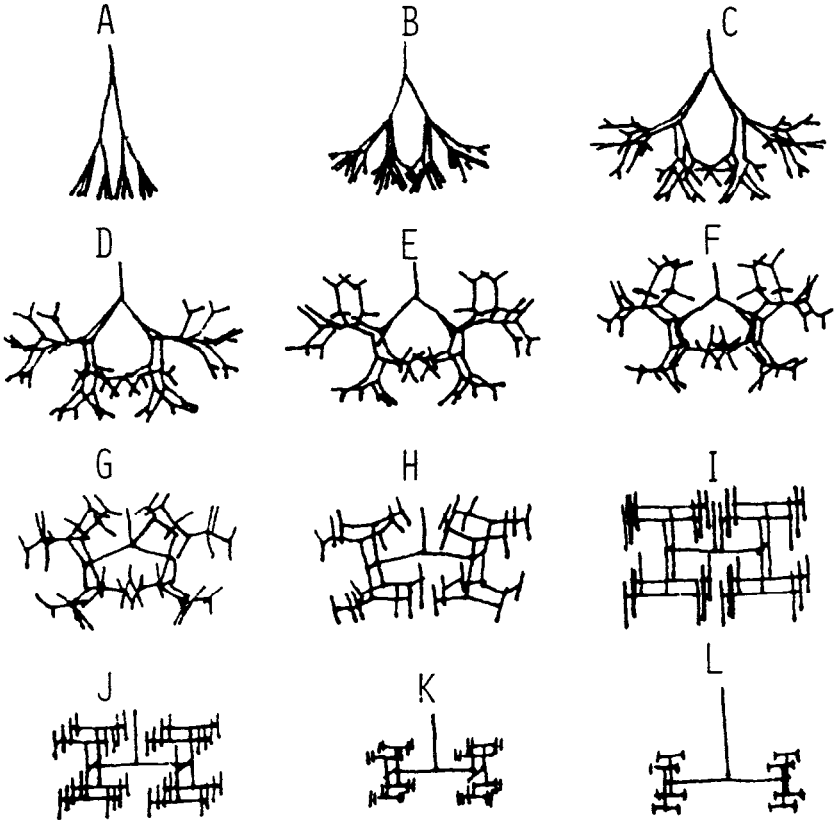

Fig. 1. A–I show graphs of symmetrical trees with branching angles from 10 to 90° in steps of 10°, with a length ratio of 0.9; I–L represent symmetrical trees with branching angles of 90°, and length ratios changing from 0.9 to 0.6 in steps of 0.1 (redrawn from Ref. [22]).

ability is 0.3, and if $\delta = 1.0$, the probability is 0.4; for all other values of δ higher than 2.0 the total probability is 1.00. A symmetrical tree is generated if the probability of $\delta = 0$ is 1.00. A few selected examples of computer generated trees are shown in Figs. 2(a) and (b). The computed trees in Fig. 2(b) compare quite favorably in morphology with two intersegmental branches of a normal, human bronchial tree [Fig. 2(c)]. The form of the computer generated trees was found to be quite sensitive to branching angles and length ratio, implying that in "real" lungs the average values are closely controlled, in spite of the presence of a wide range of individual types of bifurcation[22]. Horsfield and Thurl-

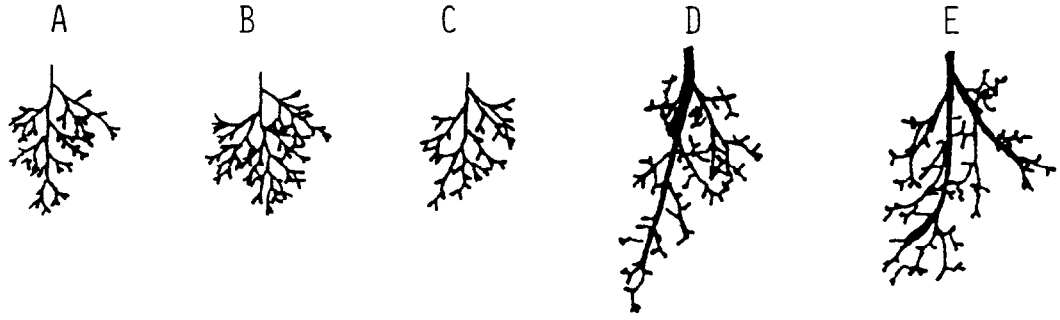

Fig. 2. A–C represent three different trees calculated by the computer with $1/Rxl(H) = 0.935$; D and E show two representations of actual human bronchial trees (redrawn from Ref. [22]).

beck[22] also suggested, based on their computer simulation, that an optimality principle might be determining the formation of the bronchial tree, such that the length of lobules increases by the cube root of the volume. Minimized "costs" in the formation of the bronchial tree may include the lumen volume, surface, frictional power loss and drag. Such costs are functions of the branch radius[15, 19]. The cost minimization would also cause the diameter, length, angle and branching pattern to be all closely inter-related; therefore, computer modelling may assist one in determining which functions are minimized[19].

B. *Arterial branching and arteriosclerosis*

The branching pattern of the arterial network is similarly presumed to be an optimal structure. Such optimal design considerations involve the angle of entry (θ_1 and θ_2) formed by the daughter branches with the axis of the parent branch. The junction angle ψ is simply $(\theta_1 + \theta_2)$[23]. If the radius of the parent branch is r_0 and the radii of the daughter branches are, respectively, r_1 and r_2, then the minimum lumen volume and minimum power loss models yields an optimal geometry of the arterial branch, subject to the following constraints:

$$\cos \theta_1 = \frac{(r_0^4 + r_1^4 - r_2^4)}{2r_0^2 r_1^2}, \tag{1}$$

$$\cos \theta_2 = \frac{(r_0^4 + r_2^4 - r_1^4)}{2r_0^2 r_2^2}, \tag{2}$$

$$\cos \psi = \frac{(r_0^4 - r_1^4 - r_2^4)}{2r_1^2 r_2^2} \tag{3}$$

(from Ref. [23]).

According to Zamir[24], these equations lead us to the optimal junction angle for minimal surface and drag,

$$\cos \psi = \frac{(1 + \alpha^3)^{2/3} - \alpha^2 - 1}{2\alpha}, \tag{4}$$

as well as to conditions for minimum volume and power loss,

$$\cos \psi = \frac{(1 + \alpha^3)^{4/3} - \alpha^2 - 1}{2\alpha^2}, \tag{5}$$

where α is the symmetry ratio r_2/r_1.

Because drag force and power loss are flow-dependent criteria, however, a general flow study is necessary in order to derive the optimal geometry for drag force and power loss. Such considerations become particularly important in arteriosclerosis since as arteriosclerosis progresses the area ratio decreases and the power loss and drag both increase. A general flow equation[15]

$$f = kr^x \tag{6}$$

needs therefore to be considered; in the above equation f is the flow, k is a constant and x is a parameter which is determined by the character of the flow (e.g. for laminar flow $x = 3$, while for turbulent flow $x = 7/3$).

The radius equation then becomes

$$r_0^x = r_1^x + r_2^x. \tag{7}$$

In arteriosclerosis, x is expected to decrease markedly as turbulent flow sets in. However, according to Zamir[24], the range of x is large even for normal arteries. The general flow equation (6) yields

$$\cos \psi = \frac{(1 + \alpha^x)^{2-4/x} - \alpha^{2x-4} - 1}{2\alpha^{x-2}} \tag{8}$$

for minimum drag, and

$$\cos \psi = \frac{(1 + \alpha^x)^{4-8/x} - \alpha^{4x-8} - 1}{2\alpha^{x-4}} \tag{9}$$

for minimum power loss through friction.

This approach may also be useful in conjunction with the computer generated trees of Horsfield and Thurlbeck[19, 22] for modelling bronchial structures and also for detailed hemodynamic calculations on a digital computer. Related applications are recently concerned with artificial valve optimization by computer dynamic simulation of restricted blood flow in the heart caused by the presence of such valves.

A model of arterial bifurcations related to the model discussed above was recently developed by Zamir[24], who reported that such structures are optimal both globally, in terms of the cardiovascular system as a whole, and locally, in terms of the orderly flow through the bifurcation.

3. MODELS OF THE CARDIOVASCULAR SYSTEM AND ARTERIAL FLOW

A computer model of the pressure-flow relationships for the arterial system was developed by Weygandt, Cox, Karreman and Cole[25], in a state variable form which is suitable for the investigation of the control of blood pressure and flow in the mammalian cardiovascular system. This model involves "lumped" parameters as shown in Fig. 3, and was suggested to be applicable to steady state, both mean and pulsatile, as well as transient processes in the cardiovascular system. Two parameters in this model are particularly important: the carotid sinus pressure, which is the major input to the neural control loop, and the mean renal pressure, which is the input to the renal-endocrine-electrolyte system. The numerical analytical method of Gear[26, 27] was employed to solve sets of stiff differential equations which were expressed in vector form. The computer model based on such equations yielded a simulation of the simultaneous blood pressures and blood flows in several arteries, for a given instantaneous output of the heart to such arteries.

Examples of these computer results for pressures and flows versus time are shown in Fig. 4 (after Weygandt *et al.*[25]). The peaks of pressure pulses in Fig. 4 occur steadily later because of transmission lags and increase from the ascending aorta to the femoral artery. This is also observed experimentally[28]. Calculated pressures in various arterial elements were also found to be in agreement with the experimental results. This model supercedes the previous models of Noordegraaf[27], Jager[29] and DePater[30], which were designed for analog computer modelling. A more detailed description of the Weygandt *et al.* model of the cardiovascular system was presented by Doubek[31], and the mechanisms of the vasomotor control were investigated with this digital computer model:

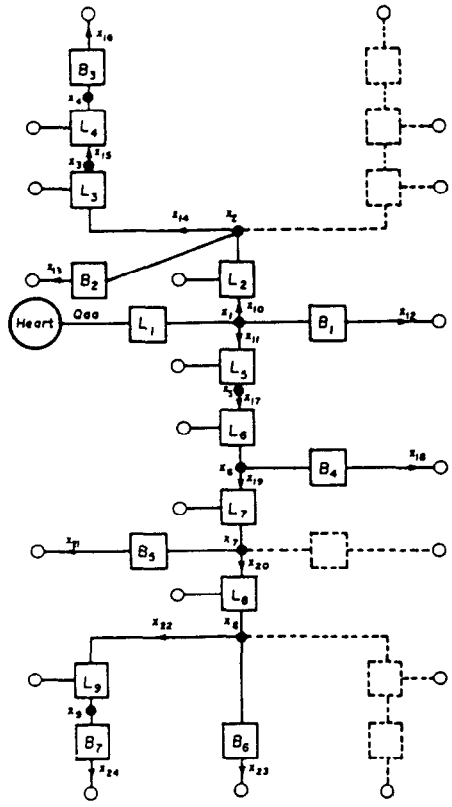

Fig. 3. Structure of a model of the arterial system (from Ref. [25]).

the problem was formulated as a Riccati state regulator, and it was assumed that the optimization criterion is the minimization of expended energy per cardiac cycle. Analog electrical circuits were also employed to facilitate computation. An example of such an analog circuit is reproduced in Fig. 5 from Ref. [31] (see also Table 1). Both the steady state and the perturbed response were calculated. Examples of the simulated waveforms are

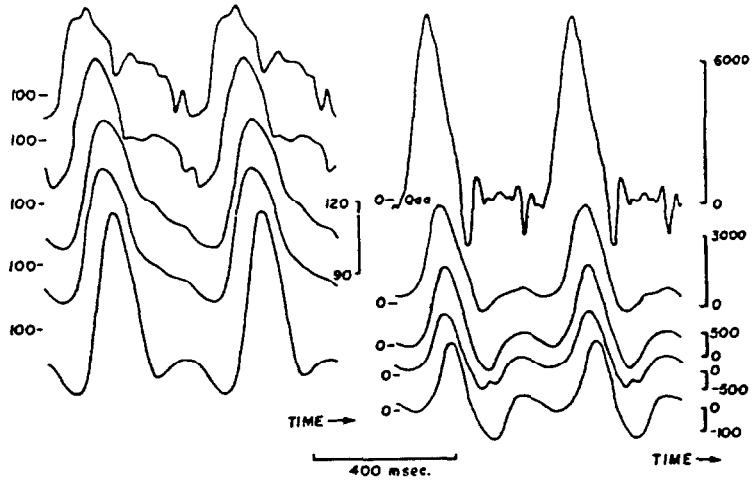

Fig. 4. Computer calculated graphs of pressures and flows in the arterial system as a function of time. Starting from the top left-hand side, pressures in mm Hg in the ascending aorta, the carotid artery, the descending aorta, the aorta above renal and femoral. Starting from top right-hand side, flows in $cm^3/sec.$ at the input from the heart, in the ascending aorta, in the carotid artery, in the descending aorta, in the aorta above renal (from Ref. [25]).

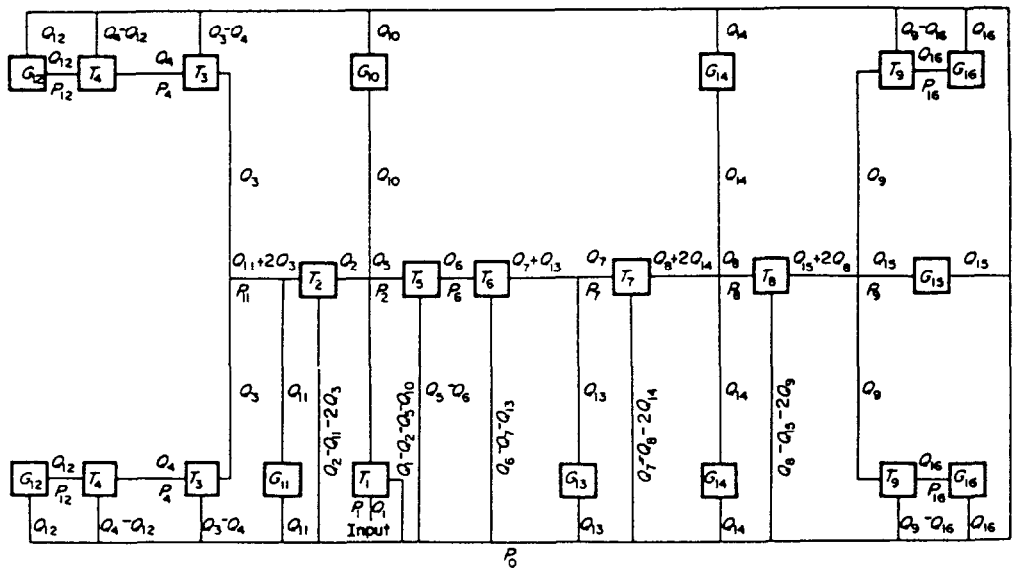

Fig. 5. Schematic representation of an arterial model (from Ref. [31]). In this model, the total arterial compliance C_p depends linearly on the arterial pressure p; R and P_i define the relationship between the total peripheral run-off and the arterial pressure.

represented in Fig. 6, following Doubek[31], and were calculated for a sequence of five heart beats. This investigator concluded that the least energy regulation of blood pressure by peripheral resistance change due to carotid sinus pressure change provides an optimal control that involves a "proportional plus rate set point controller". The model, however, did not include the necessary physiological constraint of maintaining sufficient blood flow to the brain, under various blood pressure conditions.

A much simpler model with only four lumped parameters was recently employed by Dujardin and Van Gelder[32] to simulate the relationship between slowly changing arterial

Table 1. Physical correspondence for block diagram in Fig. 5 (from Ref. [31])

Symbol	$x(i)$	Description	Symbol	Description
P_2	$x(1)$	Pressure in aortic arch	P_0	*Venous* pressure
P_{11}	$x(2)$	Pressure in brachiocephalic artery	G_{10}	Left subclavian bed
P_4	$x(3)$	Pressure in proximal carotid artery	G_{11}	Right subclavian bed
P_{12}	$x(4)$	Pressure in carotid sinus	G_{12}	Carotid Bed
P_6	$x(5)$	Pressure in thoracic artery	G_{13}	Mesenteric bed
P_7	$x(6)$	Pressure in diaphragmatic artery	G_{14}	Renal bed
P_8	$x(7)$	Pressure in abdominal artery (at renal)	G_{15}	Caudal bed
P_9	$x(8)$	Pressure at bifurcation of aorta	G_{16}	Femoral bed
P_{16}	$x(9)$	Pressure in femoral artery		
Q_2	$x(10)$	Flow in brachiocephalic artery	T_1	Aortic arch longitudinal section
Q_5	$x(11)$	Flow in proximal descending aorta	T_2	Brachiocephalic longitudinal section
Q_{10}	$x(12)$	Flow in left subclavian artery	T_3	Proximal carotid longitudinal section
Q_{11}	$x(13)$	Flow in right subclavian artery	T_4	Distal carotid longitudinal section
Q_3	$x(14)$	Flow in proximal carotid artery	T_5	Proximal descending aorta longitudinal section
Q_4	$x(15)$	Flow in distal carotid artery	T_6	Mid descending aorta longitudinal section
Q_{12}	$x(16)$	Flow in carotid sinus	T_7	Abdominal longitudinal section
Q_6	$x(17)$	Flow in mid descending aorta	T_8	Renal longitudinal section
Q_{13}	$x(18)$	Flow in mesenteric and celiac arteries	T_9	Iliac longitudinal section
Q_7	$x(19)$	Flow in proximal abdominal artery		
Q_8	$x(20)$	Flow in aorta below renal		
Q_{14}	$x(21)$	Flow in renal artery		
Q_9	$x(22)$	Flow in iliac artery		
Q_{15}	$x(23)$	Flow in caudal artery		
Q_{16}	$x(24)$	Flow in femoral artery		

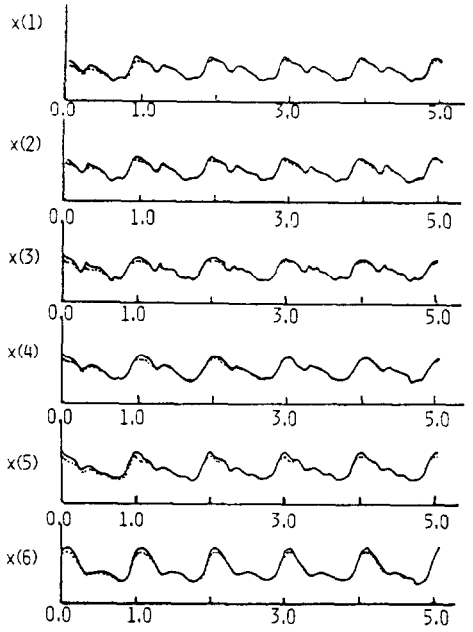

Fig. 6. Plots of normal (solid lines) and controlled (dashed line) x-matrix elements for five heartbeats, representing computer simulated waveforms (according to Ref. [31]).

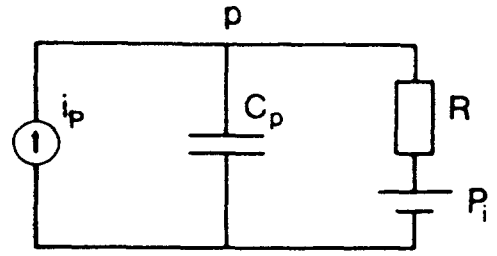

Fig. 7. Schematic model of the arterial system during diastole for a system to which an external pump is connected; the pump flow rate is i_p (from Ref. [32]).

flow and the resulting pressure change. A schematic of the simulated arterial system is shown in Fig. 7.

Experimental observations of the arterial pressure decay following cardiac arrest, as well as the arterial pressure during heart pumping, were employed to determine the values of the four model parameters by a least square adjustment procedure performed by a PDP 11-34 computer. The dynamic compliance C_p which is the derivative of the aortic volume with respect to pressure was borrowed from the earlier work of Cope[33], and is also related to the initial paper of Bergel[34]; other relevant models of the arterial system were previously reviewed by Kenner[35].

Related studies were concerned with blood flow in arteries, with and without stenosis[36–41]. The effects of the concentration profile of red cells on blood flow in the artery were investigated, and the arterial wall shear stress was calculated as a function of the relative fluidity of the blood[42]. It would seem that a more detailed computer simulation of hemodynamics/ flow in the artery with stenosis is warranted and is also likely to yield definitive results.

4. COMPUTER MODELS OF CARCINOGENESIS AND CANCER CHEMOTHERAPY

Computer simulation studies of carcinogenesis are closely related to theoretical studies of the cell cycle, the control of cell division and the growth of cell populations[43–52]. In a computer model of erythroleukemia, Düchting[51] considered a control process of cell proliferation of the form shown in Fig. 8 (also see Fig. 9). The simulation of this process was performed on an AEG-Telefunken TR440 digital computer using the ASIM

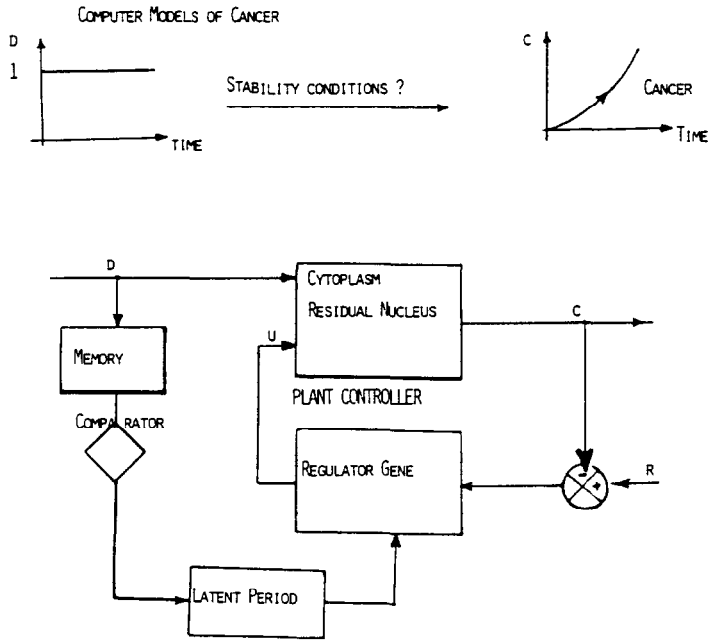

Fig. 8. Block diagram of a control model of cell proliferation (from Ref. [51]). r is the reference input, for examples, hormones; c is the controlled variable, such as the deviation of the number of cells from the steady-state value; d represents disturbances such as carcinogens: (u) represents the control signal, for example, enzymes with specific regulatory roles.

computer program listed in Table 2. This program is written in the block-oriented language for Analogous SIMulation.

The digital logic device in this model ascertains and registers the presence of each cell in a specific compartment; the analog transfer elements were integrators and switching components. The model is therefore a combination of analog and digital devices, and the simulation process is in this case more complex than in the more popular, digital-only models. This model mimiced malignancy through an uncontrollable increase in compartment population, but as many other computer models of carcinogenesis, is limited by the lack of a detailed, experimental analysis of the parameters controlling carcinogenesis. An attempt to introduce such parameters into a model of malignant "stem" cell growth was recently made by Rittgen[53]. Rittgen's basic model is sketched in Fig. 10, where G_1, S, G_2, M, Q_1 and Q_2 are cell cycle phases; Q_1 and Q_2 are the resting phases, while S is the synthesis phase. Mitosis starts either after G_2 or after Q_2, and the daughter cells begin in the resting phase Q_1. The simulation was executed with a special stochastic system[54].

With this model it was possible to calculate the number of malignant proliferating, maturing and mature cells, as a function of time. The simulated malignant cell population growth was exponential, with growth velocities depending on the cell cycle parameters.

Computers and cancer chemotherapy

A model conceptually similar to the Rittgen simulation, but simpler, was applied to the analysis of cancer chemotherapy (Fig. 11, after Chuang and Soong[55]). A FORTRAN IV program was developed for a PDP 15/76 computer which was employed for simulations of scheduled chemical treatments with cell-cycle specific, phase specific and cycle non-specific drugs. It also allowed for Gompertzian tumor growth and variation of kinetic parameters in relation to tumor size. Typical simulated curves of synchronization and

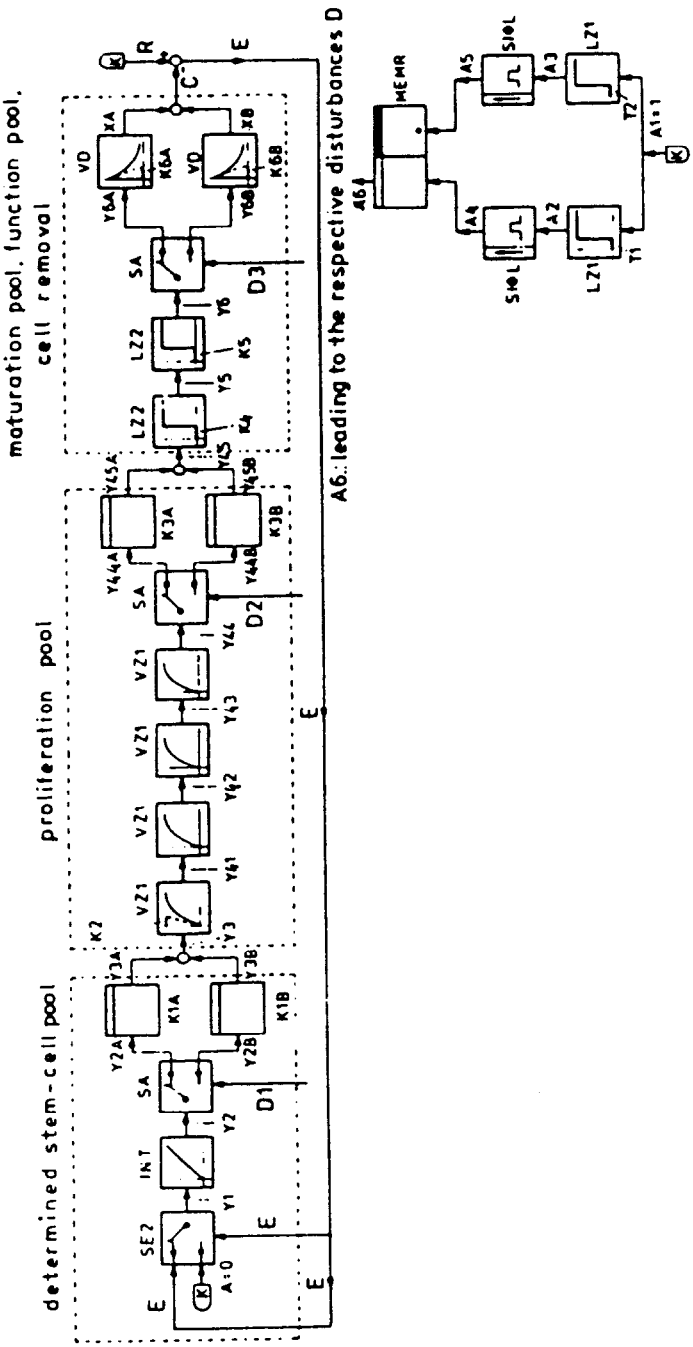

Fig. 9. A model of the erythropoiesis control system (from Ref. [51]). Y_1 = determined stem cells; Y_3 = committed stem cells; Y_{41} = proerythroblasts; Y_{42} = macroblasts; Y_{44} = polychromatic erythroblasts; Y_{45} = orthochromatic erythroblasts; Y_5 = orthochromatic erythroblasts; Y_6 = *erythrocytes/reticulocytes*; C = controlled variables = red blood cells; R = reference input = desired number of erythrocytes (related to the required tissue oxygen); E = error or deviation = quantity of erythropoietin; D = disturbance(s) such as viruses, x-rays UV, vitamin or iron definiency, bleeding, sudden hypoxia.

Table 2. Computer program ASIM (from Ref. [51])

```
*----REGELKREIS MIT TOTZEIT UND NICHTSTETIGEM ELEMENT STRUKTUR
Y1 = SE2(XD,A,XD)
Y2 = INT(0,Y1)
Y2A,Y2B = SA(Z1,Y2)
Y3A = K1A * Y2A
Y3B = K1B * Y2B
Y3  = Y3A + Y3B
Y41 = VZ1(0,K2,Y31)
Y31 = Y3
Y62 = KB*Y61
Y61 = VZ1(0,K7,Y45)
Y42 = VZ1(0,K2,Y41)
Y43 = VZ1(0,K2,Y42)
Y44 = VZ1(0,K2,Y43)
Y44A,Y44B= SA(Z2,Y44)
Y45A = K3A * Y44A
Y45B = K3B * Y44B
Y45  = Y45A + Y45B
Y5   = LZ2(K4,Y45)
Y6   = LZ2(K5,Y5)
Y6A,Y6B = SA(Z3,Y6)
XA   = VD(0,K6A,Y6A)
XB   = VD(0,K6B,Y6B)
X    = XA + XB
XD   = W - X
A1   = 1
A2   = LZ1(TZ1,A1)
A3   = LZ1(TZ2,A1)
A4   = SIML(0,A2)
A5   = SIML(0,A3)
A6   = MEMR (0,A4,A5)

*----------PARAMETER
A = 0
W = 100
H1 = ABS(XD) - 1.E.10
K1A = 0.02
K1B = 0.025
K2  = 0.25
K3A = 12
K4  =1
K5  =2
K6A =30
K6B =10
K7  = 0.1
K8  = 0.2
Z1  = 0
Z2  = A6
Z3  = 0
TZ1 =50
TZ2 = 0
K3B =10

*--------BEARBEITUNG

SKIP H1
RZEIT (0.,0,1,160.)
PLOTTER (A4Q,T/D,15,X/ERYS,7)0.,160.,T,=
        =200.,200.,X
END
```

thymidine blocking effects in cancer chemotherapy are reproduced in Fig. 12 from Ref. [55].

Complications, not considered in this model, can arise in cancer chemotherapy due to the fact that tumor cells can begin to divide parasynchronously following interruption of the treatment. The agreement between this model and the two experimental animal tumor systems, L1210 leukemia and Lewis lung carcinoma, cannot yet be considered as conclusive because of the paucity of experimental data available.

In an interesting report by Swan and Vincent[56], the problem of minimizing the total amount of cycle nonspecific cytotoxic drug in the body of the patient was investigated. Their solution was in terms of optimal control theory and their theoretical results were compared with clinical data stored in a computer at the Arizona Medical Center. For patients suffering from bone cancer known as multiple myeloma, a treatment with melphalan, combined with intravenously administered cyclophosphamide, and an oral, fixed dosage of prednisone was pursued; then the optimal control data was compared with the clinical data. The optimal treatment suggested by the Swan and Vincent model[56] is a relatively small dose at the beginning, followed by a gradually increasing dose as the cancer cells decrease in number. The total amount of drug accummulated with such a treatment appears to be a minimum but the authors warn that their model assumes that the drug effectiveness parameter does not change significantly due to a change in the drug "program"; they also suggest that clinical tests should be run to determine the nature and extent of variation of the drug effectiveness parameter. As in the model of Chuang and Soong[55], tumor growth was assumed to be Gompertzian, similarly to the earlier studies of Laird[57] and also as in the clinical applications of the Gompertz model by Sullivan and Salmon[58] to tumor growth and regression in IgG multiple myeloma in

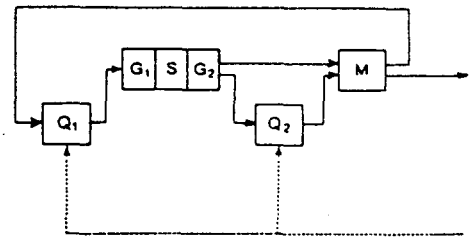

Fig. 10. Cell cycle scheme for a stem cell (according to Rittgen[53]). G_1, S, G_2 and M are known steps of the cell cycle, with G_1 and G_2 representing the "gap" intervals, S representing the synthesis step, and M representing mitosis. Q_1 and Q_2 are resting phases.

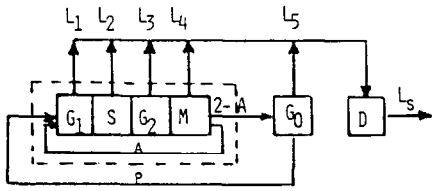

Fig. 11. A model of tumor growth and of the drug treatment effects (according to Ref. [55]). The proliferative compartment has the four phases G_1, S, G_2 and M. Cells may die either naturally or because of the drug treatment, as determined by the functions $L_i(t)$, $i = 1, \ldots, 5$. when leaving G_1, S, G_2, M or G_0 such cells enter the dead cell compartment D. After each binary fission, $(2 - A)$ cells enter the nonpoliferative compartment G_0, while A cells $(1 \leq A \leq 2)$ continue their proliferation cycle. Loss from the tumor site is determined by I_h. A proportion p of G_0-cells may re-enter the proliferative cycle at G_1.

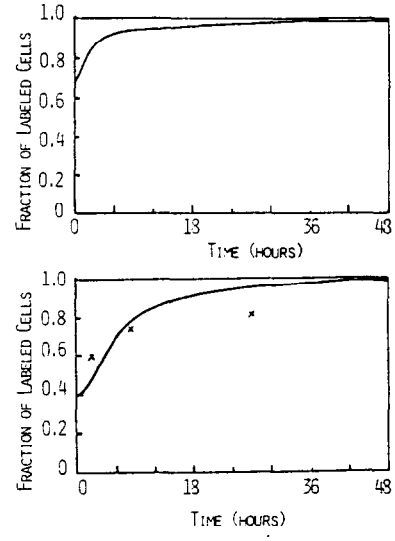

Fig. 12. Simulated CL curves of synchronization and thymidine blocking effects in cancer chemotherapy are shown together with observed values (from Ref. [55]).

humans. In a subtle development of the optimal control approach to cancer chemotherapy, Zietz and Nicolini[59] proposed that the optimum treatment should keep the tumor size low and the normal population high, for as long as possible, during the treatment, while achieving tumor cell kill. Their mathematical model is also based upon the Gompertzian growth and the earlier studies of Nicolini and Kendal[60] and Nicolini *et al.*[61]; the model leads to an expression of switching times for drug administration, and rest, which could

not be explicitly evaluated. Therefore, it was suggested that computer analysis will be needed to determine the optimum treatment strategy (optimal trajectory), and the numerical values of the switching function. An algorithm was then developed to uniquely define the switching function. This algorithm, when applied to two cell populations for a treatment period of 21 units, and a weighting of 4:1 normal-to-tumor cell division rate, predicted that the optimum treatment would be dose administration for the first 8 time units, followed by a rest for the next 13 time units. It was pointed out, however, that additional computations will be needed to improve the algorithm. The model was claimed to be also suitable, with some modifications, for the optimization of chemotherapy with cycle-specific drugs.

A microprocessor model of perturbed cell renewal

Düchting[62] reapproached the problem of computer simulation of carcinogenesis at the more basic level of perturbed cell renewal by considering the interactions between adjacent cells on a two-dimensional grid. Such questions were also considered previously by Gardner[63], Lindenmayer[64], Reshodko and Bures[65], Ransom[66] and Arbib[67]. The approach is close to what Arbib describes as a "tessellation" model, and involves basic concepts from automata theory (see also Sec. 10). Düchting's simulation of disturbed cell renewal[62] was carried out by means of an Intel 8080 microprocessor and we expect that his model could also be programmed on the now popular IBM PC/ATT microprocessor. The organization of the programs run by the Intel 8080 for this simulation is reproduced in Fig. 13 from Düchting[62]. This simulation yielded some interesting results, such as the onset of metastasis after "surgery" even if only one "malignant" cell is left amongst the "normal" cells of the grid (Fig. 6 in Ref. [62]); in the case of no surgery, the model predicts that normal cells would eliminate the few malignant cells present. Related to this

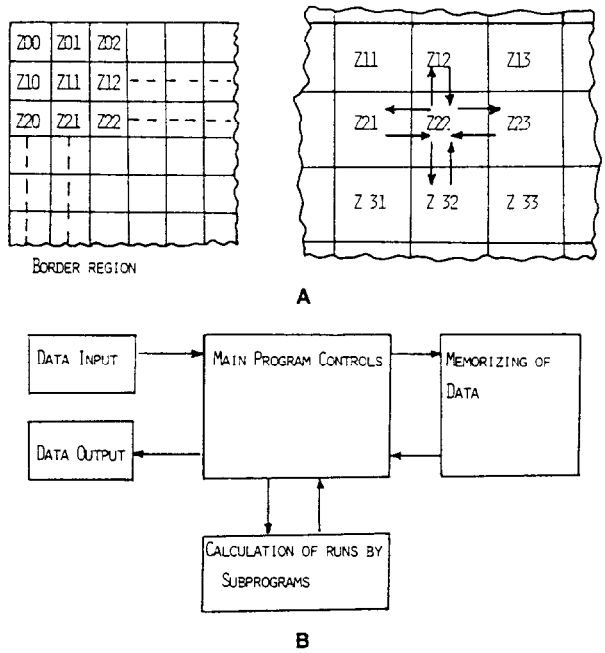

Fig. 13. A. Organization of the Intel 8080 program for modelling cell renewal (according to Düchting[62]). B. Grid configuration of cells, or tesselation model of cell renewal (after Düchting[62]).

tessellation approach to population growth, Lieberman considered in an earlier report[68] a stochastic model in which the population distribution is confined within a limited space. The simulation was carried out with an IBM Model 360 and showed that the size and abundance of organisms are linked by a logarithmic relationship if the organisms are limited by a single resource.

It would be interesting to adapt this model to the study of tumor growth, under conditions of limited nutrient supply since the tumor cell proliferation is strictly dependent upon the local availability of nutrients supplied by tumor vessels[69]. The tumor vascularization itself is, however, induced by the elaboration of a tumor antigenic factor (TAF) by the tumor cells[70]. In a detailed model of tumor growth, Liotta *et al.*[71] considered both vascularization and necrosis of tumors by taking into account both diffusion and proliferation of tumor cells. Coupled diffusion equations with a nonlinear source and sink terms described the proliferation, migration and necrosis of tumor cells. According to Liotta *et al.*[71], their diffusion model is superior to lumped parameter models of tumor growth such as that of Saidel *et al.*[72] because "the lumped-parameter simulation does not yield any information about the spatial distribution of the tumor cells and vessels in the tumor." The results of the diffusion model are qualitatively similar to those determined by the experiment (Figs. 1 and 3, respectively, in Ref. [71]). One major limitation of this diffusion model of tumor growth is that the tumor was assumed to be spherically symmetric. Other limitations of the model are discussed in Ref. [71].

5. BIOLOGICAL AND BIOCHEMICAL OSCILLATORS

A number of important biological systems incorporate nonlinear oscillators. Amongst these are the protein biosynthetic pathway and its controllers[73], interacting populations of biological organisms[74, 75], and neural networks[76]. Many other biochemical and biological oscillators are known and have been investigated in some detail[77–81]. For the Goodwin model, Singh[82] reported an analytical solution, while for the two-species Volterra system, Frame[83] obtained a convergent power series expansion for the period of oscillation. A detailed analysis of these two examples inspired Singh[82] to devise a method applicable to a large class of nonlinear oscillators which is based on the Hamiltonian approach. Although such Hamiltonian nonlinear oscillators might not be representative of biological oscillators, their investigation may suggest new approaches to biological problems such as neuroelectric activity and control of protein biosynthesis.

A particularly important case of a biochemical oscillator is that of a biochemical chain with feedback inhibition, enzymatic removal and catalyzed input[84]. The addition of enzymatic removal to feedback inhibition in a biochemical chain was suggested to increase the possibility of enhanced oscillations[85]. In one of the simple cases considered by Landahl[84], the interesting feature of confocal limit cycles was found; depending upon the initial values of the state variables x and y, the biochemical system can either approach a stable point with damped oscillations or it can oscillate around that point in a state limit cycle. These cases are illustrated in Fig. 14 (from Landahl[84]). Such results may apply to a larger class of biological systems such as a population of organisms that produces a pollutant affecting the birth rate (cf. Landahl[84]).

For more complex cases, such as an array of coupled, asymmetrical Van der Pol oscillators, both analog and digital computer simulations were reported by Linkens[86]; coupled Van der Pol oscillators were employed as a model of the spontaneous electrical rhythms recorded from the gastrointestinal tract (Fig. 15) of humans and laboratory animals. Algebraic equations were obtained for the array of coupled oscillators and a numerical simulation of such equations was carried out, followed by fast Fourier transform (FFT) spectral analysis. Accurate measurements of the spectral components were also

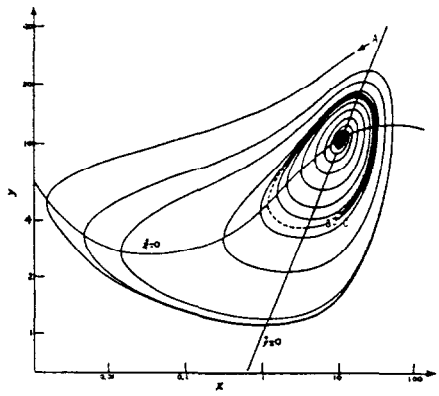

Fig. 14. Example of a stable point (10.53, 10.53), surrounded by an unstable limit cycle (dashed curve) and a stable limit cycle (heavy curve), of a biochemical oscillator with parameters defined in Landahl[85].

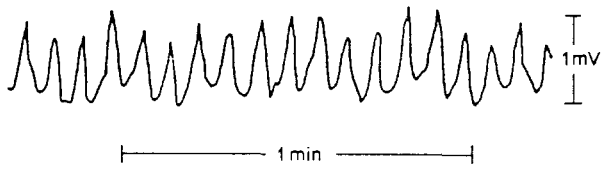

Fig. 15. Typical experimental recording of the electrical activity of human duodenum, showing an asymmetrical waveform with a small third harmonic distortion (according to Linkens[86]).

made with a Bruel and Kjaer analog spectrum analyzer Type 2107, and the results were compared with the FFT of the simulated waveform[87]. The procedure allowed the estimation of both d.c. and all harmonic components, as well as the phase shifts. Representative results are reproduced in Figs. 16 and 17 from Refs. [86] and [88], respectively; these results show good agreement with the experimental data. The analysis can be extended to any number of asymmetrical Van der Pol oscillators coupled together by a linear network comprising parallel resistive, capacitive and inductive elements (Fig. 18 from Ref. [88]). The method was successfully used to predict oscillation frequencies and harmonic content for the human, small intestine electrical activity. Further details of the analysis and computer simulations of the Van der Pol oscillators are found in the earlier papers[87–96]. The original paper of Van der Pol is Ref. [97], and a generalized Van der Pol equation was published subsequently by Nijenhuis[98].

A more general formalism for biological oscillators was proposed by Rosen[99], based on activation–inhibition functions. Thus, if one considers a general "dynamical system",

$$\frac{dx_i}{dt} = f_i(x_1, \ldots, x_n), \tag{10}$$

x_j is said to *activate* x_i in a state $(x_1^0, \ldots, x_n^0)$ if the derivative $\partial/\partial x_j(dx_i/dt) = u_{ij}(x_1^0, \ldots, x_n^0)$ is positive[100], and x_j *inhibits* x_i if this derivative is negative when evaluated in the state $(x_1^0, \ldots, x_n^0)$. Therefore, the functions $u_{ij}(x_1, \ldots, x_n) = \partial/\partial x_j(dx_i/dt)$ specify the relations of activation and inhibition between the state variables. For a harmonic oscillator $dx/dt = y$ and $dy/dt = -x$; its activation–inhibition functions are $u_{11} = 0$, $u_{12} = 1$, $u_{21} = -1$ and $u_{22} = 0$[99]. If one represents the state variables x and y by nodes and the functions u_{ij} by directed paths (or channels), joining the state variables, then the acti-

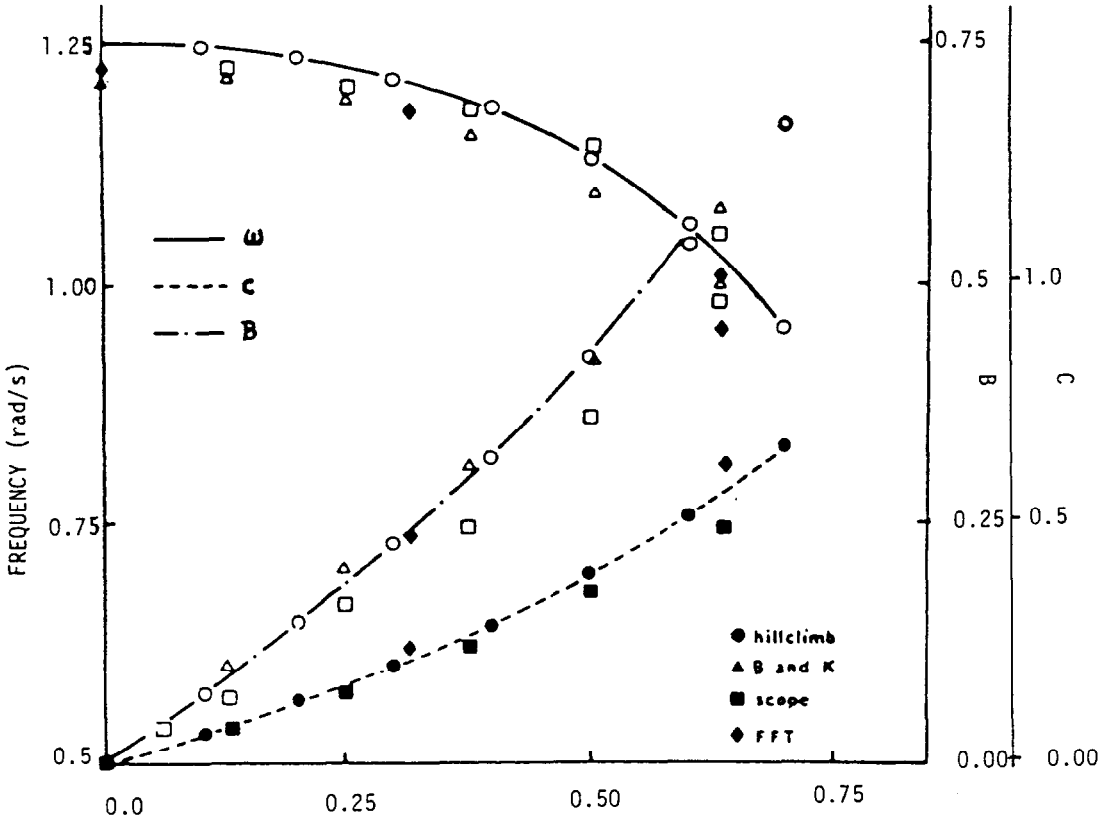

Fig. 16. Single asymmetrical Van der Pol oscillator with $\epsilon = 1.0$, $\omega = 1.25$ and variable k (according to Linkens[86]).

vation–inhibition pattern or graph of an undamped harmonic oscillator is

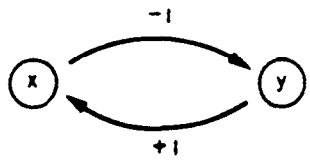

(11)

(cf. Rosen[99]). The previously considered Van der Pol oscillator has the activation–inhibition pattern

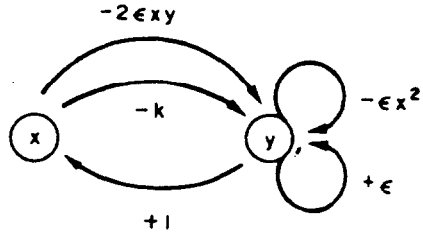

(12)

with $u_{11} = 0$, $u_{12} = 1$, $u_{21} = -2x - k$, and $u_{22} = 1 - x^2$, while the simplest (prey–

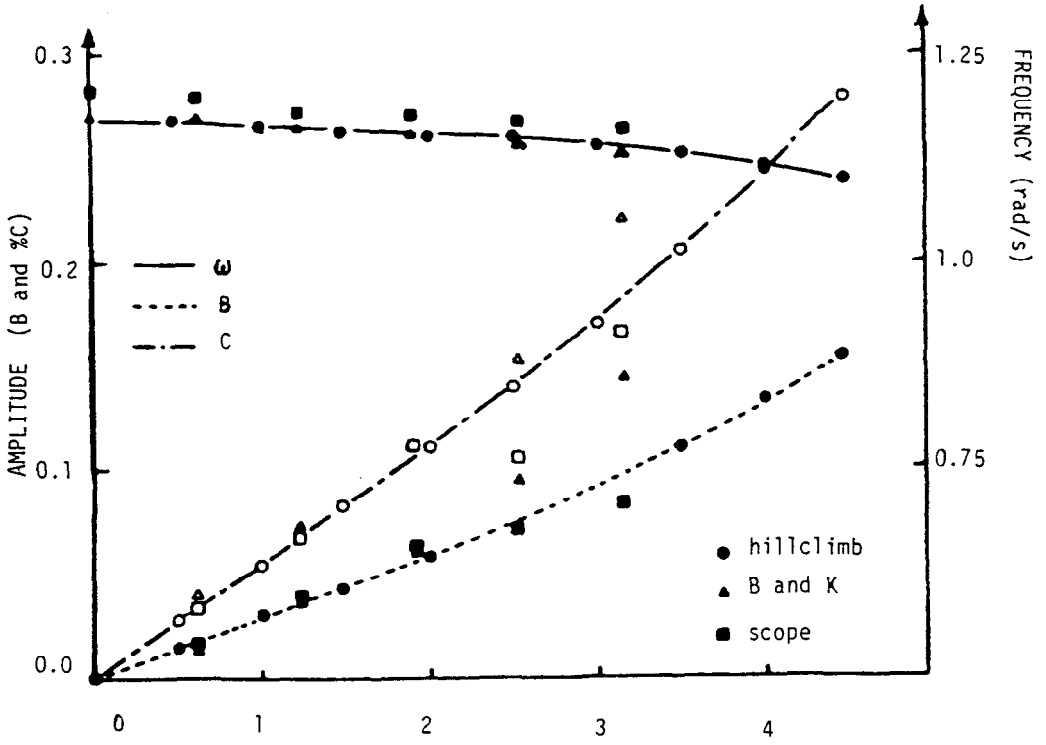

Fig. 17. Two inductively-coupled, asymmetrical Van der Pol oscillators showing the effect of changes in k for $\epsilon = 0.1$, $\omega = 1.25$, in-phase mode (according to Linkens[86]).

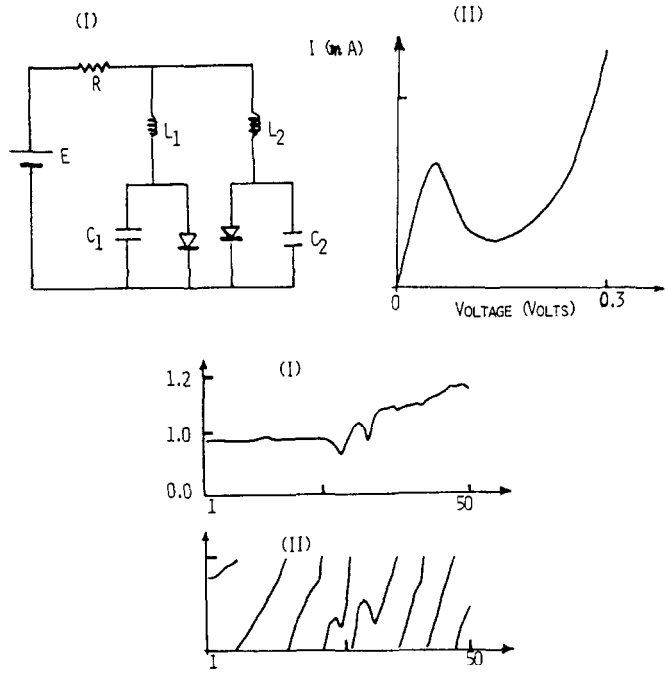

Fig. 18. A. Oscillations in an electronic network with two tunnel diodes: I. the circuit; II. the characteristic of the tunnel diode. B. Entrainment in a chain of oscillators after 156 iterations of the map P: I. the phase velocity; II. the phase (from Ref. [105]).

predator) Volterra system has the pattern

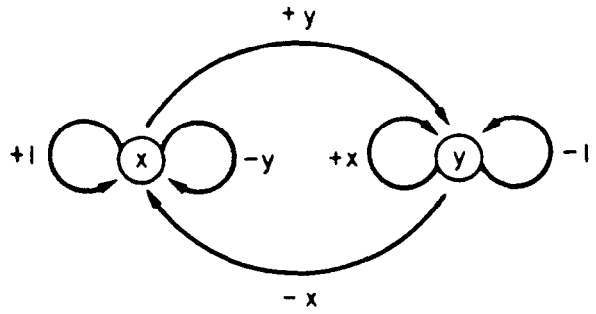

(13)

As shown by Rosen[99], this representation of system dynamics in terms of activation–inhibition patterns, or graphs, is more general than the differential equation formalism of "dynamical systems" from which it was abstracted; this is so because the activation–inhibition graphs may be applicable to dynamics which are not simply representable by the flows of a vector field[99]. The activation–inhibition graphs are useful, for example, in considering the dynamics of complex, neural and genetic networks (see, for example, Rosen[101], and Secs. 7 and 8 in this report). An algorithm for generating activation–inhibition graphs for a given dynamical system could be executed by a computer, and the analysis of complex, neural and genetic networks with specified general properties could be, therefore, simulated on a computer. A discussion of activation–inhibition patterns of neural networks was presented by Rosen[101], who also pointed out that in spite of the formal similarities between such networks and a dynamical system, they cannot be directly represented by differential equations such as (10). On the other hand, genetic networks with two-state components, as modelled by Sugita[102], are described in automata-theoretic terms and, at the same time, have a corresponding representation as dynamical systems. Such distinctions between neural and genetic networks were also noted in subsequent reports[103, 104].

The above discussion indicates that the modelling of biological and biochemical oscillators leads to the consideration of more general formalisms such as the activation–inhibition graphs, networks and automata. Such concepts are discussed in some detail in the remaining sections and provide powerful means for approaching a wide array of biological and biomedical problems. In a rather precise sense such formalisms are extensions and abstractions of the computer simulation approach to biology and medicine, and are, therefore, related to the preceding sections. To conclude this section we shall consider biological/biochemical oscillators which are modelled by networks similar to those discussed in Secs. 6 and 7. Biological organs with essential electrical activities such as the brain and the heart are often modelled by analog electronic networks. A relatively simple example of such an electronic model is shown in Fig. 19, reproduced from Ref. [105]. For this simple circuit, one can write the complete system of differential equations:

$$C_1 \frac{dV_1}{dt} = I_1 - F(V_1), \tag{14}$$

$$C_2 \frac{dV_2}{dt} = I_1 - F(V_2), \tag{15}$$

$$L_1 \frac{dV_1}{dt} = E - V_1 - R(I_1 + I_2), \tag{16}$$

$$L_2 \frac{dV_2}{dt} = E - V_2 - R(I_1 + I_2), \tag{17}$$

where V is the voltage, I is the current, R is the passive resistance, C is the capacitance and L is the inductance. The electric network in Fig. 19 exhibits "entrainment" behavior (phase locking), as shown by Gollub *et al.*[106], analogous to that of a special type of chemical oscillator called the Bruxellator[107]; the Bruxellator comprises a set of hypothetical chemical reactions with periodic fluctuations in the reactant concentrations for at least some of the reactants. Such a Bruxellator was specified in Ref. [105] by the set of reactions

$$A \underset{k_{-1}}{\overset{k_1}{\rightleftharpoons}} X, \tag{18}$$

$$B + X \underset{k_{-2}}{\overset{k_2}{\rightleftharpoons}} Y + D, \tag{19}$$

$$2X + Y \underset{k_{-3}}{\overset{k_3}{\rightleftharpoons}} 3X, \tag{20}$$

$$X \underset{k_{-4}}{\overset{k_4}{\rightleftharpoons}} E. \tag{21}$$

The Bruxellator[107] exhibits an equilibrium point which is stable, an equilibrium point which is unstable, and the stable limit cycle shown in Fig. 20. u represents the concentration of X and w represents the concentrations of $(X + Y)$, φ represents the "phase" and κ represents the phase-difference parameter. Grassman and Jansen[108] showed that a system of weakly-coupled Bruxellators gives rise both to bulk oscillations and stable-

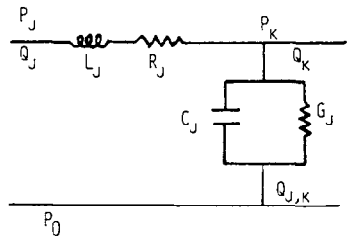

Fig. 19. Electronic model of arterial flow in longitudinal section (from Ref. [105]). P_j = input pressure, Q_j = input flow, P_k = longitudinal output pressure, Q_k = longitudinal output flow, P_0 = transverse output pressure, (venous), $Q_{j,k}$ = transverse output flow, L_j = mass of blood (inductance), R_j = arterial resistance to flow (electrical resistance), C_j = elastance of arterial wall (capacitance) and G_i = damping of arterial wall (conductance).

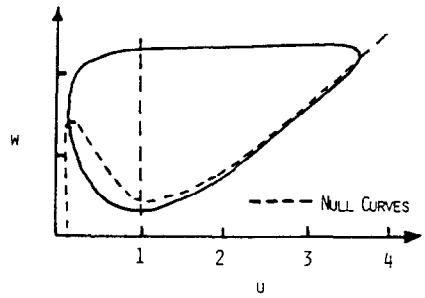

Fig. 20. Limit cycle of the Bruxellator for $n = 5$ and $\beta = 7$ (according to Ref. [107]).

phase wave patterns. Gollub *et al.*[106] showed that coupled nonlinear oscillators exhibit both periodic behavior and "chaos" (which includes phase incoherence). Phase locking of weakly-coupled oscillators has been discussed in a number of general reports[108–111], as well as in relation to specific biological systems such as the cardiac cells[112–115], the respiratory system[116], and coupled neurons[117–119].

A group of more complex biochemical oscillators was recently considered which consists of closed, positive feedback loops of catalytic reactions between biopolymers; these were called "hypercyles"[120]. Such networks exhibit limit cycles characteristic of a biochemical clock. The computer solutions of the corresponding, coupled nonlinear differential equations describing these hypercycles showed that the period τ_n of the n-component limit cycle is a multiple integer n of an elemental repeat period τ. A diagram of the n-component hypercycle is reproduced in Fig. 21 from Ref. [120]. The corresponding computer solutions for representative hypercycles are shown in Figs. 22 and 23.

The synchronous character and parametrization of the n-hypercycle is consistently approached within the limit cycle period T_n, and after the decay of the initial transients there is an orderly build-up of phase-locked species amplitudes. Because of this phase coherence and phase-locking, the n-hypercycle is resistant to external perturbations in all cases for $n \geq 5$. It is rather interesting that the catalytic feedback limit cycle has the time delay structure

$$y_1(t) = y_k(t + (k - 1)\tau_n), \tag{22}$$

$$y_k(t) = y_{k+1}(t + \tau_n), \tag{23}$$

where y are the amplitudes, t is the time and k is an integer. Equation (22) reflects the translational time invariance which is characteristic of ordered linear systems, although the hypercycles are nonlinear systems with internal feedback controls; it is precisely the feedback control which enables the nonlinear system of hypercycles to resist changes in the presence of external perturbations. Another interesting feature of the n-hypercycles uncovered by this computer analysis[120] is that as n becomes large the periodic variation in y deviates more and more from a sinusoidal oscillation, getting progressively closer to "localized" pulses. For $n = 5$, this feature is barely noticeable (Fig. 22a); on the other hand, for $n = 10$, the pulses are clearly visible (Fig. 22b). At the same time, the $n = 10$ hypercycle is highly nonlinear: y_3 must increase 19 orders of magnitude to reach half-maximum within a period of 51 time units, reflecting the extreme steepness of the pulse

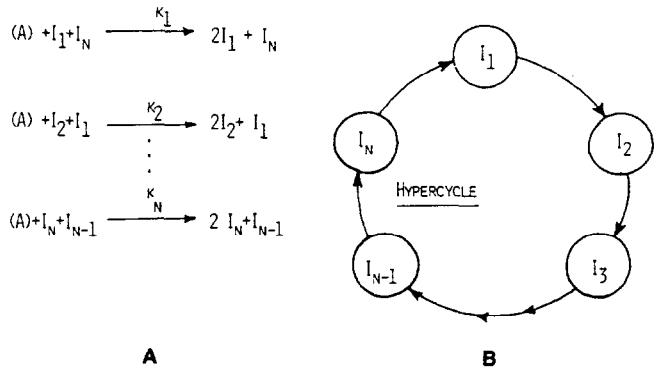

Fig. 21. Representation of the basic mechanism of catalytic hypercycles (according to Ref. [120]). Circles refer to self-instruction or autocatalysis and single arrows indicate a catalytic reaction. The network (B) of second-order autocatalytic reactions (A) forming a closed loop is called a hypercycle.

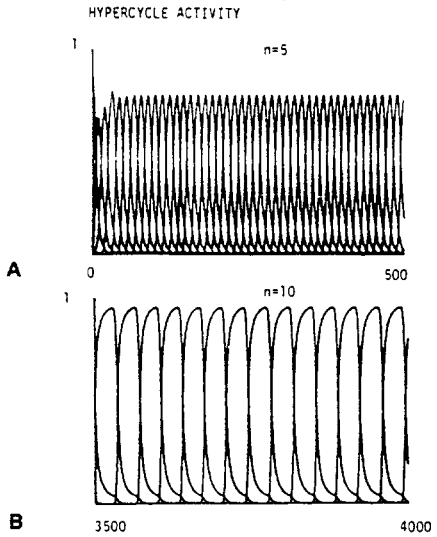

Fig. 22. Hypercycle activity for $n = 5$ (A) and $n = 10$ (B) (according to Ref. [120]).

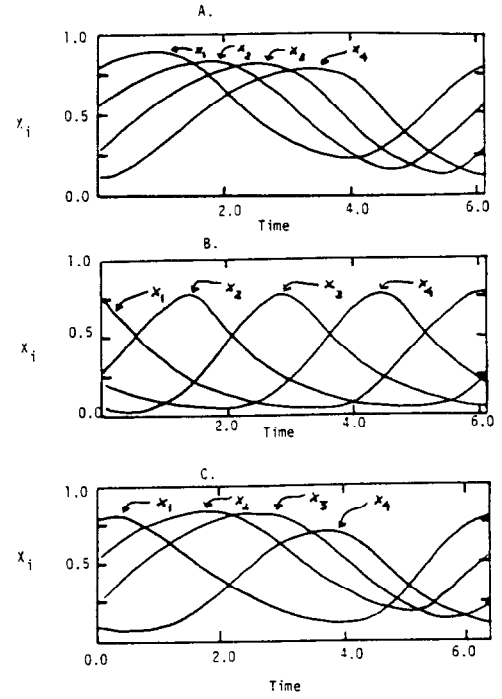

Fig. 23. Limit cycles found by numerical integration for a $k = 4$ hypercycle (according to Ref. [120]). A. $\theta_1 = \theta_2 = \theta_3 = \theta_4 = 0.50$; B. $\theta_1 = \theta_2 = \theta_3 = \theta_4 = 0.25$; C. $\theta_1 = \theta_2 = \theta_3 = \theta_4 = 0.50$, but with a different equation from that used to calculate A.

shapes in Fig. 22b. The computer solution for the $n = 13$ hypercycle (Fig. 23) compares very favorably with the approximate, analytical solution (Table II in Ref. [120], p. 350), suggesting that computer solutions of the exact equations can also be trusted for higher n values. An elementary hypercycle was previously introduced by Eigen and Schuster[121], with the purpose of reducing the complicated multistep polynucleotide replication and translation processes to the single, overall biochemical reactions. The limit cycles of realistic hypercycles, however, are smaller, in general, than those of elementary hypercycles and approach them in the limit of vanishingly small concentration ("infinite dilution").

The treatments of the electronic and biochemical oscillators discussed above proceed by solving systems of differential equations and then by analysis in detail of the analytical or computer solutions. Alternative approaches by means of activation–inhibition graphs or automata-theoretic means are more generally applicable, even to very complex networks, and can provide insights into the complex oscillatory behavior of biological systems, as discussed in Secs. 6 and 7.

6. MODELS OF NERVE CELLS

Neurophysiology has been a very fertile field for the application of mathematical modelling and computers to physiological problems. The celebrated work of Hodgkin and Huxley[122] is an outstanding example of the precision of mathematical modelling and its power in unraveling the complex interactions amongst the components of nerve mem-

branes. The recent construction of high-speed digital computers has further stimulated the development of sophisticated neural models. At the same time, the ease with which differential equations of a neural model can be solved numerically with a computer might suggest that mathematical analysis without a computer is redundant; however, this is not so because a complex nonlinear model of a neuron will often have solutions that are remarkably sensitive to one or more parameter values[123]. Furthermore, the fact that the solutions of certain differential equations resemble an observed behavior of the neuron does not imply that the model gives an accurate representation of the mechanism causing that behavior. A model is considered to be adequate only if it can be used to make predictions that can be experimentally tested, *and* if the results of such testing are in agreement with the predictions of the model. As discussed by Plant[123], one has to supplement the computer and quantitative analysis of a model with mathematical techniques from the qualitative theory of differential equations (which are not programmed in the computer).

The simple case of bursting "pacemaker" neurons[123], which occur for example in the abdominal ganglia of snails and slugs, was considered from the standpoint of this qualitative theory. Such nerve cells as the pacemakers generate "bursts" of action potentials separated by intervals of lower or zero activity (Fig. 24); this behavior is observed even in isolated cells, in the absence of any external input. One of the important questions considered for such systems is the modelling and separation of electrical activity other than the action potentials in the burst. Experiments with tetrodotoxin (TTX) added to pacemaker nerve cells have shown that the action potentials gradually disappear and that only the TTX-insensitive "slow-wave" signals are left behind. The mechanism(s) for generating such slow-wave potentials can be identified by phase-plane analysis[123]. Take for example the mechanism of generating a voltage which contributes to its own oscillation, or the so-called regenerative behavior in the Hodgkin–Huxley model. The corresponding "autonomous" system is represented by the differential equations

$$\frac{dV}{dt} = f_V(V, x),$$
$$\frac{dx}{dt} = f_x(V, x), \tag{24}$$

where x is the variable which the voltage V "oscillates against". The behavior of the solutions of these equations can be followed by projecting the three-dimensional plot of V as a function of time t onto the (V, x) plane or "phase plane", (Figs. 25 and 26). The solution of this model is a periodic oscillation such as the slow wave when the curve in Fig. 26 is closed. The curve is then called a limit cycle. A part of the slow-wave limit cycle will be below the threshold for action potentials, and the other part will be above, as shown in Fig. 26. If a brief perturbation, such as a strong hyperpolarizing current pulse is injected into the nerve cell at various times during the burst, the regenerative model predicts that the time interval required to return to the next burst will entirely depend on the point in the previous burst at which the impulse was applied. Furthermore, the impulse should be sufficiently strong to temporarily "kill" the burst. Strumwasser[124] performed such an experiment and found that the results agreed with the predictions of the regenerative model; therefore, it is likely that the major component of the generation process of the slow wave in pacemaker nerve cells is a regenerative one, as represented by Eq. (24), and discussed in Ref. [123]. Plant[123] went further than the phase-plane analysis,

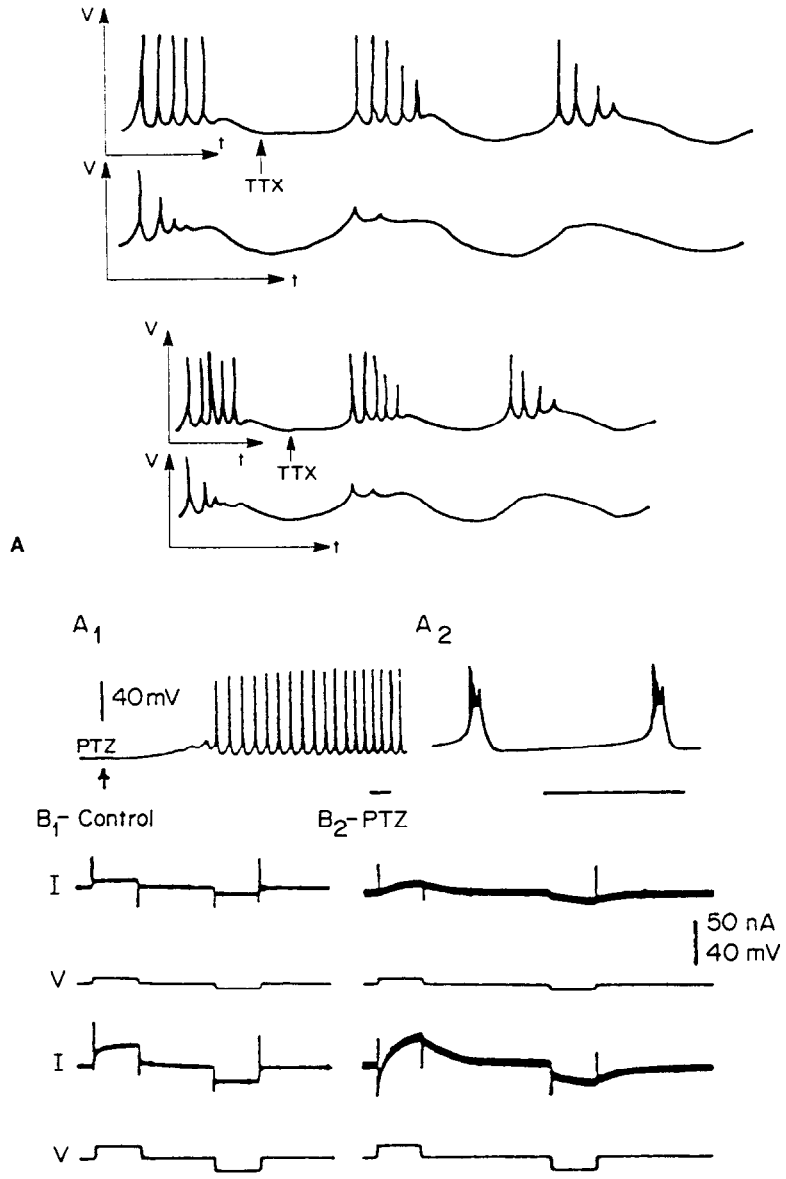

Fig. 24. Action potentials of nerve cells that serve as pacemakers. A. TTX-insensitive "slow-wave" (from Ref. [123]). B. PTZ (pentylenetetrazol) effects on Aplysia neurons (from Ref. [126]): A_1 - upon addition of 0.5% PTZ the cell depolarizes and fires bursts of 2–3 spikes triggered by slow oscillations; A_2 - 25 min later, damped paroxysmal discharges; B_1 - control experiment by voltage-clamped LGC cell in saline (no PTZ added); B_2 - same as B_1 but with PTZ added. Note the slowly developing current (I trace), and the slow tail current produced by 10 sec depolarizing or hyperpolarizing voltage pulses (V trace). Holding potential: −45 mV; voltage pulses: 6 and 12 mV. Horizontal bars: 10 sec.

in an attempt to identify the variable x, and employed singular perturbation theory. He proposed that the slow wave is generated by ions moving down their electrochemical gradients in response to voltage-dependent conductance changes, very similar to the Hodgkin–Huxley model[122]. With the assumptions of neglible leakage conductance and very slow conductance components, inwardly and outwardly flowing ions, the analysis

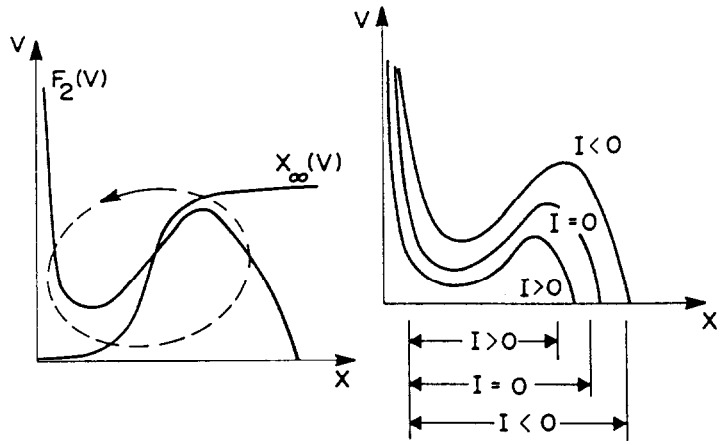

Fig. 25. Phase-plane representation (A) of the potential $V(x, y, z)$ as a function of time t and (B) $V(x)$ for different values of I, (according to Ref. [120], redrawn figure).

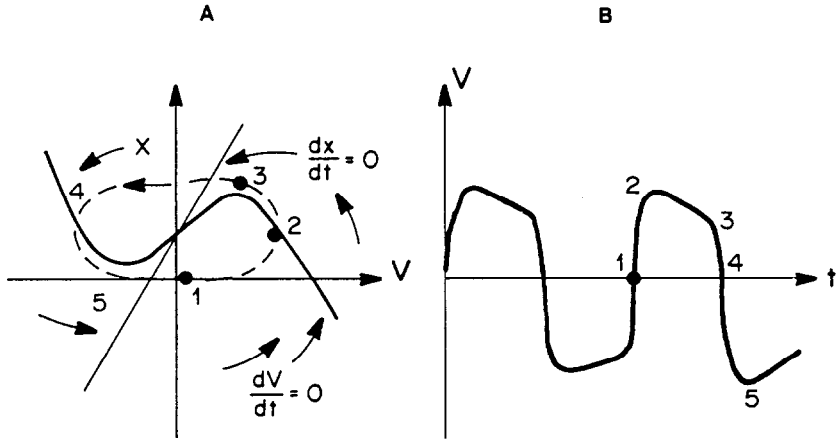

Fig. 26. Limit cycle and null points in the phase-plane representation (according to Ref. [120].

leads to the Van der Pol equations, which we already discussed in Sec. 5:

$$\frac{dV}{dt} = V - \frac{V^3}{3} - x + I,$$
$$\frac{dx}{dt} = r(V + a - bx), \tag{25}$$

where a, b and I are constants. The corresponding phase-plane analysis is represented in Fig. 27, together with the stable limit cycle solution (dashed line in Fig. 26). Introducing $s = rt$, Eqs. (25) become

$$r\frac{dV}{ds} = V - \frac{V^3}{3} - x + I,$$
$$\frac{dx}{ds} = V + a - bx. \tag{26}$$

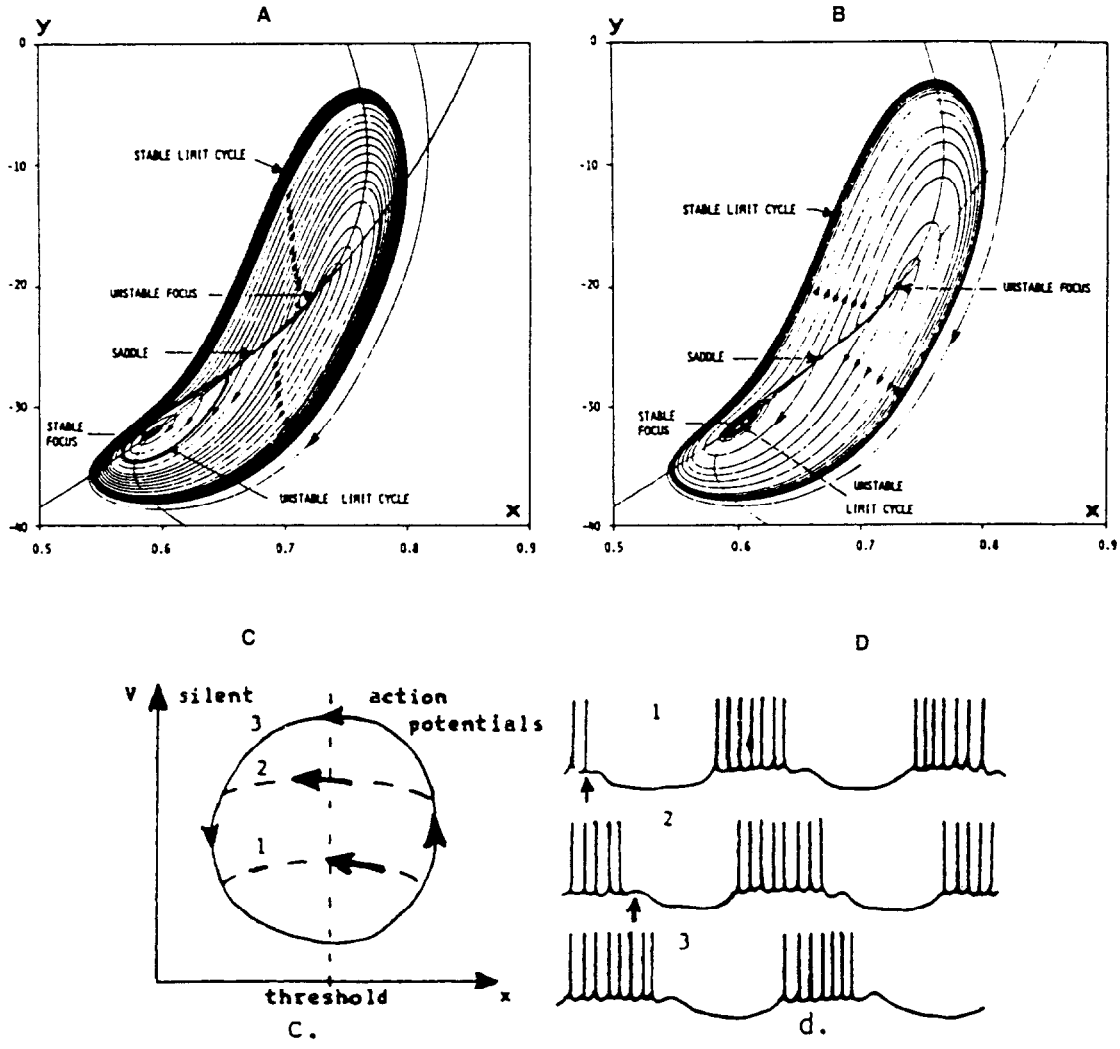

Fig. 27. A and B. Topological portraits of the fast dynamics of Aplysia neurons obtained by numerical integration for two different time instants (from Ref. [251]). C. Limit cycle and threshold in the phase-plane representation of the voltage (D) of Aplysia neurons (according to Ref. [120]).

In the limiting case of $r = 0$, called the "singular perturbation" of Eq. (26), the solution in the phase plane jumps from one point of the nullcline ($dx/dt = 0.0$ and $dV/dt = 0.0$ curve) to another point on the same curve, in a precisely defined manner. Furthermore, the solution of Eq. (26) for r small but nonzero is close to the singular perturbation solution. The singular perturbation analysis leads to the conclusions that if the slow wave is generated by the interaction of an outward current with very slow kinetics and an inward current with faster kinetics, then the effect of an injected, steady depolarizing current will be to decrease the amplitude of the slow wave; on the other hand, a hyperpolarizing current will increase the amplitude of the slow wave. The experiments of Mathiew and Roberge[125] showed that the Aplysia R15 cell has a decreased slow wave when a depolarizing current is injected into the cell, and therefore, suggest that such a mechanism is operating in the Aplysia R15 cell. The outwardly moving ion, potassium, would carry the very slowly changing current and, according to the mathematical analysis, should

have activation kinetics. Therefore, the nerve cell membrane conductance should increase gradually as the burst continues, but should also gradually decrease as the interburst interval increases. Both predictions of this nerve model were experimentally verified by Junge and Stephens[126].

With this solution for the slow-wave component of the potential, one can write the general, global equation

$$\frac{dV}{dt} = \text{(action potential)} + \text{(slow wave)}, \tag{27}$$

and find the numerical solution for the action potentials with a computer by employing the well-established Hodgkin–Huxley equations[122]. Computer generated solutions, obtained in this manner, were presented in Refs. [127–128]; at this point, one might be tempted to consider that the model adequately describes the behavior of the pacemaker nerve cells. Two important aspects have been, however, omitted in this analysis. The first omission is the presence of a hysteresis phenomenon in the Hodgkin–Huxley equations, and was found by Hassard[129]; a periodic solution of the equations is unstable and, therefore, it is never seen in computer analyses. By employing sophisticated mathematical techniques, Hassard[129] and Rinzel[130] calculated the unstable solution which corresponds to a subcritical bifurcation, occurring at the threshold steady current. As a consequence of hysteresis, for a certain range of current values, there are also two stable solutions which exist simultaneously: a rest (or equilibrium) solution and an oscillatory (or limit cycle) solution. A stimulus can cause the system to move from one solution to the other, as indeed observed experimentally. The second aspect is the involvement of calcium ions which plays a major role in the pacemaker oscillation[131]. The model should therefore include a calcium-dependent potassium conductance; the corresponding equation describing the flow of calcium ions into the nerve cell is

$$\frac{dc}{dt} = k_i I_c - k_0 c, \tag{28}$$

and should be considered in conjunction with Eq. (26). In the above equation, c is the concentration of calcium ions in the immediate neighborhood of the nerve membrane, I_c is the ionic calcium "current" through the nerve membrane and k_i, k_0 are constants. One finds that the solution for c is[123]

$$c = G(V) = (w(V) + I)/(w(V) - g_0), \tag{29}$$

where $w(V) = g_i y(V)\,(1 - V)$. It is interesting that the equation for the c nullcline is similar to that of the V nullcline in the initial model (without calcium ions), and that the refined model [Eq. (29)], which incorporates the calcium-dependent potassium channel, exhibits similar properties to those of the initial model.

Traditional models of the neuron are essentially linear systems with a threshold which generates an output whenever the weighted sum of the inputs exceeds the threshold. The more recent models attempt to include additional processes such as nerve pulse interactions[132] and time-code to space-code translations on the axon, leading to the concept of a "multiplex" neuron[133]. The interactions of pulses travelling along a single fiber lead to velocity dispersion, while the propagation of pairs of pulses through a branching region leads to quantum pulse code transformations which involve the loss of entire pulses at axonal bifurcations. Even more complex interactions seem to occur between pulses on parallel fibers through which those pulses may form a *pulse assembly*[132]. The hy-

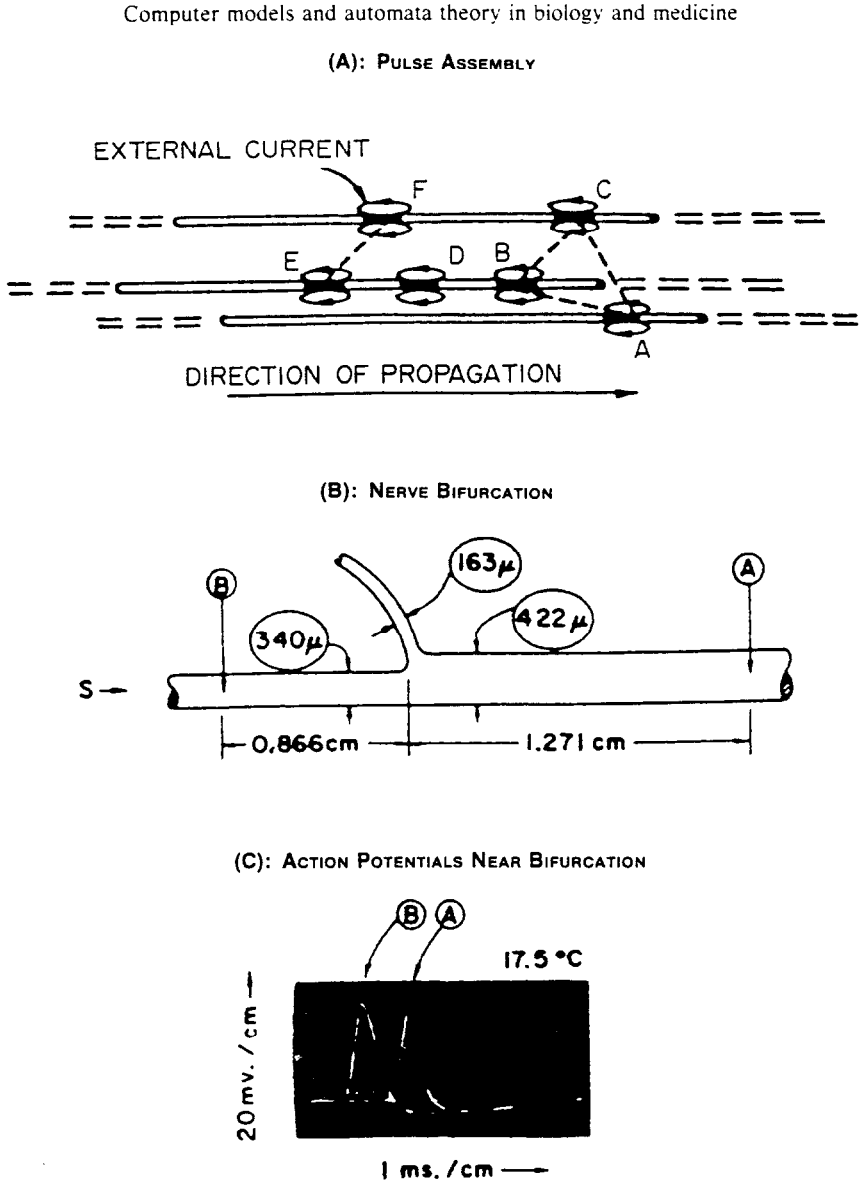

Fig. 28. Nerve pulse interactions: (A) structure of a "pulse assembly"; (B) representation of a nerve bifurcation; (C) action potentials affected by the bifurcation. (From Ref. [132]).

pothetical structure of such a pulse assembly is sketched in Fig. 28a, where the longitudinal pulse locking at a given time interval is acting between pulses B and D, and also between pulses D and E; in addition, a transverse pulse locking is acting between pulses A, B and C, and also between pulses E and F. Such a mechanism would provide a means for synchronizing the component pulses[132], as required by Waxman's "multiplex" neuron[133]. If considered in neural networks, the pulse assembly would give rise to very complex behavior, perhaps not unlike the observations of Scheibel and Scheibel[134] who reported that the appearance of nerve bundle complexes seemed closely time locked to the initial developments of discrete items of motor performance in cats. Bundles were formed during the process of maturation by rearrangements of the dendrite shafts in various parts of the nervous system, such as the brain stem reticular core, the cerebral cortex, the nucleus reticularis thalami and the ventral horn of the spinal cord.

7. COMPUTER SIMULATION AND MATHEMATICAL MODELS OF NEURAL NETWORKS

A. *Stochastic processes in neurophysiology*

From the early models of neural activity presented by Rashevsky[135, 136] and McCulloch and Pitts[2], the investigation of the properties of neural networks has developed into an area of intense research with special emphasis on stochastic aspects[137] and random nets[138]. Most modern concepts of neural networks are based on measurements of their electrical activity. The recorded potential as a function of time, $V(t)$, may be the result of the activity of a large number of neurons, as in the recording of an electroencephalogram (EEG). One of the interesting computational problems arising in connection with EEG interpretation is the power requirement and distribution in such a neural network[139]. Such analyses indicate that one needs to have as an input to network computation, the intra- and extracellular recordings of electrical activity for at least a pair of nerve cells; cellular neurophysiology is in fact based on measurements of electrical activity of single cells. Because of technical limitations, the observation of dynamic patterns of activity of the nervous system is difficult, at best; therefore, stochastic models of neural networks are to a large extent deductively based on indirect evidence. Several reviews on stochastic processes in neurophysiology have appeared[140–143] which indicate that various types of stochastic processes need to be considered in neurophysiology. One class of neurophysiological problems is concerned with the time series of action potentials, or the spike-train activity of neurons.

Repetitive action potentials, such as those in Fig. 29, are considered as a "point process", and one important problem is the generation of a continuous process (for example, nerve membrane noise) from point processes. For a membrane area which has N independent ionic channels, one can calculate the spectral densities of voltage $S_V(\omega)$ and current fluctuations $S_I(\omega)$. Furthermore, one can derive a multistate model in which there is only one conducting state and a number of other states, all of zero conductance. Such a model is in effect a gated channel with more than one gate per channel, as in the Hodgkin and Huxley model[122] for the K^+ conductance of the squid axon. The transition diagram of such a channel with 16 microstates is illustrated in Fig. 30 from Ref. [137]. If the activity of a channel is like a random telegraph wave, with only one conducting state, the opening and closing gate processes are independent stochastic processes; the activity of a channel can be considered as a sequence of short, random duration pulses.

A major theme in cellular neurophysiology is the coding of analog signals as a train of action potentials. This corresponds to a transformation between continuous and point processes. A one-dimensional model for the flicker noise was proposed by Holden and Rubis, as illustrated in Fig. 31. The model involves nearest-neighbor interactions between channels. When a channel opens, it leads to a pulse in the membrane current. The "spectrum" of the pulse train can be, therefore, calculated as the spectrum of the point process multiplied by the modulus squared of the Fourier transform of the pulses. A random process obtained by superposition of N point processes corresponding to channels will

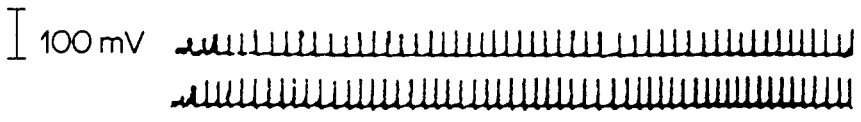

Fig. 29. Action potentials recorded simultaneously from two endogeneously active snail neurons. (From Ref. [120].)

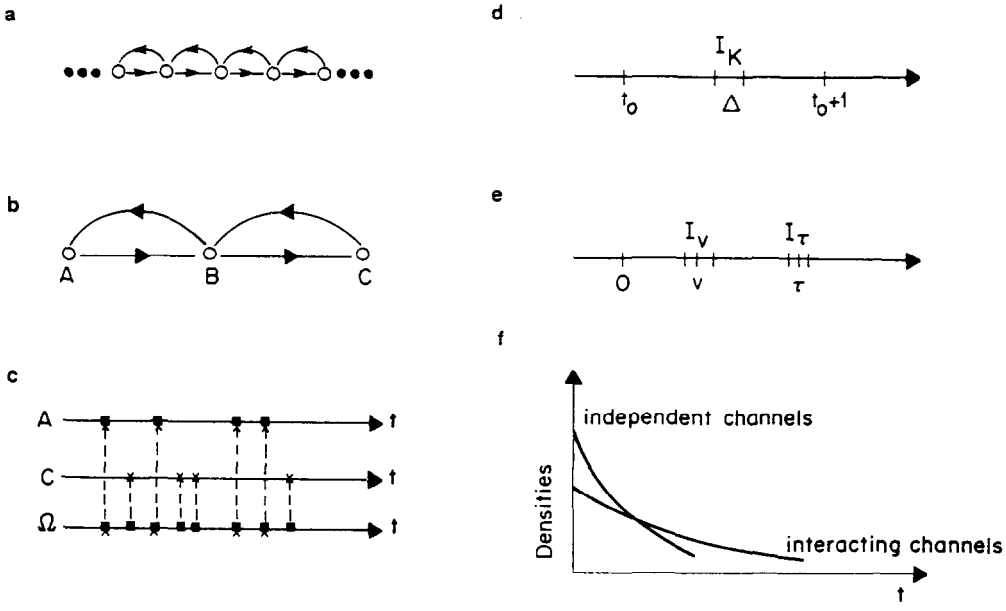

Fig. 30. Microstates for a Hodgkin–Huxley K^+-selective gated channel (according to Ref. [137]).

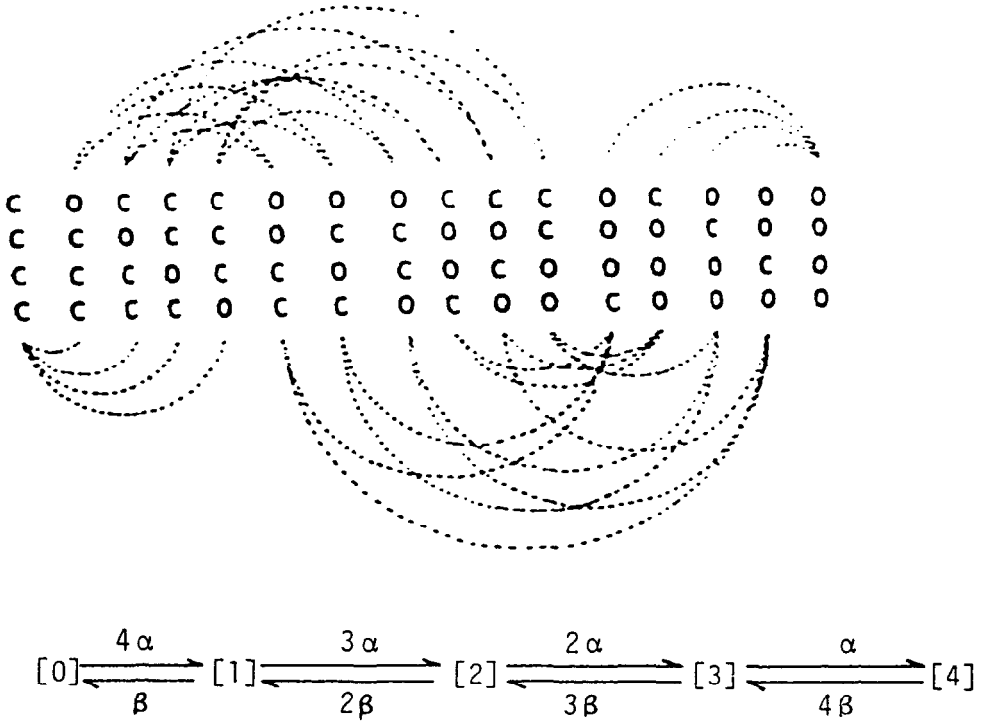

Fig. 31. One-dimensional model for the generation of flicker noise, including nearest-neighbor interactions (from Ref. [137]).

be characterized by an autocorrelation function

$$R(\tau) = NR_{ii}(\tau) + N(R_{i,i+1}(\tau) + R_{i+1,i}(\tau)), \tag{30}$$

with τ a real number and R_{ii} the autocorrelation function of the point process associated with each channel; $R_{i,i+1}$ and $R_{i+1,i}$ are the cross-correlation functions of a process with the right- and left-hand neighbors in the one-dimensional model in Fig. 31. The calculation of both the autocorrelation and cross-correlation functions of a network involve the use of a digital computer. It can be shown, however, analytically[137] that R is of the form

$$R(\tau) = c/\tau^{(1+\nu)} + d/\tau^{2(1+\nu)}, \tag{31}$$

where c and d are constants.

Using a Laplace transform, the power spectrum of the current can be calculated from R, and can be shown to have a dependence ω^{-a} on frequency, with a values between 0 and 1, for larger values of time[137]. Such a model accounts for the steady-state flicker noise component of the spectral density of fluctuations in ionic current of a neural network; the model also predicted the presence of retardation currents, that is, slowly inactivating currents with an anomalously low temperature dependence. Local accumulation, or depletion of ions, close to the nerve membrane surface may, however, explain the observation of such slow inactivation processes in a neural network.

B. *Reaction-diffusion networks*

The "traditional" models of the brain have considered the neuron as a simple logic element of the on-off switch type. Such models are often statistical in nature, and are only applicable to large neural networks. A review of such models was provided by Amari[144]. The opposite case of a single but physiologically realistic neuron was considered by Kirby and Conrad[145]. The latter is focusing on the biochemical processes that may be relevant to information processing by a neuron, or by a neural network. The microscopic features of such a network model are the enzymatic processes in the neuron, while the macroscopic properties are the membrane isopotentials. Kirby and Conrad[145] presented the results of computer simulations of an "enzymatic neuron", considered as a reaction-diffusion network which simulates the cyclic nucleotide system. Its implications for selectional learning and the relation to conventional "two-factor" models were also discussed. A fundamental property of the reaction-diffusion neuron is its "dual dynamics", related to the correspondence between its microscopic and macroscopic computation modes. The enzymatic neuron model is defined as an abstract membrane, tessellated into a finite number of compartments, $k = 1, 2, \ldots, n$. Each compartment k exists in a definite state u_k which may change in time. $u_k(t)$ is defined as the state of the compartment k at time t; the compartments are subject to external binary inputs $x_k(t)$ that may change their state. The neuron is also endowed with "excitases" which are enzyme-like elements that respond to the state and determine if the neuron fires. Furthermore, the enzymatic neuron has two basic properties:

1. Its internal state u is a linear transformation of the input signals at any given time t.
2. Each compartment containing an excitase has a certain threshold and a ceiling; if the state u_k exceeds the threshold but does not exceed the ceiling, then the entire neuron will fire.

Networks of enzymatic neurons were envisaged which differ in their excitase contents but share the threshold and ceiling values, as well as the contributions w_{ki} of inputs x_i

to the states u_k. Evolutionary learning algorithms[146] varied the excitase configurations and selected only those neurons which exhibited responses appropriately tuned to the environment coded by $x(t)$. An illustration of the enzymatic neuron and its tessellated membrane is reproduced in Fig. 32 from Ref. [145]. The reaction-diffusion network[147] is an oriented graph, the nodes of which contain the states of the network. Each node k has a set of neighbors $V(k)$. The transition rule of such a system is a local one, that is the trajectory of a node is influenced only by the external inputs to that node, and by the states of its neighbors. This rule has the form

$$\frac{du_k}{dt} = \sum_{j \in V(k)} d_{jk}(u_j - u_k) + R_k(u_k). \tag{32}$$

Each $u_k(t)$ is the state of the node, or compartment k. d_{jk} are the "transfer coefficients" of the reaction-diffusion network. A realization of this model was then proposed based on the hypothesis of cyclic 3',5'-monophosphate (cAMP). Cyclic AMP has been shown to be involved in a chain of reactions which affect the membrane potential of the neuron[148, 149]. The hypothetical postsynaptic actions of cyclic AMP are illustrated in Fig. 33 from Ref. [145]. Depolarization of the presynaptic membrane causes the neurotransmitter to be released in the synapse where it may bind to receptor molecules on the

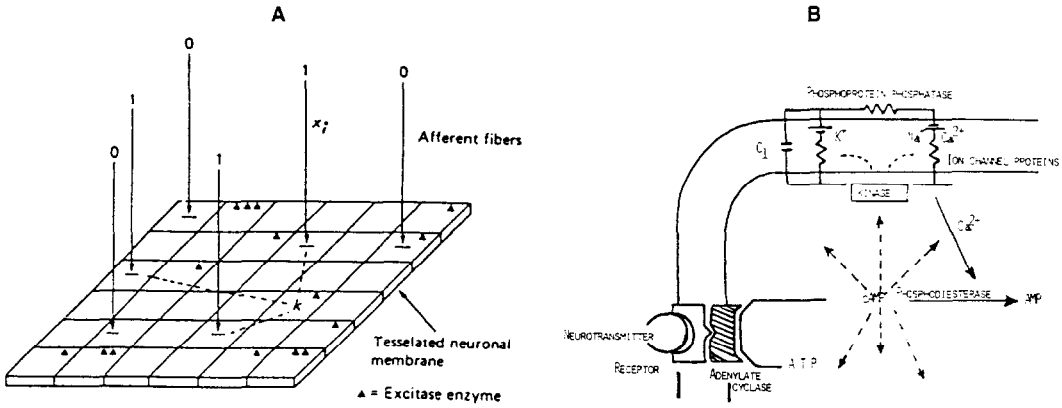

Fig. 32. The enzymatic neuron model[145]. A. Dotted lines indicate the influence of binary input signals x_i on an arbitrary compartment k; the strength of such an influence is given by the matrix coefficient w_{ki}, (according to Ref. [145]). B. Postsynaptic actions of cyclic AMP in the enzymatic neuron model.

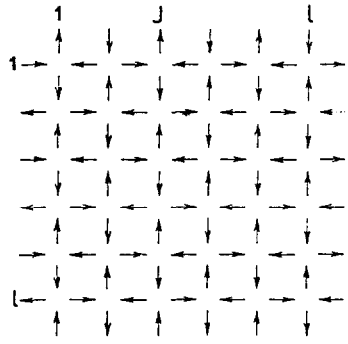

Fig. 33. Scheme of connections of a planar lattice for a special "random" network (from Ref.1 [178]). A module takes its inputs and outputs among its neighbors; the structure is completed at the boundaries by connecting symmetrical nodes. Directions of arrows have period 2 and yield the shortest feedback loops in the network.

postsynaptic surface. The occupied receptors are then considered to diffuse along the lipid bilayer surface to reach an adenylate cyclase enzyme which triggers the formation of cAMP from ATP. The input, therefore, triggers a sharp cAMP gradient which lasts for less than 10 msec. Subsequently, such a sharp gradient is dissipated as cAMP diffuses across the membrane into the cell. Phosphodiesterase brakes down the diffused cAMP inside the neuron, and one of these processes is Ca^{2+} activated. As the neuronal membrane is depolarized, there is a sudden influx of Ca^{2+} ions which activates a phosphodiesterase that breaks down the cyclic nucleotide. The effect of neuron firing on its state was taken to be

$$F(t) = 1.0 \Rightarrow u(t + dt) = hu(t), \qquad \text{with } 0 < h < 1,$$

and F being the binary firing function. Thus, in this neuronal model, the state variable is the cAMP concentration. By assumming Michaelis–Menten kinetics for the phosphodiesterase activity, the reaction term becomes

$$R_k(u_k) = A_k - u_k P/(u_k + K), \tag{33}$$

where P is the maximum rate of cAMP hydrolysis, A_k is the basal rate of cAMP production and K is the saturation constant. The reaction-diffusion network associated with the enzymatic neuron is subject to the basic equations [145]

$$\frac{du_k(t)}{dt} = A_k - \frac{P_k u_k}{(u_k(t) + K)} + \sum_{j=0}^{n} d_{jk}(u_j(t) - u_k(t)), \tag{34}$$

$$u_k(t + dt) = u_k(t)\,((h - 1)F(t) + 1) + Ix_k(t), \tag{35}$$

$$F(t) = \max H(u_k(t)z_k - \theta_k). \tag{36}$$

Equation (34) is summed over all "compartment", or synapse, interactions. In Eq. (36), H is the threshold Heaviside function ($H = 1$ for positive values of the argument and 0 elsewhere). Several computer simulations of this reaction-diffusion network were tested using both CSMP and FORTRAN programs. A general simulation used a patch of membrane tessellated into a 6×6 array of compartments, as shown in Fig. 32. In over 100 simulations of the enzymatic neuron, the model exhibited one general type of behavior: the frequency of firing is directly related to the distance between the kinases and those compartments with high cyclase activity. An interesting property of this reaction-diffusion network (the "enzymatic neuron") is that local disturbances are rapidly dissipated. As a result, autonomous firing of the neuron is observed in the absence of external signals when kinase enzymes are present in a particular compartment which has a permanently "excited" level of adenylate cyclase activity (which causes a constant, local production of cAMP). Equations (34)–(36) do not provide, however, a description of the information-processing capabilities of the reaction-diffusion network. To complete the reaction-diffusion network model, Kampfner and Conrad[146] proposed *selectional algorithms* which result from a competition between similar networks in performing a specified task. The only difference allowed between networks is in their excitase configuration z; only those networks whose configuration produces the most appropriate response function will survive. The set of all inputs to the networks is a space X, which is the set of all maps x: $T \to \{0, 1\}^n$, where T is the time continuum. The output space Y of the neuron is defined as the set of all maps F: $T \to \{0, 1\}$, and the reaction-diffusion network in an excitase configuration z is said "to compute a map", $R(z)$: $X \to Y$. Clearly, such a definition is very similar to that of an automaton, as discussed in Sec. 10. This is not surprising since

neural networks were also shown to be represented by metabolic-replication $[(M, R)]$ systems[150], which have corresponding automata representations[151–154]. The set of such computations of the reaction-diffusion network Ω will range over all n-compartment reaction-diffusion neurons that are subject to Eqs. (34)–(36). The computational power of such neural networks is probably less than that of an universal Turing machine since the latter can compute any finite state automaton[155], such as the enzymatic neuron. However, Kirby and Conrad proposed that the reaction-diffusion neurons should have a broader class of inputs x: $T \rightarrow \{0, 1\}^n$ than a discrete, structureless set, so that continuous dynamics can perform more complex computations than a universal Turing machine. With the introduction of such continuous dynamics, the reaction-diffusion neuron becomes somewhat similar to Rashevsky's "two-factor system"[156]. The states of two-factor systems are determined by pairs of real numbers (q_1, q_2) which evolve according to the equations

$$\frac{dq_i}{dt} = b_i I - \lambda_i q_i, \qquad i = 1, 2, \tag{37}$$

as discussed in Ref. [157]. The variable I in Eq. (37) is an external "forcing" parameter acting on the system such that the system "fires" when $q_1 > \theta q_2$, with θ being a threshold. By setting $dq_2/dt = 0$, the two-factor model acts like the enzymatic neuron: q_1 would be the cAMP, λ_1 would represent a phosphodiesterase and q_2 would be the inverse of the protein kinase concentration. The distinctive feature of the enzymatic neuron is its ability to carry out many local, microscopic computations prior to undergoing a global (macroscopic) state change. Therefore, the reaction-diffusion neuron is primarily a model of transient processes which are extremely sensitive to input timing. If nucleotide levels are near threshold, the inputs into an autonomously firing neuron are essentially ignored but they will reset the firing rhythm if they arrive when compartments have low concentrations of nucleotides. Furthermore, the continuous-time version of the neuron in the reaction-diffusion network allows for additional computational power; the class of computations generated by a reaction-diffusion neuron is associated with performance in selectional learning algorithms. The most distinct feature of the reaction-diffusion model is that the mapping, or coding, from microscopic inputs to macroscopic outputs occurs at the microscopic level via selective, continuous processes that are being controlled, however, by a discrete parameter—the kinase configuration. The broader meaning of this interesting model of the neuron is that the medium of computation is highly significant; this biological computation style was considered to be quite distinct from that of artificial intelligence, in the sense of being more powerful than finite-state logic devices in performing higher level tasks (also more efficient and adaptable). The future study of neural networks made of enzymatic neurons will be undoubtedly a challenging task for computer simulations.

C. *Cycle structure, Boolean mappings and self-organization of binary random networks*

Random switching nets are being extensively used as models of biological systems. Perhaps, the most important example is that of neural net models of the central nervous system which were developed from formal, McCulloch and Pitts[136] "neurons". The linear case was originally discussed by Pitts[158], and a nonlinear, stochastic extension was analyzed by Landahl, McCulloch and Pitts[159]. More recently, Kauffman[160–164] has proposed binary random nets as models of the cell genome. Reviews of the formal, neural networks were presented by Griffith[165], Arbib[166], and Szentagothai and Arbib[167]. Arbib[168] showed that a network of on-off formal neurons can always be

constructed to simulate any given finite-state sequential machine, or automaton. Even the randomly connected networks of formal neurons are sufficiently complex so that their study is "an empirical exploration using computer models" (that is, by computer simulation, cf. Muir and Warner[169], Harth *et al.*[170], Amari[144]). Studies of actual neural systems have, however, focused on simpler networks which exhibit regularity, or symmetry. Examples are studies of cerebellum and retina where structural regularities were discovered. Another example is that of a one-dimensional chain modelling the propagation of the alpha rhythm[171]. In such a model, the inhibition strength is a function of the distance between neurons. Similarly, in a discrete, planar model of lateral inhibition, Hartline and Ratcliff[172] assummed that the inhibition is distance dependent. Sherlock[173] noted that the analytical limitations in the study of random switching networks are the major hindrance in obtaining biologically relevant solutions. However, in certain cases, such as the completely random switching net, a complete mathematical analysis was reported. Other complete studies include those of neural networks as reviewed by Rashevsky[135], von Foerster[174] and Stubbs[175], as well as the propagation of excitation in the myocardium[176].

Kauffman[162] and Walker and Gelfand[177] proved that completely random Boolean networks with only two or three inputs per module were much more stable than networks made of modules with larger numbers of inputs per module.

A random Boolean network is usually defined as a set of interconnected N elements, or modules. Each module has binary response (0 or 1) to inputs, and at any discrete instant of time t the net is in one of 2^N distinct states. The net operates on a discrete time scale such that its state at a time t determines precisely its state at time $(t + 1)$. The completely random net is in a state which is selected as equally probable from its 2^N possible states. Formally, the net can be defined[169] as a pair (X, ϕ), where X is a set and ϕ: $X \times X \to R$, is a function from the product $X \times X$ to the set of real numbers R. Each element of X is also called a node of the net and ϕ is the connection function of the net. A state of N is a function ψ: $X \to A \subset R$. $\psi(x)$, with $x \in X$, is called the *activity* of x, and Ω denotes the set of states of the net.

If X is a set of neurons and ϕ (x, x') is chosen as a measure of how strongly is the neuron x' connected with neuron x, then the activity set of formal, McCulloch–Pitts neurons is $A = \{0, 1\}$. Any net can be alternatively described in terms of its transition matrix[178]: if the net states are placed in one-to-one correspondence with integers ranging from 1 to 2^N, one can form a $2^N \times 2^N$ matrix T whose elements are

$$T_{ij} = \begin{cases} 1 & \text{if state } i \text{ follows state } j, \\ 0 & \text{otherwise.} \end{cases}$$

This transition matrix T can be also viewed as a transformation from the set into itself, T: $\Omega \to \Omega$.

Computer simulations of such random Boolean nets are aimed at determining their "stability" and behavioral pattern. More specifically, since the number of net states is finite, and the state transition is deterministic, after starting the net in an initial state it will eventually go through a sequence of states and reach again the initial state; such a sequence of net states is called a *cycle*. The number of distinct states in the cycle is called the cycle length. Prior to cycling one has a "run-in" sequence. Gelfand[178] summarized in a recent review a series of basic properties of completely random Boolean nets:

1. the expected number of transient states of the net is of the order of 2^N;
2. the expected number of cyclic states is of the order $2^{N/2}$;
3. the expected number of cycles is of the order N;
4. the probability that any particular state is cyclic is of the order $2^{-N/2}$;

5. the expected number of cycles of length r converges to r^{-1};
6. the expected number of states on cycles of length r converges to 1;
7. the expected cycle length is of the order $(N^{-1})\,2^{N/2}$.

Note that each module of a network is an automaton which computes its internal state with a Boolean function of two variables—its input signals.

An alternative matrix approach to random Boolean networks was proposed by Fogelman-Soulié *et al.*[179] who considered a network specified by the incidence matrix A with N columns and lines. The element A_{ij} of A is 1.0 if module i has an input from module j and is zero otherwise. An element F_i of the Boolean function matrix specifies the number of the Boolean function which is used to compute the output of module i (see Table I in Ref. [179], p. 718). Starting with an initial condition matrix X_0, which describes the states of all modules at time $t = 0$, the matrices $X_1, X_2, \ldots, X_n$, representing the state of the network at time $1, 2, \ldots, n$, can be computed using the Boolean functions. When the network enters a limit cycle, after a period T, one has $X_{m+T} = X_m$. Kauffman[162] showed that random nets (with matrices A, F and X_0 set at random) with connectivity $k = 2$ evolve toward limit cycles in relatively short periods. During the limit cycles there are some modules which change state at least once; these are called "oscillating" modules. An aggregate of closely connected oscillating modules was called a *subnet* by Atlan *et al.*[180]. In the particular case of the network of a plane lattice with connections between nearest neighbors such as the one shown illustrated in Fig. 33, the system evolves under Boolean mappings toward an organization of independent subnets where modules belonging to different subnets behave as if they had no functional modules. The network undergoes a partial loss of its random character. In the initial state, the network is random and its internal connections are also random. Once the network reaches its limit cycle, the oscillation is no longer random and the network has become self-organized. A strong local correlation is present: a module has a high probability to oscillate if its neighbors are oscillating. Such subnet organization is relatively stable against perturbations, including the application of external noise to one module[180], or even "amputation". The organization into subnets exists, in general, for random connection networks and not only for planar lattices. A classification of the Boolean mappings according to their effect on the dynamical properties of random networks is possible[179, 181] and it shows some interesting correlations with the cycle structure of homogeneous networks. For example, Boolean mappings of type 6 (XOR) or 9 (equivalence) (see Table 3) lead to a period of $2^n - 1$ time units in a homogeneous network if the gates are appropriately selected as feedback inputs. The systems thus defined are pseudorandom sequence generators[179]. These networks have very different behavior from Kauffman networks even though they are built with a random distribution of mappings and connections; there exists no stable component and the period of the limit cycle increases proportionally with 2^N. One-input transfer mappings, on the other hand, lead to a majority of elements oscillating during the limit cycles, and the period of the network is the least common multiple of the periods of the subnetworks[179]. Yet another type of mappings provide an algorithm for obtaining the maximum period of a homogeneous network operating either with AND or OR; such reducing mappings are allowing for a decomposition of the network into fully connected subnetworks. The dynamics of the network can be represented in this case in matrix form

$$X_t = AX_{t-1}, \text{ or } X_t = A^t X_0,$$

where X_0 is the matrix of the initial conditions. The periods of such networks are related to the number and size of loops in the network: according to Thomas[181], the complexity of the state transition graphs depends on the complexity of the feedback loops in the network. For inhomogeneous networks a more involved three-step algorithm is required

Table 3. Boolean functions numbered 0, . . . , 15 according to the decimal representation of their table of values

2 \ 1	0	1
0	0	0
1	0	0

0 Contradiction

2 \ 1	0	1
0	1	0
1	0	0

1 NOR

2 \ 1	0	1
0	0	0
1	1	0

2 $\overline{\Rightarrow}$

2 \ 1	0	1
0	1	0
1	1	0

3 $\bar{t}_2$

2 \ 1	0	1
0	0	1
1	0	0

4 $\overline{\Leftarrow}$

2 \ 1	0	1
0	1	1
1	0	0

5 $\bar{t}_1$

2 \ 1	0	1
0	0	1
1	1	0

6 XOR

2 \ 1	0	1
0	1	1
1	1	0

7 NAND

2 \ 1	0	1
0	0	0
1	0	1

8 AND

2 \ 1	0	1
0	1	0
1	0	1

9 Equivalence

2 \ 1	0	1
0	0	1
1	1	1

10 t_1

2 \ 1	0	1
0	1	0
1	1	1

11 $\Leftarrow$

2 \ 1	0	1
0	0	1
1	0	1

12 t_2

2 \ 1	0	1
0	1	1
1	0	1

13 $\Rightarrow$

2 \ 1	0	1
0	0	1
1	1	1

14 OR

2 \ 1	0	1
0	1	1
1	1	1

15 Tautology

Table $\begin{pmatrix} d & b \\ c & a \end{pmatrix}$ is numbered $a(2)^3 + b(2)^2 + c(2) + d$.

to follow the effects of Boolean mappings[179]. The first step is to decompose the network into fully connected subnetworks; then a search for the stable components is carried out by analyzing connected loops for consistency, namely, those whose connection nodes are in the same state. The second step was to search for the input frontier of the stable component. Such a frontier is made of stable elements who may have transfer or reducing functions as Boolean mappings. This step defines the different oscillating subnets. Finally, the dynamics of the oscillating subnets thus defined are directly investigated. Because the subnets are smaller the analysis is substantially easier. Such a Boolean mapping analysis shows also that short periods are essentially due to the presence of nodes with reducing or transfer mappings that allow the appearance of frontiers between oscillating and stable components[179].

D. *Connectivity, symmetry and dynamics of random nets*

Connectivity of random nets has been defined in a number of different ways, reflecting the different approaches to network behavior. Shimbel[182] and Rapoport[183] defined the output connectivity as the number of connections sent out by each individual node or module in the network. They applied this concept to the study of neural networks. Solomonoff and Rapoport[184] defined the *total* network connectivity as the fraction of nodes that can be reached in one or more steps from a given node. Gardner and Ashby[185] showed that the stability of a network is directly related to the proportion of nodes to which any one node is directly connected (the "*connectance*" of the network). Another measure of connectivity is the expected pathlength, defined as the mean number of steps

between any two nodes of a network. The interrelations between the different types of connectivity were investigated by Stubbs and Good[186]. They defined an $N \times N$ connectivity matrix M for a network of N nodes. Their preferred definition of connectivity for a node I of the network was the proportion of nodes to which I is connected. The network connectivity γ was then defined as the expected value of this proportion with respect to a probability measure defined on the smallest field containing all subsets of a set of $N \times N$ matrices whose row sums are equal to a constant a. Computer simulations were then employed to explore the output connectivity of the neurons of the brain[186]. The network connectivity defined as in Ref. [186] was computed as a function of output connectivity for up to 100 000 nodes. The simulated network connectivity (Table I in Ref. [186]) decreased with increasing number of nodes for an output connectivity of 1.0 but increased for output connectivities up to about 4. For output connectivities higher than about 5, the network connectivity was close to 1.0, independently of the number of nodes. Computer simulation also provided the values of the expected pathlength and radius ([187], p. 31) as a function of the output connectivity up to 1000 (for numbers of nodes up to $N = 10\,000$). For $a > 1$, the expected pathlength decreased with increasing output connectivity (Table II on p. 301 in Ref. [186]). The relation between the expected pathlength L and the connectance a/N is given by Theorem 2 in Ref. [186], p. 299:

$$\text{If} \quad a/N \to c > 0 \quad \text{when} \quad N \to \infty, \quad \text{then} \quad \gamma > 1 \quad \text{and} \quad L \to 1 + \exp(-c).$$

This theorem was verified also by numerical computation (in a computer simulation) up to $N = 1000$. If one models the human brain by a randomly connected network the number of nodes, the neurons, is of the order of 10^{10}[188]. Hunt and Stubbs[189] determined experimentally that the average number of steps between two neurons is 15. With this value, the output connectivity of the brain for a net radius of 15 was calculated to be ~10.5[186]. With this value of the output connectivity, the total connectivity of the brain was slightly less than 0.999999; of the 10^{10} neurons in the human brain only some 300 000 neurons would not be reached. Stubbs and Good[186] suggested that the value of 10.5 for the output connectivity may mean that neural connectivity may be genetically specified.

A major concern of such direct connectivity studies of random nets is the local and global stability of the nets[160–164, 190–195], but long-range indirect connections may also be important[196–197]. Furthermore, in real systems, regularities or symmetries do occur. As in the case of Boolean mappings discussed above, such symmetries are directly determining the dynamics of the networks. Spatial symmetries of differentiable neural models were amongst the cases investigated[198, 199], as were the bifurcation phenomena in nonlinear dynamics[200]. A group-theoretical approach to the symmetries of net dynamics was recently proposed by Muir and Warner[201]. The existence of a symmetry group for a network was shown to permit "motions" in which groups of neurons behave collectively[201]. The possibility of spontaneous symmetry breaking for homogeneous networks was also considered to arise as a result of external perturbations and may induce complex dynamics in spite of the simplicity of homogeneous networks. Such models could exhibit short-term memory but may be incapable of long-term memory[201, 202], for which a stable cyclic pattern of activity was proposed.

Another aspect of connectivity, which is of interest but is little investigated in the study of neural networks, is the strength of a connection between neurons; the probability for triggering of a neuron is related to its connections to other neurons. Muir[203] proposed to attach to every pair of neurons a real number representing the strength of their connection, and argued that a neural net could be treated as a group quotient, lattice-valued relation. A lattice-valued relation (lvr) on a set A (such as the set of neurons) was de-

fined[203] as a function λ: $A \times A \to L$, with L being a lattice. If $L = I = \{0, 1\}$, with the partial ordering $\geq$ one obtains a fuzzy relation on A[204]. The strength of connections between neurons could be represented for a neural network N as an lvr, Γ: $N \times N \to L$. For $L = I$, this lvr can represent a neural network with stochastic behavior (firing pattern). Further aspects of the lvr theory concerning the hierarchy of biological organization and quantitation of the strength of the relations between the components of a biological organism were recently discussed by Warner[205]. The lvrs may be useful not only in the study of neural networks and hormonal control but also in the analysis of the genetic nets discussed in Sec. 9. For numerical lvrs the question of computing the strength of connections for specific classes of neural networks, or random networks, may also be approached with a digital computer but has not been addressed so far.

E. *N-ary random nets*

Binary switching nets have been useful as simplified models of complex biological systems. Walker[206] recently proposed a generalization of the Kauffman binary net[160] to n-ary random nets. The n-ary random network is made of N logic elements which have exactly k inputs. The output of an element can be arbitrarily branched and can carry at a given time one of P states. Similarly, each input can carry one of P states at a given instant. The output state of an element in the net of time $(t + 1)$ is determined by a function of the state of its inputs at time t. Furthermore, all inputs in the net are interconnected. Once outputs are assigned to inputs and functions are assigned to elements, the assignments are kept fixed while the net behavior is observed. The net behavior is generated in a stepwise manner from the net state and a sequence of transient states is produced, followed by a sequence which repeats itself. The two parts are, respectively, called "run-in" and "cycle" sequence, as in the case of binary nets. The length of a sequence is defined as the number of distinct net states in the sequence. Walker[206] employed computer simulation to examine net behavior over a range of values of N, k and P. Values of N ranged from 5 to 250, and one hundred nets with different connections, etc., were simulated for each N, K and P combination; in a special case, 1000 nets were monitored to study the net behavior. Cycles and run-in lengths were recorded from such computer simulations. An example of such a computation is given in Fig. 34, where the median cycle length is plotted as a function of the log of the net size, log N. For $k = 2$ and $P = 2$ the median cycle lengths were somewhat different from those calculated by Kauffman for the binary net[160]. The genetic control system can be considered, for example, as a binary net[160]; the calculations for n-ary nets showed that small alphabet nets are relatively more attractive as behavioral complexity increases, but the higher-order nets have also higher output variety which may provide a selection advantage even though the alphabet size is increased.

Although such models are well suited for size-complexity studies of neural networks, their applications seem to be primarily concerned with genetic control systems, or genetic networks. The latter are more complex than the simple, random net behavior, as discussed in Sec. 9.

F. *Stochastic dynamical systems*

Questions related to the behavior of neural networks[207] and the development of the nervous system[208] can also be approached by stochastic dynamical models, that is, by employing random difference and differential equations. Stochastic dynamical systems (SDS) can also be used to describe some of the nonequilibrium cooperative phenomena in open systems. Approximations of discrete stochastic models by diffusion processes[209, 210] also lead to stochastic differential equations.

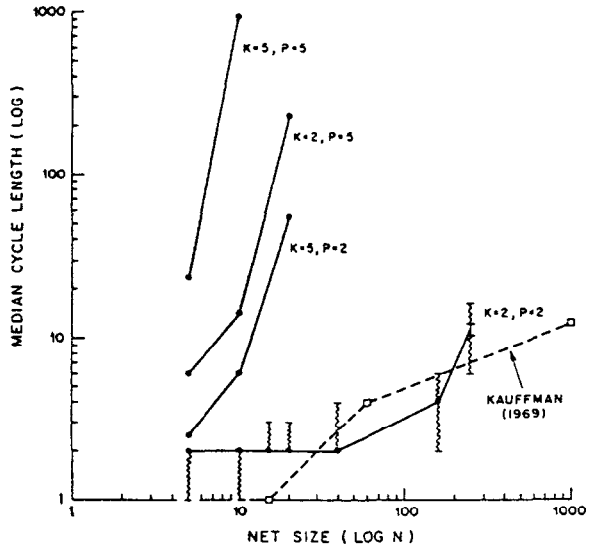

Fig. 34. Median cycle length (in log scale) as a function of the net size (log N) for selected values of the input connectance K, and of the output variety P. Dashed line shows the data from Kauffman[161] for comparison. Straight line and full circles from Ref. [206].

The qualitative behavior of SDS without solving the equations has been the subject of studies by Friedman[211], Bhattacharya[212], Hasminskii[213], Kesten and Ogura[214], and Kliemann[215]. The stability of SDS was treated by Kliemann and Rumchin[216], Arnold and Kliemann[217], and Arnold *et al.*[218]. The transient behavior of SDS was recently discussed by Kliemann[215]. The qualitative behavior of nonlinear stochastic systems with colored (Markovian) noise was investigated and applications were developed in terms of diagrams for the state-space, transients and stationary solutions[215], although the examples were noncomputable with a digital computer.

The basic approach in previous qualitative theories of SDS was to find an appropriate Lyapunov function, just as in the case of deterministic systems. Kliemann's approach[215] was to use directly the systems and noise dynamics because this is more readily applicable to transient processes and stationarity in degenerate systems such as the stochastic pair (x, η), represented by the stochastic differentials

$$\begin{cases} \mathrm{d}x = f(x, \eta)\,\mathrm{d}t, \\ \mathrm{d}\eta = a(\eta)\,\mathrm{d}t + A(\eta)\,\mathrm{d}W_t, \end{cases} \tag{38}$$

with η being a nondegenerate diffusion process in R'''. This qualitative SDS approach, although unaided by computer, is a potentially powerful tool for the investigation of reaction-diffusion networks as models of neural systems such as the brain, and could be of value to neurophysiologists for modelling the transient behavior of neural systems.

The SDS theory is considerably more general and complex than the discrete, random Boolean network theory. Its relationship to the reaction-diffusion network model[145] discussed in Sec. 7B would also be of interest for further evaluation of the enzymatic neuron theory.

8. COMPUTER SIMULATION AND COMPUTABILITY OF BIOLOGICAL SYSTEMS

The ability to simulate a biological organism by employing a computer is related to the ability of the computer to calculate the behavior of such a dynamical system, or the

"computability" of the system.* However, the two questions of computability and simulation are not equivalent. Since the question of computability can be given a precise answer in terms of recursive functions, automata theory† and dynamical systems, it will be appropriate to consider it first. The more elusive question of adequate simulation of biological systems by a computer will be then addressed and a possible connection between the two answers given will be considered.

A. *Are biological systems recursively computable?*

An answer to this question was recently given by Conrad and Rössler[219] who showed that although a system can be computation universal it may not be effectively programmable if its translator has "chaotic" dynamics; such chaotic dynamics were encountered in certain models of biomolecular reaction kinetics[220]. At this point, let us introduce the concepts of recursive function, recursive computer, computation and program in order to be able to formally discuss recursive computability of a system, be it biological or nonbiological.

A function is called *recursive* if there is an effective procedure, or computation, for calculating it (p. 211 in Ref. [155]).

A *recursive computer* C[155] on the alphabet Y is a partial recursive function f_C: $Y_b^* \to Y_b^*$. $Q = Y_b^*$ is called the set of complete states of C. (The qualifier "partial" refers to the fact that the recursive function may not be defined for all its values.) If at an instant t the computer has n registers, the jth register containing the word Y_j, one can say that the *complete state* of the computer is the word $Y_1 b \cdots b Y_n$ of Q; also if the state of the computer C is $\xi \in Q$ at time t, the state of C will be $f_C(\xi)$ at time $(t + 1)$, and may be therefore undefined, although not necessarily so. The computer is in a halting state $\xi \in Q$ when $f_C(\xi) = \xi$.

A *computation* by the computer C[155] is defined as any finite sequence $\xi_0, \xi_1, \xi_2, \xi_3, \ldots, \xi_n$ of elements of Q such that $\xi_{j+1} = f_C(\xi_j)$ for any $j < n$ and $j \geq 0$; $\xi_n = f_C(\xi_n)$ and $f_C^*(\xi)$ is defined as the end result of a computation starting with $\xi \in Q$. If f_C is total, the end result of a computation is unique, and is always defined.

A program P for the computer C is defined[155] as a pair of mappings α: $(X^*)''' \to Q$, β: $Q \to (X^*)''$ which are partial recursive on the union set $(X \cup Y)_b$. α is used to read in the data and appropriate instructions into memory, which will continue until the computation stops; then β is used to "read" the results from the computer registers. The partial recursive function f_C^* defining the computer is related to α, β, and a partial function C_P: $(X^*)''' \to (X^*)''$, which is said to be "computed by C with the program P". This relationship is given by the following commutative diagram, which also defines C_P:

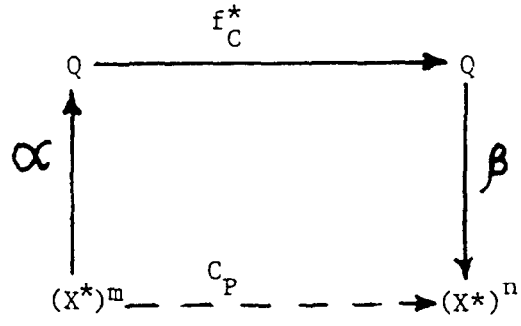

(39a)

That is, $C_P = \alpha \circ f_C^* \circ \beta$.

---

* The contributions made to this section by an anonymous referee are gratefully acknowledged.

† Please also refer to Sec. 10 where basic automata theory concepts are briefly reviewed.

The question at the beginning of this section is, therefore, if the function $C_P = \alpha \circ f_C^* \circ \beta$ is sufficient to mimic or simulate the dynamics of any biological system. The argument introduced by Conrad and Rössler[219] is that the read-in function should be a translator with "chaos" in order to be able to simulate certain biomolecular reactions in a biological system. Thus, suppose that one programs a digital computer in the usual sense; this can be represented by the commutative diagram (39a) above, in which Q is the state set, or "state space", of the computer and with the functions α and β being used by the programmer to implement the function C_P. The idea of the Conrad–Rössler paper[219] was to interpose a "chaotic translator" between the programmer and the computer; such a chaotic translator can be constructed, or envisioned, as follows. Let g be a map $X \to R^3$ (with R^3 being the three-dimensional Euclidean space), and let h: $R^3 \to X$ be a (left) inverse of g, that is, $h \circ g = 1_X$, with 1_X being the identity map $X \to X$ and "$\circ$" the usual map composition law. Furthermore, let us consider a dynamical flow induced by the Lorenz equations Φ_{τ_c}: $R^3 \to R^3$, that is, with $\Phi_{\tau_c}(x, y, z)$ being defined as the point (x', y', z') to which the system flows after the interval of time τ_c if started at the point (x, y, z). When coupled to the programming diagram (39a) such a dynamical flow induces the following representation:

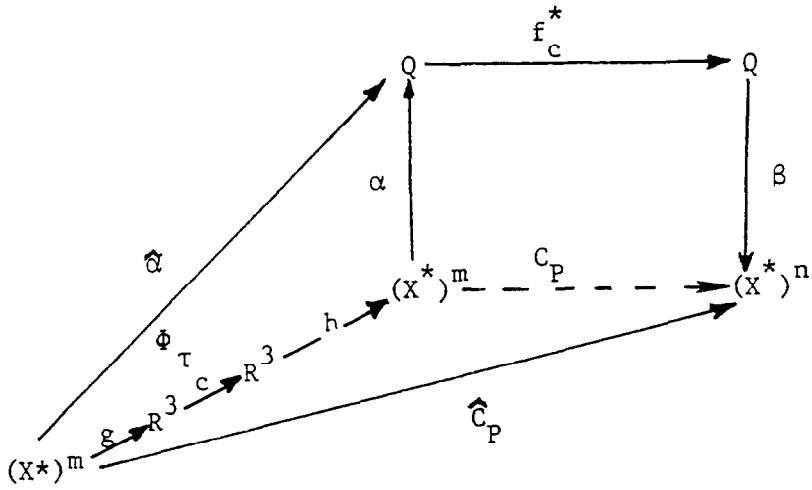

(39b)

Because arbitrarily small differences will produce permanently distinct aperiodic trajectories, there is no single partial recursive function f_C^* that will allow the computer to calculate the encoding function $\hat{\alpha}$ if $\tau_c > Q \mid \Delta_t$. Therefore, a system that does possess a dynamical flow which is induced by the Lorenz equations would not be recursively computable.

B. *Can one simulate all biological systems with computers?*

This important question of universal computation of biological systems can be answered uniquely only by giving an appropriate definition of the concept of "simulation". If one defines formally "computer simulation" to be restricted to (partial) recursive computation of biological dynamics by a digital computer, then it would follow from Sec. 8A that such a simulation is not generally possible for biological systems. However, if one employs dynamical analogy[221] to define simulation, then the computer prospects for simulation may appear somewhat brighter since one can now define a class of systems S' that are analogous to a computer Q, as represented by the commutative diagram

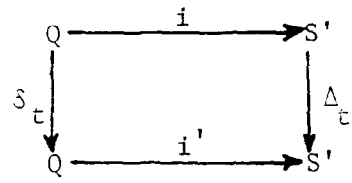

(40)

by selecting i and i' to be isomorphisms. If the computer is digital, then $\delta_t = f_C^*$ is the partial recursive function defined in Sec. 8A that will allow one to compute, or "simulate", the behavior of a certain class of dynamical systems; such recursively computable systems may be certain components or subsystems of a biological system that do not incorporate any chaotic behavior. Furthermore, if one were to lift the restriction that Q be a discrete set, and define instead a new kind of "computer" with a topological state space (incorporating chaos), then a dynamic analogy can be considered between such a novel "topological computer" and an intact biological system. This type of topological computer may include, for example, topological automata that have topological semigroups[222] for state spaces instead of algebraic semigroups as the conventional automata or sequential machines[155]. The *analogy* will be replaced in this case by *conjugacy* (p. 508 in Ref. [223]) as a form of similarity between dynamical systems. A topological computer would thus be endowed with a topological semigroup and could simulate a biological system if its computation function f_c was topologically conjugate[222] to the transition function f_2 of the biological system ($f_c \tilde{\phi}\ f_2$), that is, $\phi f_2(x) = f_c(\phi(x))$, $x \in T$, with ϕ being a homeomorphism

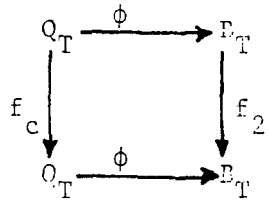

(41)

Topological conjugacy ensures that if $f_2 \tilde{\phi}\ f_c$ for some given parameter set, then the functions f_2 and f_c have equivalent dynamical behavior over that parameter set. The general case of state spaces with both algebraic and topological structure was also considered by means of *adjointness of functors* defining dynamical equivalences between systems possessing such complex state spaces[224].

CONJECTURE. There is a universal simulation of biological systems by an algebraic-topological "computer," by means of a pair of adjoint functors which defines the dynamical equivalence of the computer with any selected biological system.

9. COMPUTER SIMULATIONS AND ALGEBRA OF GENETIC NETS

A. *Binary genetic nets*

Metabolic stability and epigenesis in genetic systems were modelled by Kauffman with formal "binary genes"[160]. Such models are particularly applicable to bacterial genetic control systems[225]. Kauffman found that large genetic nets of binary elements which have very large numbers of possible states, exhibit remarkably ordered and stable behavior without requiring any special structural organization. Such "genetic nets" enter rapidly their stable limit cycles in their state space and have very few different limit cycles.

A Kauffman (genetic) net of size N and connectivity k consists of N interconnected binary elements (Fig. 35), each having k inputs and only one output. The elements of a Kauffman net were described[160] as "formal genes". The inputs and outputs of each

formal gene take only one of the two possible values denoted by 0 (zero) and 1, at any instant in time t. The interconnection of formal genes is random, each input is connected to one and only one output, and each input has an equal chance of being connected to any output. Therefore, as in the case of neural binary networks, the input-output relation of each formal gene is defined by one of 2^{2^k} possible Boolean mappings of k binary variables. Furthermore, the assignment of Boolean mappings is such that each element in the net has an equal chance of being assigned any of the 2^{2^k} Boolean mappings.

The state of a Kauffman net is specified at any instant in time by the states of the N element outputs, which means that this genetic net has 2^N distinct states. In terms of automata theory (see Sec. 10) the Kauffman net is a deterministic, "autonomous", finite-state sequential machine; the machine is autonomous in the sense that there are no external inputs to the genetic net[173]. Although the Kauffman net is random, its state transitions are not probabilistic events. Kauffman[160] also imposed the restriction that the network is in some well-defined state at time t, and operates on a discrete time scale, like a clock with a period τ. The behavior of a Kauffman net can be also represented in the form of a state transition diagram (Fig. 36), which is a directed graph whose vertex set is the state space of the net, and whose arcs are the state transitions.

Kauffman[160] used computer simulation to study the behavior of genetic binary nets with low connectivity ($k = 2$ or 3), and numbers of elements between 15 and 8192. For $k = 2$, Kauffman found that the number of limit cycles r of a net with N elements was $r = N^a$, with $a = 0.5$, and that the median limit cycle length was $L = N^b$, with $0.3 < b < 0.6$. When $N = 1000$, $r = 30$, but the number of possible states is $n = 2^N = 10^{300}$, which is astronomical. Nets with such a large number of states entered very quickly a very small number of very short cycles. Sherlock[173] proposed an analytical description of Kauffman nets in terms of the state transition matrix. An example of such a matrix is

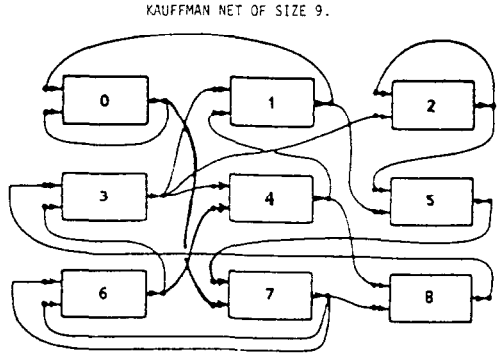

Fig. 35. A Kauffman net of connectivity $k = 2$ and size $N = 9$ (according to Sherlock[173]).

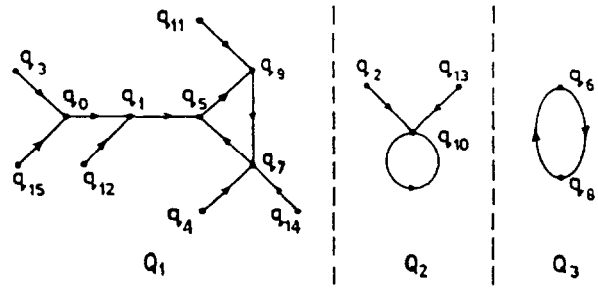

Fig. 36. A possible state transition diagram for a $N = 4$ Kauffman net (from Ref. [173]).

reproduced from Ref. [173] in Fig. 37. The matrix provides a complete specification of the state transition graph.

The states of the Kauffman net can be represented as vectors: $q(t + \tau) = Aq(t)$, where A is the transpose of the adjacency matrix[187] specifying the state transition digraph; in terms of the digraph, A is defined as

$$A = \{a_{ij}\}, \qquad a_{ij} = 1 \tag{42}$$

if there is an arc from the vertex j to the vertex i, and $a_{ij} = 0$ otherwise. This matrix form is convenient for an algebraic analysis of the dynamics of the genetic nets. The representation also has the advantage that the matrix elements a_{ij} of A can be calculated from a specified "wiring diagram" (Fig. 35) of the network, together with the assignment of the Boolean mappings to the network elements. With the matrix representation the number of states involved in the limit cycles are readily calculated[173] through matrix element manipulation. Specifically, the fractional distribution $f(l)$ of limit cycle lengths is

$$f(l) = \sum_{j|N_c} n_l^j \left(\prod_{l=1}^{N_c} l^{n_l^j} n_l^j ! \right)^{-1}, \tag{43}$$

where n_l^j is the number of occurrences of integer l in the partition j of N_c into the sum $N_c = \sum n_l^j$ which corresponds to a partitioning of Q_c into any of the sets of disjoint limit cycle subsets C_J that give rise to n_1 stable states, n_2 cycles of length 2, etc. The number of occurrences of cycles of length l was calculated[173] as

$$M(l) = N_c f(l) \tag{44}$$

where N_c is the number of different ways of distributing N_c distinct objects among the partitions. Using a computer algorithm, Sherlock[173] evaluated numerically $f(l)$ for all N_c up to 20. Within the 24 bit (~seven decimal digit) precision of the digital computer, Sherlock[173] found that

$$f(l) = 1/l, \tag{45}$$

for $1 \leq l \leq N_c$, $N_c \leq 20$. This $1/l$ distribution of cycle lengths is also observed in a computer simulation of Kauffman nets for cycle lengths up to 50 (Fig. 7 on p. 699 in Ref. [173]). Sherlock[173] also found that $N_c = L^2$, where L is the median cycle length and,

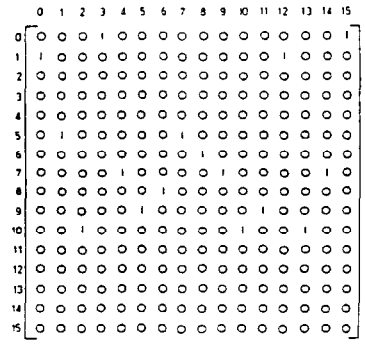

Fig. 37. Example of a state transition matrix corresponding to the state transition graph in Fig. 36 (from Ref. [173]).

therefore, with $L \simeq \sqrt{N}$[160] he obtained $N_c \simeq N$; that is, for $k = 2$ random nets with N elements the cardinality of the cycle state set is approximately equal to N. With this value of N_c, the fraction F_c of the total number of states involved in the limit cycle is

$$F_c = \frac{N_c}{n} \simeq \frac{N}{2^N}. \tag{46}$$

This relation is in agreement with Kauffman's "experimental" findings[160] by computer simulation of formal genetic nets. However, for connectivities higher than 2, the fraction F_c calculated algebraically was no longer $\sim N/2^N$, as in the computer experiments (simulation of random nets). The deviation from the behavior obtained by Kauffman for $k = 2$ increased rapidly with the size of the net and, therefore, it is possible that biologically relevant models of genetic systems may not have $F_c \simeq N/2^N$ (see Fig. 7 on p. 722 in Ref. [173]), but may have instead $\log F_c \sim (-N)$. Even more complex behavior is expected for n-ary genetic nets; such nets are discussed next.

B. *N-ary genetic networks*

A *genetic network*, or *net*, is defined as an assembly or aggregate of interacting genes. Genetic interactions can be either direct, as in the case of gene "clustering", or they can be indirect—via intermediates, products and metabolic pathways. Perhaps the best known simple example of a genetic net is the one introduced by Jacob and Monod[225] for the genes related to lactose metabolism in the Gram-negative bacterium *Escherichia coli*. Such genes were shown to lie near one another in the same region of the bacterial chromosome and were considered to act as a functional unit, or "operon". Within the operon, a "regulator" gene, three "structural" genes and an "operator" gene were postulated to exist and to play different functional roles. The three structural genes are under the control of the same operator gene, while the operator gene itself responds to, or is controlled by, the regulator gene. In the case of two interacting operons, which define a two-component genetic net, the situation can be represented schematically as in Fig 38.

Let us consider the possible dynamics of the genetic network in Fig. 38. If we postulate discrete states for the genes, then one can readily calculate the dynamics for "all-or-none" type of genes (that is, the case in which the genes are either fully active or completely inactive). The more general case of n discrete states, which are defined by n discrete levels of gene activities, is more difficult to treat and requires the introduction of special

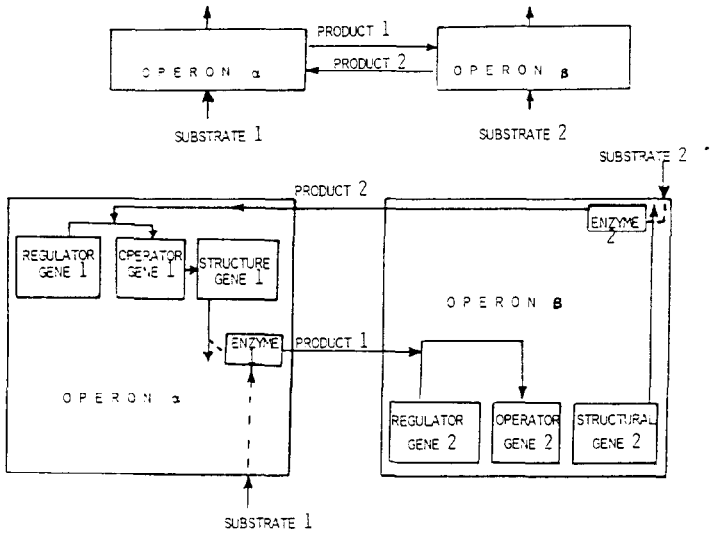

Fig. 38. Two-component genetic net with two operons α and β (from Ref. [226]).

mathematical concepts. A general, two-component genetic net with n states is presented in Fig. 39 and the generalization to *m-component genetic nets* is now transparent. This n-state black-box representation can be used in principle to determine the behavior of any genetic net. However, it has the disadvantages of being tedious and limited in its scope for deriving general theorems concerning genetic network dynamics. An alternative approach was, therefore, introduced in which genetic nets and their activities are defined in terms of n-valued logic and their associated Łukasiewicz algebras[226]. Mainly because the n levels of activity of a gene are ordered (in the sense that the lowest level corresponds to no activity or 0, while the higher levels or corresponding states are in the order of increasing activity up to full activity which is labelled by 1), the statements concerning such genetic activities are also ordered under a *symbolic ordering relation* $\subset$ forming therefore a distributive lattice of a special kind. Such a distributive lattice is called an *n-valued Łukasiewicz algebra* (or *L-algebra*). Certain maps σ_i: $L \to L$ and N: $L \to L$, which are endomorphisms of an L-algebra associated with an n-state genetic net[226] are employed to model the dynamics of genetic systems in the absence of mutations. In order to represent genetic mutations certain transformations of L-algebras are defined. These are morphisms f: $L_1 \to L_2$ of L-algebras and possess certain specific properties such as

$$f*N = N*f \qquad \text{and} \qquad f*\sigma_i = \sigma_i*f \qquad \text{for any } i = 0, 1, \ldots, n-1 \tag{47}$$

(see also details on p. 254 of Ref. [227]). All "genetic" L-algebras together with the possible L-morphisms representing genetic mutations are then forming a *subcategory* G_L of the *category* Luk_n of all n-valued Łukasiewicz algebras and L-morphisms between them. The basic properties of G_L were reported in Ref. [226]. In the particular case of two-state genes, the n-valued algebras are reduced to Boolean ones and the category G_L^B of such Boolean algebras is equivalent to a special subcategory called the category of centered L-algebras G_L^C. This equivalence between G_L^B and a full subcategory of G_L^C is expressed by two *adjoint functors* C and D:

$$G_L \xrightarrow{C} G_L^B \xrightarrow{D} G_L, \tag{48}$$

with the functor C being full and faithfull (see also p. 254 in Ref. [226] and references cited therein). The *centers* of a centered Łukasiewicz algebra are $(n-2)$ elements (statements about gene activities), $a_1, a_2, \ldots, a_{n-1} \in L$, for which

$$\sigma_i(a_j) = \begin{cases} 0 & \text{for } 1 \leqq j < n-j, \\ 1 & \text{for } n-j < i \leqq n-2. \end{cases} \tag{49}$$

The corresponding genes would have degenerate states in the sense that $(n-j)$ states will all be characterized by no activity while the remaining states will yield full activity. An organism at a given stage of its development may have some genes of the all-or-none type, as well as some nondegenerate ones. Therefore, the collection of genes of an organism, or its corresponding genetic net, will be generally represented by a mixture of

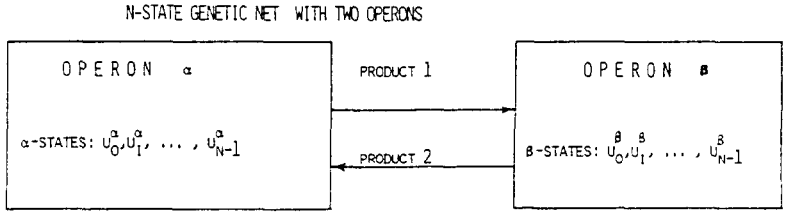

Fig. 39. N-state genetic net with two operons α and β.

centered Ł-algebras and noncentered ones. The corresponding category of genetic nets of an organism and their dynamic transformations will be a subcategory of G_L, and therefore of Luk_n, but will not be in general a subcategory of G_L^B, or of Bl, the category of Boolean algebras. A simple example of a nondegenerate genetic net is provided by the multiple genes which were discovered in the lampbrush chromosomes in oocytes of the crested newt *Triturus cristatus carnifex*[228], after we postulated the genetic n-states[226]. The transcription of multiple genes can be readily represented as a particular dynamic process of an m-state genetic network with its 0 state corresponding to all multiple genes being inactive and the 1 state corresponding to all m genes being fully operational. There is strong experimental evidence that the transcription of multiple genes, or "satellite" DNA, on lampbrush loops in oocytes does indeed occur and correlates somehow with structural heteromorphism of the organism, as well as a lack of chiasma formation in the chromosome arm in *Triturus cristatus*[228]. The evolutionary significance of this "unusual" transcription of satellite DNA appears obscure at present, and further hybridization experiments involving DNA/ nascent RNA transcripts from clone pTcS1 will be necessary in order to determine the transcription mechanism in such cases.

Another particularly interesting example of n-state transcription units was recently reported for the rDNA gene sequences of *Physarum*[229]. In this case, the subunits on the ribosomal gene transcription unit were shown to be in a molecular configuration which was distinct (in some unspecified way) from the oligomers of the nucleosomes present on the inactive rDNA regions. Different chromatin subunit structures could be isolated from different functional regions of a single gene[229]. These experiments open up the exciting possibility of carrying out detailed kinetic studies of individual genetic activities and should allow for a direct comparison with the theoretical predictions based on abstract molecular models of such genetic systems. In particular, the polymerase binding rates and certain transient conformational changes of nucleosomes on functional genes could be derived from computer simulations.

10. AUTOMATA THEORY AND METABOLIC-REPLICATION MODELS IN BIOLOGY

Before considering the applications of automata theory in biology we shall introduce the basic concepts needed for such models.

A. *Algebraic theory of automata*[230, 155]

An *automaton* is a quintuple $M = (X, Y, Q, \delta, \lambda)$, where X is a finite input alphabet, or set of inputs $\{a_1, a_2, \ldots, a_m\}$, Y is a finite set of outputs $\{y_1, y_2, \ldots, y_n\}$, Q is a finite set of memory states $\{q_1, q_2, \ldots, q_k\}$, δ: $Q \times X \to Q$ is the next state (transition) function and λ: $Q \times X \to Y$ is the output function.

Automata can also be represented by state transition graphs, similar to those of random nets, or by Boolean matrices and output vectors. A more powerful, algebraic representation of an automaton is its description as a semigroup of state transition maps; the state transition maps associated with single-input symbols can be multiplied to find the state transition maps produced by input sequences (strings of inputs). The set of state transition maps of the automaton when endowed with the multiplication operation of the transition maps has a semigroup structure. The algebraic theory of automata which deals with such semigroup structures is useful for solving the following problems:

1. automata decomposition into the simplest, "irreducible" components;
2. finding the standard version of any automaton;
3. classifying automata according to their most general and essential properties.

B. *Basic theorem for decomposition of automata*

The state transition maps are of two basic types:
(a) collapsers—two distinct states are carried onto the same next state under the input;
(b) permutations—states are being only permuted under such maps; the permutations are 1-1 onto functions of the state set.

Krohn, Rhodes and Tilson[231, 232] have found the basic decomposition theorem of automata: *any automaton can be decomposed into irreducible components that have either only permutations or are amongst four types of elementary collapser automata.* Permutations form a group and, therefore, *the automata decomposition theorem states that any automaton, or "machine" semigroup, can be decomposed into a group and collapser semigroups of four basic types.*

C. *Tessellation automata and biological development*

Cellular automata have been used as models for the development and growth of biological organisms. An example, provided by Arbib[233] will be used to illustrate this approach. In a similar vein is the preceding work of Smith[234], Wagner[235] and Arbib[236].

A "module" equipped with 22 instructions, a bit register, BR, and a number of inputs is the basic unit (Fig. 10.1 on p. 352 in Ref. [233]) of a tessellation structure. Copies of the module are placed at a lattice point, in a planar configuration. An array of modules defines the tessellation. Directions within the tessellation are defined using the coordinates (m, n) for each module:

u = up, defined by increasing n;
d = down, defined by decreasing n;
r = right, defined by increasing m;
l = left, defined by decreasing m.

For example, a group of four neighbor modules, or "cells", in such a tessellation structure will have the coordinates $(m-1, n)$, (m, n), $(m, n-1)$, and $(m+1, n)$. The tessellation is a "tissuelike" structure where a collection C of cells is *comoving* if $\alpha \in C \Rightarrow \beta \in C \Leftrightarrow W(\alpha, \beta)$, with W being the relation of "welding" on cells: $W(\alpha, \beta) \Leftrightarrow \alpha$ and β are welded neighbor cells, that is, $\exists\ \gamma$ such that $W(\alpha, \gamma)$ and $W(\gamma, \beta)$. The neighboring cells are said to be welded if either of the cells is joined to its neighbor, so that they "change" their position together in the array; "moving a cell" in direction x means in fact moving the contents of the cell registers in the x direction. The comoving set, therefore, is really a pattern rather than a set of cells in the tessellation. The basic idea is that if any cell moves in one direction all the cells in the comoving set move in the same direction. Arbib[233] showed that any finite automaton or Turing machine can be simulated by a tessellation structure. Tessellation structures can be used not only to generate new cell configurations but also to construct automata by acting on neighboring squares. A tessellation structure capable of constructing and simulating a Turing machine was called a "CT-machine"[233]. Arbib proved the existence of a CT which is also self-reproducing (p. 370 in Ref. [233]). Figure 40 shows such a CT-machine, with P being its program and $\mathcal{T}$ being its tape configuration; the reproduced machine $(\mathcal{V}, \mathcal{U}, \mathcal{W})$, which is the "offspring", also includes the program to reproduce itself.

Such abstract constructions were designed to address the question: how can a complex, multicellular organism grow from a single cell assumming that each cell behaved like an automaton and executed a finite program?

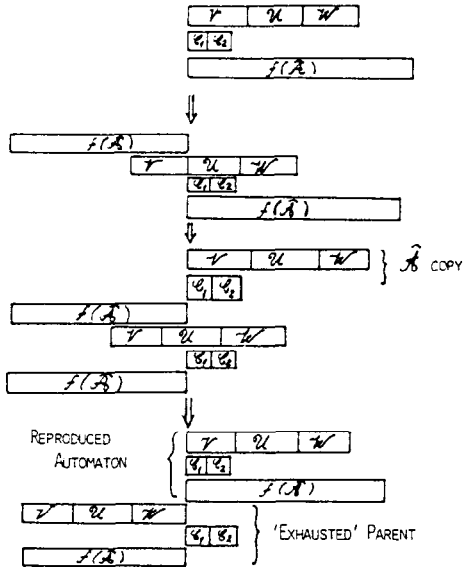

Fig. 40. Model of self-reproduction in the form of a CT-machine (according to Arbib[233]).

The process represented in Fig. 40 shows how a multicellular organism can reproduce itself but it does not indicate how a multicellular organism can grow and develop from a single cell.

The tessellation model presents a number of differences from the behavior of a real biological organism: the program of the machine is contained in a string of automata rather than in a single cell, the specification of the machine is complete within each module but it is incomplete in a biological cell, and the construction assummes that the modules are passive, in the sense that any subassembly will remain fixed and inactive until the whole tessellation structure is complete. Biological development, however, is an active process, generated through the multiple interactions and "induction" between the subassemblies. In the tessellation model, growth is simulated by an increase in the number of cells in a comoving set; cell division is mimiced by modular activity at the construction site in the tessellation. When a module "divides" the original module is preserved at the initial site, while its replica has been produced at a neighboring location in the lattice. In such a model, a module $\hat{c}(A)$ produces initially a copy of itself which is rendered "dormant", that is nondividing. Then, $\hat{c}(A)$ produces $c(A)$ which builds A, and before A is turned loose, it is attached to the copy of $c(A)$. Upon reaching "maturity", module A reproduces by releasing such a copy $\hat{c}(A)$ into the tessellation. The design of a differentiated organism would be, however, much more complex than such a tessellation process; one would have to use subroutines to build differentiated tissues and employ higher-level routines to assemble such differentiated tissues in the correct anatomical position.

Models employing molecular automata rather than cellular ones may be closer to the molecular biology approach to differentiation, growth and development. A category of such models comprises metabolic-replication, or (M, R), systems and was designed by Rosen[150].

D. (M, R)-*Systems*

The simplest (M, R) system[151] is defined by a set of mappings $H(A, B)$ of the form $f: A \rightarrow B$, together with a set of mappings $H(B, H(A, B))$ of the form $\Phi: B \rightarrow H(A, B)$, such that $\Phi_f(b) = f$ for $f(a) = b$. A is the set of inputs and B is the set of outputs of the

(M, R) system. By defining the mappings f as states of the (M, R) system, one can associate with each (M, R) system an automaton[151]. A set of mappings β: $H(A, B) \rightarrow H(B, H(A, B))$ ensures the "self-reproduction" of the (M, R) system since it associates with a mapping f the corresponding Φ_f mapping that replicates f. In a more recent version[237], (M, R) systems have an associated dynamical realization so that their state space is a topological structure rather than a discrete set. An example of the simplest (M, R) system is given in Fig. 41, which also contains a proposed realization of such an (M, R) system in molecular terms. (M, R) systems were shown to form a category[151] which is a subcateogry of the category of all automata[153, 154]. The basic algebraic properties of this category of (M, R) systems were considered in relation to their possible biological realizations[153, 154], and a generalized form of (M, R) systems with variable algebraic and topological structure was proposed[238]. Such extensions of (M, R)-systems theory will be discussed in Sec. 11 together with other organismic structures and molecular set theory.

An interesting possibility is the computer simulation of dynamical realizations of specific (M, R) systems with structures selected to simulate a particular group of biological organisms. The approach would be similar to the computer simulation of Kauffman nets and one may expect to obtain from such a simulation biologically relevant results.

11. NATURAL TRANSFORMATIONS OF ORGANISMIC STRUCTURES

In a recent report, relational theories of organismic sets[239], metabolic-replication systems[237] and molecular "sets"[240] were shown to have a similar foundation, and thus can be studied within a unified theory which employs a categorical framework[241]. This is possible because all relational theories have a molecular basis. Complex structures such as genomes, living cells, organs and organisms were mathematically represented in terms of molecular properties and molecular entities such as "molecular sets". The definition of organismic sets, for example, requires that certain quantities are determined from experiments: these quantities are specified by a special set of values of general observables which is derived from physicochemical data[241]. Such observables are directly represented by *natural transformations* in category theory, and are also encountered in theories of metabolic-replication $[(M, R)]$ systems, as well as molecular set theory (Ref. [240]).

Since the problem of uniquely decomposing such organismic structures into simpler, functional (or active) components appears to be an unsolvable one in the general case, we have adopted a complementary procedure which begins by building up specific structures corresponding to specific biochemical, genetic or organismic systems. We have then examined their properties in terms of their mathematical representations such as the generating formalisms[241]. It is interesting that energetic considerations ultimately lead to molecular models and natural transformations[241, 242] or natural equivalences in particular cases[243]. A detailed investigation of the natural transformations of organismic structures is therefore necessary in order to understand certain basic themes of relational

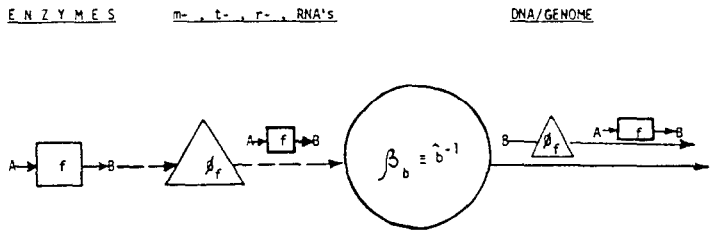

Fig. 41. Diagram representation of the simplest (M, R) system (according to Ref. [238]).

theories in biology, such as observability of molecular processes, realizability conditions for relational models/theorems, unicity of representation, dynamics /kinetics of biomolecular reactions and molecular evolution.

When attempting to compare mathematical results of relational theories with recent advances and experimental observations in molecular biology one invariably finds that a theoretical-molecular model approach, such as the procedure adopted by us, is really needed in order to be able to realize the experimental implications of relational results.

Most theoretical studies of molecular models are, however, taking a very different course and are merely the result of formalizing a fixed set of experimental observations, without pursuing its wider implications for a synthesis of theoretical knowledge in biology. On the other hand, relational theories are still developing and may reach a stage when their predictions will make a strong impact on the molecular biologist's veiw, which so far has been "to divide and conquer." Our abstract molecular models of organismic and genetic structures in terms of natural transformations could help bridge the gap between relational and molecular biology.

A. *Molecular automata and molecular models in categories*

We showed in an early report[242] that energetic considerations of nerve excitation and conduction lead to a physical, molecular model of these processes, and allow one to analyze in physical terms the behaviors of neurons and neuronal networks. From quite a different standpoint we later considered n-state genetic networks[226] using n-valued logic in categories, and derived general theorems concerning the decomposition and dynamic properties of such networks in a general fashion. Some of these properties were found to be similar to those of neuronal networks, but the analogy was far from being complete. In these two partially analogous biological networks we found that a full, general treatment required the use of the mathematical theory of categories and functors[226]. Recently, it became possible to derive a synthesis of the three different approaches to relational biology—the organismic set theory[239], the theory of (M, R) systems[237] and the molecular set theory[240]. In our synthesis[241], natural transformations of organismic structures play a central role. The unifying concept of natural transformation is provided by the standard theory of categories and functors, initially developed as a general theory of natural equivalences[244] by Eilenberg and MacLane in 1945.

A simple introduction of such a synthesis is based on set-theoretical models of chemical transformations[240]. Consider the simple case of *unimolecular chemical transformations*[240]:

$$T: A \times I \rightarrow B \times I, \tag{50}$$

where A is the original sample set of molecules, $I = [0, t]$ is a finite segment of the real time axis and $A \times I$ denotes the indexing of each A-type molecule by the instant of time at which each molecule $a \in A$ is actually transforming into a B-type molecule [see also Eq. (3) in Ref. [240]). $B \times I$ denotes the set of the newly formed B-type molecules which are indexed by their corresponding instants of birth. As a flexible means of formalization, any chemical component-molecular set A of a biochemical subsystem in a living organism may be regarded as a variable quantity, or as a molecular set variable (msv), which spans certain allowable molecular sets (that is, those which are actually observed or realized if a molecular model was considered). The functional dependence of these msvs on time (in the mathematical sense) was then regarded as a kind of ≪"relation" from the time axis to the class of molecular subsets as "range"≫. This was termed the "wide-sense" kinetics of molecular set theory[240]. The transitions from one possible value (or state) of an msv to the next allowable value (s) will occur with some definite probabilities—in

a statistical sense. While the concentration, or cardinality, of a molecular set component is constant, the set itself can change continuously its composition; this is the biologically significant factor in the operation or functioning of an organism.

At this point, one can easily categorize the transformations of a molecular set A by simply using the endomorphisms $f: A \to A$ and by considering the new set of all possible transformations of A, which will be denoted by $H(A, A)$. The molecular sets and their transformations can now be organized into a *category* M and certain functors h^X between such categories of molecular sets can now be defined. (For definitions of the concepts of category and functor please see Ref. [245].) Specifically, the functor $h^A: M \to \text{Set}$, with Set being the category of sets, is defined by

$h^A(X) \equiv H(A, X)$ for any X in M as object, and $h^A(t) = m: H(A, A) \to H(A, B)$ for any morphism $t: A \to B$ in M, and B a molecular set of reaction products of type "B."

The flexible notion of molecular set variable (msv) is exactly represented by the morphisms v in the diagram

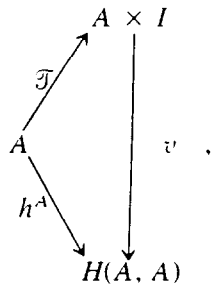

(51)

where morphisms v are induced by the inclusion mappings $A \xrightarrow{\mathcal{J}} A \times I$ and the commutativity conditions $h^A = v \circ \mathcal{J}$. The naturality of this diagram simply means that such conditions hold for any functor h^A defined as above.

The unimolecular chemical reaction is thus represented by the natural transformations $h^A \xrightarrow{\eta} h^B$, as one can readily check in the commutative diagram

$$\begin{array}{ccc} h^A(A) = H(A, A) & \xrightarrow{\eta_A} & h^B(A) = H(B, A) \\ \downarrow h^A(t) & & \downarrow h^B(t) \\ h^A(B) = H(A, B) & \xrightarrow{\eta_B} & h^B(B) = H(B, B) \end{array} \tag{52}$$

if the states of the molecular sets $A_n = a_1, \ldots, a_n$ and $B_n = b_1, \ldots, b_n$ are represented by certain endomorphisms in $H(A, A)$ and $H(B, B)$, respectively. In the case of *multimolecular reactions*, the canonical functor of category theory

$$h: M \dashrightarrow [M, \text{Set}] \tag{53}$$

assigns to each molecular set A the functor h^A and to each chemical transformation $A \xrightarrow{t} B$ the natural transformation $h^A \xrightarrow{\eta} h^B$. As an example, let us consider the "replication maps" of (M, R)-system theory. These "maps" were shown to be representable by natural transformations (details are given in Ref. [238]). The machinery associated with metabolic and genetic activities of the "simplest", or primordial organism, could be simply

visualized as in Fig. 41. This is, of course, Robert Rosen's simplest (M, R) system. Molecular candidates for the components of this metabolic-replication model are indicated at the top of the diagrams in Fig. 41. The corresponding molecular model is well established in molecular biology on an experimental basis. One quantity often omitted from this model is energy. Energy could be readily introduced into the model as an input/output element for each component of the (M, R) system. A more physical approach would, however, introduce energy by defining an observation process on a molecular set and then convert it into the molecular set formalism by defining the appropriate natural transformations. A few details of this formalization are given below and full details will be presented elsewhere. An observation process on a molecular set will involve the preparation of a certain msv, A, (with preparation in the quantum-mechanical sense) into a selected state, or field of states, A_u^*. The process is described by a morphism α: $H(A, A) \rightarrow R$. For the chemical product "B" of a reaction, γ: $H(B, B) \rightarrow R$ is an observable of the msv B, which is measured in some specially prepared state (or field of states) B_u^*. The preparation itself can be subject to an uncertainty δ in the set of real numbers R. α and γ are connected together in the commutative diagram

$$\begin{array}{ccc} H(A, A) & \overset{c}{- - - - - - - - \rightarrow} & H(B, B) \\ & {\scriptstyle\alpha}\searrow \quad \swarrow{\scriptstyle\gamma} & \\ & R & \end{array} \tag{54}$$

with c being "uniquely" defined as a morphism c: $A_u^* - - \rightarrow B_u^*$, within the uncertainty range δ. Among such observables of an msv, energy is an essential one since it places limits on the possible reactions and products, although it changes such restrictions to probabilistic statements. In our formalism, therefore, energy is represented as a morphism, and has quite general properties. In specific cases it will be necessary to define more precisely the energy and the statistical conditions related to the uncertainty range δ. Our definition of energy as a morphism is natural both formally and conceptually. Formally, the diagram (54) is natural both in α and γ, as well as certain "reactions" c. Conceptually, energy is one of the general observables of any organismic structure (for details please see pp. 433–434 in Ref. [241] and literature cited therein). As shown previously, the general observables of any organismic structure are natural in the categorical sense[244]. Natural transformations thus establish a formal and energetic link between organismic structures, (M, R) systems and molecular sets. By employing the canonical functors f and the natural transformations η as a translation device between (M, R) systems, molecular and organismic sets, once a result is obtained in one of these theories it can be readily translated into the others without losing generality. The translation in terms of molecular set theory is particularly important for physicochemical representations of abstract molecular models, such as the (M, R) systems, because molecular-set models have relatively direct interpretations in experimental/physicochemical terms. In practice, one is still left with the question of deciding which abstract model is actually realized in molecular biology, that is, defined by experimental data.

B. *Natural transformations in protein biosynthesis and embryogenesis*

As a particular example of protein biosynthesis let us consider the synthesis of approximately 50 different ribosomal proteins (or r-proteins) in the Gram-negative bacterium *E. coli*. The r-protein genes are arranged in many different operons, apparently placed at

separate locations on the *E. coli* chromosome[246]. The *r*-protein biosynthesis is very well coordinated in *E. coli* and the question of how this is achieved is an important one. From a theoretical standpoint, this system is a good example of a genetic network. The experiments indicate that the overall regulation of *r*-protein biosynthesis responds to changes in growth conditions and these may be primarily mediated by changes in the rate of transcription of the *r*-protein genes. By comparing, however, the transcription rates of *r*-protein mRNA in haploid and merodiploid strains, it was found that the expression of *r*-protein genes in the str-spc region is controlled by a post-transcriptional mechanism[246]. Such a mechanism could involve the inactivation and degradation of the excess of *r*-protein mRNA. Nevertheless, it is equally possible that the translation of intrinsically active *r*-protein mRNA is blocked by other means; the "overproduced" mRNA could be more labile and this may impair its participation in *r*-protein biosynthesis. This example leads to an abstract molecular model similar to the one shown in Fig. 41. Thus, if the set of *r*-proteins is denoted by $H(A, B)$ then the set of *r*-protein mRNAs will be represented by some subset of $H(B, H(A, B))$; the genome region which is transcribed into *r*-protein mRNAs will be then represented by a subset of $H(H(A, B), H(B, H(A, B))$, as in the standard (M, R)-system theory. As shown by Rosen[150], the "metabolic" components, such as the *r*-proteins, can be reorganized into a finite category M. Let any two sets of M be X and Y, and let $t: X \to Y$ be a mapping of M. If Set is the category of all sets and mappings of sets, then one can define a special functor $h^X: M \to \text{Set}$ as

$$\begin{cases} h^X(Y) = H(X, Y) & \text{for any set } Y \text{ in } M, \\ h^X(t) = m: H(X, X) \to H(X, Y) & \text{for any } t: X \to Y, \\ h^X(g)(t) = gt: H(X, X) \to H(X, Y') & \text{for any } g: Y \to Y' \text{ in } M, \end{cases} \tag{55}$$

where X is a certain fixed object in M. The functor h^X carries Y into $H(X, Y)$ without acting on the elements of Y. A family of functors of the type h^X, which is obtained by varying X in M, will produce all sets of the form $H(X, Y)$. The set of *r*-proteins $H(A, B)$ can thus be generated by considering $h^A(B)$ for A and B sets in M. In order to construct the sets $H(B, H(A, B))$ which represent the *r*-protein mRNAs, one can use the canonical functor $h: M \to [M, \text{Set}]$. The functor h is defined by the assignments

$$S \rightsquigarrow h^X \qquad \text{and} \qquad t \rightsquigarrow h^X \to h^Y, \tag{56}$$

where $t: X \to Y$ and $[M, \text{Set}]$ is a category of functors from M to Set. An *embedding* $I: M \to \text{Set}$, carries any X of M into the same set X of Set, and any morphism $t: X \to Y$ of M, into the corresponding mapping of Set. The *natural transformations* $\Phi: I \to h^X$ with X varying in M now define the "genetic" maps ϕ_f, that is, the elements of $H(X, H(X, Y))$. In the particular case of certain natural transformations $\phi_r: I \to h^A$, we obtain a representation of the *r*-protein mRNAs; kinetic calculations derived from such a model and the "wide-sense" kinetics of molecular set theory are in broad agreement with the experimental observations of *r*-protein biosynthesis in *E. coli*. A categorical representation of *r*-protein biosynthesis thus consists of a functor h^A—generating models of the *r*-proteins—and certain natural transformations $\phi_r: I \to h^A$—generating the models of *r*-protein mRNAs. The generalization of this formalism to any protein biosynthetic process is immediate by considering the appropriate h^P functors and $\phi_P: I \to h^P$ natural transformations. During protein biosynthesis the composition of the biological system will vary as a result of certain multimolecular reactions taking place; such processes induce certain natural transformations $\nu: \alpha \to \alpha^*$ and $\omega: \gamma \to \gamma^*$, with $\alpha, \alpha^*: \text{Set} \to R$ and $\gamma, \gamma^*: \text{Set} \to R$ being certain special functors. From the definitions of natural transformations and multimolecular reactions [relations (52) and (53), respectively] one obtains the commutative

diagram

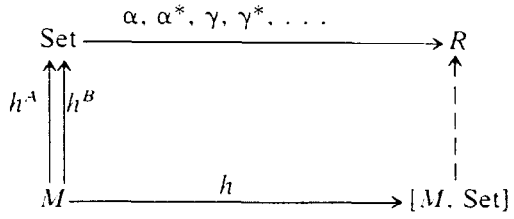

(57)

with L playing the role of a generalized observable. In this diagram, the canonical functor h assigns to each molecular set A the functor h^A and to each chemical transformation t: $A \rightarrow B$, the natural transformation η: $h^A \rightarrow h^B$. The advantages of employing natural transformations over the use of the standard maps t: $A \rightarrow B$ of molecular set theory are:

(1) the natural transformations η are not restricted to mappings; and

(2) A and B can be truly varying structures rather than simple discrete sets.

This generalization of molecular set theory, (M, R)-systems theory and organismic set theory is important for kinetic modelling of protein biosynthesis since the states of molecular structures (previously discrete sets) can be defined in quantum-mechanical terms, for example. Calculation of transition probabilities between such states may be thus possible starting from physical first principles, in favorable cases; such calculations would employ standard quantum-mechanical approaches, such as the Dirac or the Heisenberg representation. Even without making use of such detailed formalisms it is possible to derive some of the basic properties of protein biosynthetic processes. For example, the msv associated with the final form of a synthesized polypeptide, can be shown to be representable as the direct limit of the intermediate forms in its synthesis (for a definition of direct limit and an example see p. 482 in Ref. [224]). On the other hand, a cell at the end of its synthesis stage will be represented by the projective limit of certain metabolic-replication systems associated with selected intermediate stages. This projective limit is constructed as a Cartesian product of sets of states/inputs/outputs and transition/output functions of the corresponding (M, R) automata or sequential machines (for details of the construction and the relevant definitions see Ref. [153]). The cell dynamics, including protein biosynthetic processes, are thus subject to the following natural restriction:

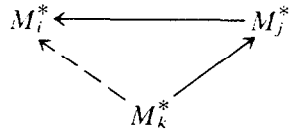

(58)

is commutative for any i, j, k belonging to an ordered set I, and such that $i \leqq j \leqq k$. The ordered set in this case corresponds to the set of cellular events, and the M_j^* components are some selected (M, R) systems which represent certain cell stages at which different mRNAs are being synthesized. In this model, a complete cell, or organism, can be built from certain intermediate stages as a Cartesian product of the sets defining the selected stages. The problem is, of course, one of defining experimentally such stages. In the case of developing embryos, tests for nuclear equivalence showed that somatic nuclei from the blastula stage to early stages of organogenesis become progressively restricted in their ability to promote "normal" development when transplanted into enucleated eggs[247]. Up to a certain stage, however, the nuclei were equivalent, in the sense of being capable of inducing normal development. From a dynamic viewpoint such nuclei are adjoint, that

is, their associated dynamical systems have an adjointness relation between them, which is unique up to an isomorphism (Proposition 1 in Ref. [224]). Essentially, there exist certain adjoint functors[248] between the categories defining any two such dynamical systems. These adjoint functors are present only if there exists a certain natural equivalence (see relation (4) on p. 479 and related details in Ref. [224]). When the nuclei become progressively restricted in their ability to induce normal development, the associated dynamical systems become only weakly adjoint (see also Theorem 3 on p. 483 in Ref. [224]) because the dynamic isomorphisms of the kind

$$S[A, U(B)] \xrightarrow{\sim} S'[K(A), B], \tag{59}$$

which existed for equipotent nuclei, are now replaced by certain dynamic epimorphisms

$$S[X, V(Y)] \rightarrowtail S'[W(X), Y]$$

(which are related to two weakly adjoint functors V and W: $S \xrightarrow{W} S' \xrightarrow{V} S$). The categories S and S' generate the dynamical systems D and D', respectively.

Since a weak adjoint functor is not necessarily a proper functor (as it may be multivalued on morphisms), weak adjointness does not generally require the existence of a certain natural equivalence, or even of certain natural transformations. At this point, we conjecture that the weak adjoint functors which represent embryological development are in fact proper functors, that is they are not multivalued on morphisms. We expect that certain natural transformations can be always defined to model the development of an organism because we were able to show their involvement in the construction of molecular sets, (M, R) systems and organismic structures. If we consider certain functors Δ: $S_0 \rightarrow S_0$ which define a dynamic transformation of an organismic structure (such as a cell or an embryo) then the natural transformations between such functors are a means of recovering the effects of dynamic transformations at the level of the components in the organismic structure S_0.

While natural transformations appear to be universally present and provide useful means for unifying relational theories of biological systems—starting from the molecular level and including the cellular and organismic levels—any molecular models in molecular biology will require additional specific assumptions and restrictions. The wide-sense kinetics of molecular set theory[240] is one such assumption. Since it only requires that transitions between molecular set variables occur with definite probabilities, the approach will be valid for most chemical and biological systems that are multistable or metastable, but may run into difficulties for systems with chemical chaos.

The remarkable stability of certain genome regions results in a series of fundamental properties which are preserved not only throughout the development of an organism but also during evolution. In the case of embryological development, adjoint functors, natural equivalences, weakly ajoint functors and epimorphic transformations provide descriptions of biodynamics in algebraic terms. Mathematical theorems can be therefore proven algebraically for developing organisms. Another example of the remarkable stability of certain genome regions is provided by the sequence "homology" existing between 16S rDNA from *Zea mays* chloroplasts and the 16S rRNA of *E. coli*[249]. Although these two biological systems are separated by a large phylogenetic distance, extensive homology between them was observed; out of 1541 residues from *E. coli* 16S rRNA, 1144 positions are identical in maize 16S rDNA. Unlike this "structural" region of the cistron, the immediately adjacent "spacer" region containing the nucleotide positions 1542–1729 were quite distinct in the two systems. Such observations have implications for genetic engineering attempts; an *in vitro* system from *E. coli* can be used for efficient translation of plant chloroplast mRNAs. Our natural transformation models can be employed to predict

such homologies in molecular biology and could be therefore used in conjunction with genetic engineering experiments. Related experiments in the more complex organisms are the tests for nuclear equivalence in nuclear transplant experiments. We have presented an analysis of such experiments from a relational viewpoint by means of natural equivalences and adjoint functors, and derived the consequences of nuclear transplant experiments for theories in relational biology.

12. N-VALUED LOGIC IN MATHEMATICAL MEDICINE

An early attempt to model the diagnostic process in medicine was made ten years ago using Boolean algebras, two-valued logic and computer simulations of the diagnostic process[250]. This approach pictures diagnosis as a series of yes and no decisions based on the examination of the patient which finally involves two types of statistical variables: a continuous type representing numerically the results of biochemical and clinical tests, and a discrete or macroscopic qualitative type variable which represents the patient's condition and his/her case history. Another important ingredient of the medical diagnostic process which was, however, ignored previously is the logical concept of *contingent*, sometimes assimilated with the logical category of "possible". The degrees of possibility are readily represented in n-valued logic by taking the value 0 for false, 1 for true, and by allowing for $(n-2)$ degrees of possibility between false and true. The manipulation of logical statements with n possible truth values (in the logical sense) is conveniently carried out by algebraic means. These play the role which Boolean algebras played for two-valued logic. Thus, an *n-valued Łukasiewicz algebra* is a distributive lattice with a first element (0) and a last element 1, which is subject to the following axioms:

(I) There exists a map N: $L \to L$ so that $N(N(X)) = X$, $N(X \cup Y) = N(X) \cap N(Y)$, and $N(X \cap Y) = N(X) \cup N(Y)$ for any $X, Y \in L$ and with $\cup$ and $\cap$ being the composition laws of the lattice. The symbol $\cup$ stands for the nonexclusive logical OR and $\cap$ stands for the logical conjunction AND; N is the logical negation.

(II) There exist $(n-1)$ maps σ_i: $L \to L$ with the following properties:

(a) $\sigma_i(0) = 0$, $\sigma_i(1) = 1$ for any $i = 1, 2, \ldots, n-1$;

(b) $\sigma_i(X \cup Y) = \sigma_i(X) \cup \sigma_i(Y)$, $\sigma_i(X \cap Y) = \sigma_i(X) \cap \sigma_i(Y)$ for any $X, Y \in L$ and any $i = 1, 2, \ldots, n-1$;

(c) $\sigma_1(X) \subset \sigma_2(X) \subset \cdots \subset \sigma_{n-1}(X)$ for any $X \in L$, and with $\subset$ being the canonical order in the lattice;

(d) $\sigma_h * \sigma_k = \sigma_k$ for $h, k = 1, 2, \ldots, (n-1)$;

(e) $\sigma_i(X) \cup N\sigma_i(X) = 1$, $\sigma_i(X) \cap N(\sigma_i(X)) = 0$ for any $X \in L$;

(f) If $\sigma_i(X) = \sigma_i(Y)$ for any $i = 1, 2, \ldots, n-1$, then $X = Y$;

(g) $\sigma_i(N(X)) = N(\sigma_j(X))$ for $i + j = n$ (Ref. [227]).

While the maps σ_i can be used to put order amongst the possible choices according to the results of diagnostic tests, one will still need to be able to change the type of tests, their significance, or the degree of possibility for a given choice to be true. In order to be able to model such significance changes we need to introduce morphisms of L-algebras: these are mappings f: $L_1 \to L_2$ with the following properties:

$$\text{(M1)}\quad f(0) = 0, \qquad f(1) = 1, \qquad f * N = N * f; \tag{60}$$

$$\text{(M2)}\quad f(X \cup Y) = f(X) \cup f(Y), \qquad f(X \cap Y) = f(X) \cap f(Y) \qquad \text{for any } X, Y \in L; \tag{61}$$

$$\text{(M3)}\quad f * \sigma_i = \sigma_i * f, \qquad \text{for any } i = 0, 1, \ldots, (n-1). \tag{62}$$

The aggregate of all L-algebras and morphisms between them can be organized as a category, Luk_n. In our model of medical diagnosis, Luk_n represents both the process of ordering possible diagnostics according to their degree of possibility (or, if necessary, probability of occurrence), or the choice of a new significance for specific results/data in the case history. The probabilities can be readily introduced through lvrs as discussed in the

previous section and in Ref. [169]. The special case of *centered L-algebras*, that is, those algebras which have $(n - 2)$ elements called centers, encompasses the previous model of Boolean algebras in medical diagnosis. An efficient diagnostic procedure would impose a number of restrictions on the structure of the subcategory D_n of Luk_n which represents the diagnostic decisions. For example, D_n should perhaps be loop-free in the sense that a chain of morphisms with the same orientation must not have the same beginning and end L-algebra. Such loops were previously called cycles[226]. This restriction on D_n corresponds to unalterable decisions, that is, decisions which cannot be reversed. From a practical viewpoint, this restriction may appear too severe; parallel reasoning and intuitive jumps are, however, permitted, and in this respect, too, our present model is an extension of the previous Boolean approach.

Categorical structures such as Luk_n could be hardwired on a digital computer as an aggregate of interconnected n-state black boxes, or else coded in numerical form using appropriate software. Such developments will be considered elsewhere.

We conclude that an algebraic model of medical diagnosis is now possible by taking into account the rather subtle aspects of diagnosis, such as parallel reasoning and contingent thinking. Our model is effectively a subcategory D_n of Luk_n, the category of all L-algebras. Further developments will be needed to render some of our algebraic structures computable on a digital computer. Our approach thus opens the possibility of detailed analyses of medical diagnosis using n-valued logic and L-algebras.

CONCLUDING REMARKS

Computer simulations in biology and medicine are of increasing variety, subtlety and importance; the number of computer simulations in these fields is increasing almost exponentially. Selected examples of such simulations, ranging from branching studies of arteries to biochemical oscillators, neural networks, genetic nets and molecular automata were discussed with a view to the underlying, or unifying trends.

Automata theory and other algebraic models of biological systems provide sophisticated means for simulating the behavior of real biological systems. Dynamical systems and analogs of biological organisms are now considered which have complex state-space structures and exhibit novel behavior when compared with the simpler networks that have become traditional in theoretical biology.

A unifying view of theoretical models in biology was discussed and new applications of natural transformations were presented. Conjectures were made indicating new possible developments of computer applications.

Limitations of present digital computers for mimicing biological dynamics were considered in relation to "chaos" and n-ary networks based on n-valued logic.

The need for n-valued logical models in medical diagnosis was discussed and the role of previous Boolean models in mathematical medicine was briefly reviewed.

The underlying theme of all examples considered is a search for more general algorithms, better suited for modelling complex biological systems, and in which computer simulation and automata-theoretic approaches play a key role.

Acknowledgment—The kind permission by several authors to reproduce figures is gratefully acknowledged.

REFERENCES

1. A. M. Turing. On computable numbers, with an application to the entscheidungs-problem. *Proc. Lond. Math. Soc., Ser. 2* **42**, 230–265 (1936).
2. W. McCulloch and W. Pitts. A logical calculus of the ideas immanent in nervous activity. *Bull. Math. Biophys.* **5**, 115–133 (1943).
3. M. Conrad and A. Rosenthal. Limits on the computing power of biological systems. *Bull. Math. Biol.* **43**, 59–68 (1981).
4. N. Rashevsky. *Mathematical Biophysics*. Dover, New York (1936).

5. K. Horsfield and G. Cumming, Morphology of the bronchial tree in man. *J. Appl. Physiol.* **24**, 373–383 (1968).
6. P. G. Holland, The maintenance of structure and shape in Three Malle Eucalipts. *Phytologia* **68**, 411–421 (1969).
7. H. Honda, Description of the form of trees by the parameters of the tree-like body: Effects of the branching angle and the branch length on the shape of the tree-like body. *J. Theor. Biol.* **31**, 331–338 (1971).
8. K. Horsfield, G. Dart, D. E. Olson, G. Filley and G. Cumming, Models of the human bronchial tree. *J. Appl. Physiol.* **31**, 207–217 (1971).
9. G. Legay, Contribution a l'étude de la forme des plantes. Discussion d'un modele de ramification. *Bull. Math. Biophys.* **33**, 387–401 (1971).
10. L. B. Leopold, Trees and streams: the efficiency of branching patterns. *J. Theor. Biol.* **31**, 339–354 (1971).
11. S. Oohata and T. Shidei, Studies of the branching structures of trees. I. Bifurcation ratio of trees in Horton's law. *Jap. J. Ecol.* **21**, 7–14 (1971).
12. K. Horsfield and G. Cumming, Angles of branching and diameters of branches in the human bronchial tree. *Bull. Math. Biophys.* **29**, 245–259 (1967).
13. K. Horsfield, Some mathematical properties of branching trees with application to the respiratory system. *Bull. Math. Biol.* **38**, 305–315 (1976).
14. K. Horsfield and G. Cumming, Morphology of the bronchial tree in the dog. *Resp. Physiol.* **26**, 173–182 (1976).
15. H. B. M. Uylings, Optimization of diameters and bifurcation angles in lung and vascular tree structures. *Bull. Math. Biol.* **39**, 509–520 (1977).
16. K. Horsfield, Morphometry of the small pulmonary arteries in man. *Circulation Res.* **42**, 593–597 (1978).
17. R. Borchert and N. A. Slade, Bifurcation ratios and the adaptive geometry of trees. *Bot. Gaz.* **142**, 394–401 (1981).
18. H. Honda, R. B. Tomlinson and J. B. Fisher, Computer simulation of branch interaction and regulation of unequal flow rates in botanical trees. *Am. J. Bot.* **68**, 569–585 (1981).
19. K. Horsfield and A. Thurlbeck, Computer simulation of the geometry of the human bronchial tree. *Bull. Math. Biol.* **46**, 389–398 (1984).
20. H. Honda, P. B. Tomlinson and J. B. Fisher, Two geometrical models of branching of botanical trees. *Ann. Bot.* **49**, 1–11 (1982).
21. M. S. Woldenberg and K. Horsfield, Finding the optimal lengths of the three branches at a junction. *J. Theor. Biol.* **104**, 301–318 (1983).
22. K. Horsfield and A. Thurlbeck, Relation between diameter and flow in branches of the bronchial tree. *Bull. Math. Biol.* **43**, 681–691 (1981).
23. H. B. M. Uylings and A. M. Veltman, Characterizing a dendritic bifurcation. *Neurosci. Lett.* **1**, 127–128 (1975).
24. M. Zamir, Local geometry of arterial branching. *Bull. Math. Biol.* **44**, 597–608 (1982).
25. C. N. Weygandt, R. H. Cox, G. Karreman and M. L. Cole, Pressure-flow relationships in a model for the arterial system. *Bull. Math. Biol.* **40**, 95–106 (1978).
26. C. W. Gear, The automatic integration of ordinary differential equations. *Commun. Assoc. Comput. Mach.* **14**, 176–179 (1971).
27. A. Noordegraaf, Development of an analog computer for the human systemic circulatory system, in *Circulatory Analog Computers* (Edited by G. N. Jager and N. Westerhof). North Holland, Amsterdam (1963).
28. E. O. Attinger, H. Sugawara, A. Navarro, A. Ricetto, and R. Martin, Pressure-flow relations in dog arteries. *Circulation Res.* **19**, 230–246 (1966).
29. G. N. Jager, Electrical model of the human systemic arterial tree. Ph.D. thesis, University of Urecht (1965).
30. L. DePater, An analogue of the human circulatory system. Ph.D. thesis, University of Groningen, Rotterdam (1966).
31. E. Doubek, Jr., Least energy regulation of the arterial system. *Bull. Math. Biol.* **40**, 79–94 (1978).
32. J. P. Dujardin and B. Van Gelder, Large signal, low-frequency characteristics of the systemic arterial system. *Bull. Math. Biol.* **44**, 193–214 (1982).
33. F. W. Cope, Elastic reservoir theories of the human circulation with applications of clinical medicine and computer analysis of the ciculation, in *Advances of Biological and Medical Physics* (Edited by J. W. Lawrence and J. W. Gofman), Vol. 10. Academic Press, New York (1965).
34. D. H. Bergel, The static elastic properties of the arterial wall. *J. Physiol. Lond.* **156**, 445–457 (1961).
35. T. Kenner, Models of the arterial system, in *The Arterial System* (Edited by R. D. Bauer and R. Busse), pp. 80–88. Springer-Verlag, Berlin (1978).
36. G. R. Cokelet, The Rheology of Human Blood, in *Biomechanics. Its Foundation and Objectives* (Edited by Y. C. Fung, N. Perrone and M. Anliker), pp. 63–103. Prentice-Hall, Englewood Cliffs, N.J (1978).
37. C. K. Kang and A. C. Eringen, The effect of microstructure on the rheological properties of blood. *Bull. Math. Biol.* **38**, 135–159 (1976).
38. D. Quemada, Rheology of concentrated disperse systems and minimum energy dissipation principle. I. Viscosity-concentration relationship. *Rheol. Acta* **16**, 82–94 (1977).
39. J. B. Shukla, R. S. Parihar and S. P. Gupta, Effects of peripheral layer viscosity on blood flow through the artery with mild stenosis. *Bull. Math. Biol.* **42**, 797–805 (1980).
40. J. B. Shukla, R. S. Parihar and B. R. P. Rao, Effects of stenosis on non-Newtonian flow of the blood in an artery. *Bull. Math. Biol.* **42**, 283–294 (1980).
41. J. B. Shukla, R. S. Parihar and B. R. P. Rao, Biorheological aspects of blood flow through artery with mild stenosis: Effects of peripheral layer. *Biorheology* **17**, 403–410 (1980).

42. J. Perkkio and R. Keskinen, On the effect of the concentration profile of red cells on blood flow in the artery with stenosis. *Bull. Math. Biol.* **45**, 259–268 (1983).
43. M. Takahashi, Theoretical basis for cell cycle analysis. II. Further studies—a labeled mitosis wave method. *J. Theor. Biol.* **18**, 195–209 (1968).
44. J. C. Barrett, A mathematical model of the mitotic cycle and its application to the interpretation of percentage labeled mitoses data. *J. Natl. Cancer Inst.* **37**, 443–450 (1966).
45. R. Baserga, The relationship of the cell cycle to tumor growth and control of cell division: a review. *Cancer Res.* **25**(5), 581–595 (1965).
46. P. Tautu and M. Josifescu, *Stochastic processes and applications in biology and medicine*. Springer-Verlag, Berlin (1973).
47. G. M. Hahn, State vector description of the proliferation of mammalian cells in tissue culture. *Biophys. J.* **6**, 275–290 (1966).
48. M. Kim, K. Bahrami and K. B. Woo, Mathematical description and analysis of cell cycle kinetics and the application to Ehrlich ascites tumors. *J. Theor. Biol.* **50**, 437–459 (1975).
49. M. F. Rajewsky, Proliferative parameters of mammalian cell system and their role in tumor growth and carcinogenesis. *Z. Krebsforschung* **78**, 12–30 (1972).
50. J. Kiefer, A model of feedback-controlled cell populations. *J. Theor. Biol.* **18**, 263–279 (1968).
51. W. Düchting, Computer models of the cancer problem, in *Progress in Cybernetics and Systems Research* (Edited by Trappl, Klir and Ricciardi), Vol. 3, pp. 596–613. Hemisphere Publ., New York (1978).
52. W. Düchting, Krebs, ein instabiler regelkreis-versuch einer systemanalyse. *Kybernetik* **5**(2), 70–77 (1968).
53. W. Rittgen, Controlled branching processes and their applications to normal and malignant haematopoiesis. *Bull. Math. Biol.* **45**, 617–626 (1983).
54. W. Rittgen, Positive recurrence of multi-dimensional population-dependent branching processes, in *Lecture Notes in Biomathematics, Vol. 38. Biological Growth and Spread. Mathematical Theories and Applications* (Edited by W. Jager, H. Rost and P. Tautu), pp. 98–108. Springer-Verlag, Berlin (1980).
55. S. N. Chuang and T. T. Soong, Mathematical analysis of cancer chemotherapy: The effects of chemotherapeutic agents on the cell cycle traverse. *Bull. Math. Biol.* **40**, 499–512 (1978).
56. G. Swan and T. Vincent, Optimal control analysis in the chemotherapy of IgC multiple myeloma. *Bull. Math. Biol.* **39**, 317–337 (1977).
57. A. K. Laird, Dynamics of growth in tumors and normal organisms, in *Human Tumor Cell Kinetics*, NCI Monograph, Baltimore Vol. 30, pp. 15–28 (1969).
58. P. W. Sullivan and S. E. Salmon, Kinetics of tumor growth and regression in IgG multiple myeloma. *J. Clin. Invest.* **51**, 1697–1708 (1972).
59. S. Zietz and C. Nicolini, Mathematical approaches to optimization of cancer chemotherapy. *Bull. Math. Biol.* **41**, 305–324 (1979).
60. C. Nicolini and F. Kendal, Monte Carlo simulation of drug action in intact animals, in *Mathematical Modeling in Cell Kinetics* (Edited by A. J. Valleron), pp. 81–83. European Press Medikon, Ghent (1975).
61. C. Nicolini, E. Milgram, F. Kendall, and W. Giaretti, Mathematical models for drug action *in vivo*, in *Growth Kinetics and Biochemical Regulation of Normal and Malignant Cells* (Edited by B. Drewinko and R. M. Humphrey), Williams & Williams, Baltimore (1977).
62. W. Düchting, Simulation of disturbed cell renewal systems by means of a microprocessor system. *Int. J. Bio-Medical Comput.* **10**, 375–382 (1979).
63. M. Gardner, On cellular automata, self-reproduction, the garden of Eden and the game "life". *Sci. Amer.* **224**, 112–117 (1971).
64. A. Lindenmayer, Developmental algorithms for multicellular organisms: A survey of *L*-systems. *J. Theor. Biol.* **54**, 3–32 (1975).
65. L. V. Reshodko and J. Bures, Computer simulation of reverberating spreading depression in a network of cell automata. *Biol. Cybern.* **18**, 181–189 (1975).
66. R. Ransom, A computer model of cell clone growth. *Simulation* **28**(2), 189–192 (1977).
67. M. A. Arbib, A simple self-reproducing universal automaton. *Inform. Control* **9**, 177–189 (1966).
68. M. A. Lieberman, A stochastic model based on computer simulation using pre-empting to predict size distribution and species equitability. *Bull. Math. Biol.* **39**, 59–72 (1977).
69. I. F. Tannock, The relation between cell proliferation and the vascular system in mouse mammary tumor. *Brit. J. Cancer* **22**, 258–273 (1968).
70. J. Folkman, E. Merler, C. Abernathy and G. Williams, Isolation of a factor responsible for tumor angiogenesis, *J. Exp. Med.* **133**, 278–288 (1971).
71. L. A. Liotta, G. M. Saidel and J. Kleinerman, Diffusion model of tumor vascularization and growth. *Bull. Math. Biol.* **39**, 117–128 (1977).
72. G. M. Saidel, L. A. Liotta and J. Kleinerman, System dynamics of a metastatic process from an implanted Tumor. *J. Theor. Biol.* **56**, 417–434 (1976).
73. B. C. Goodwin, *Temporal Organization in Cells*. Academic, New York (1963).
74. A. J. Lotka, *Elements of Physical Biology*. Williams and Wilkins, Baltimore (1924).
75. V. Volterra, *Leçons sur la Théorie Mathématique de la Lutte Pour la Vie*. Gauthier-Villard, Paris (1931).
76. J. D. Cowan, Statistical mechanics of nervous nets, in *Neural Networks* (Edited by E. R. Caianiello), pp. 181–188. Springer, Berlin (1968).
77. B. Chance, E. K. Pye, A. K. Ghosh and B. Hess, *Biological and Biochemical Oscillators*. Academic Press, New York (1973).

78. N. S. Goel, S. S. C. Maitra and E. W. Montroll, On the Volterra and other nonlinear models of interacting populations. *Rev. Mod. Phys.* **43**, 231–276 (1971).
79. Th. Pavlidis, *Biological Oscillators: Their Mathematical Analysis*. Academic Press, New York (1973).
80. A. Rescigno and I. W. Richardson, The deterministic theory of population dynamics, in *Foundations of Mathematical Biology* Edited by R. Rosen), Vol. 3, pp. 283–360. Academic Press, New York (1973).
81. P. E. Waltman, The equations of growth. *Bull. Math. Biol.* **26**, 39–43 (1964).
82. V. Singh, Analytical theory of the control equations for protein synthesis in the Goodwin model. *Bull. Math. Biol.* **39**, 565–575 (1977).
83. J. S. Frame, Explicit solutions in two species Volterra systems. *J. Theor. Biol.* **43**, 73–81 (1974).
84. H. D. Landahl, Some conditions for sustained oscillations in biochemical chains with feedback inhibition. *Bull. Math. Biophys.* **31**, 775–787 (1969).
85. H. D. Landahl, Some conditions for sustained oscillations in chain processes with feedback inhibition and saturable removal. *Bull. Math. Biol.* **39**, 291–296 (1977).
86. D. A. Linkens, The method of harmonic balance applied to coupled asymmetrical Van der Pol oscillators for intestinal modelling. *Bull. Math. Biol.* **41**, 573–590 (1979).
87. D. A. Linkens and A. E. Cannell, Interactive graphics analysis of gastro-intestinal electrical signals. *IEEE Trans. Biol. Med. Eng.* **24**, 362–365 (1974).
88. D. A. Linkens, Analytical solution of large numbers of mutually coupled nearly sinusoidal oscillators. *IEEE Trans. Cct. Syst.* **21**(2), 294–300 (1974).
89. D. A. Linkens, The stability of entrainment conditions for RLC coupled Van der Pol oscillators used as model for intestinal electrical rhythms. *Bull. Math. Biol.* **39**, 359–372 (1977).
90. D. A. Linkens, Stability of entrainment conditions for a particular form of mutually coupled Van der Pol oscillators. *IEEE Trans. Cct. Syst.* **23**, 113–121 (1976).
91. D. A. Linkens and S. Datardina, Frequency entrainment of coupled Hodgkin–Huxley type oscillators. *IEEE Trans. Biol. Med. Eng.* **24**, 362–365 (1977).
92. D. A. Linkens *et al.*, Mathematical modelling of the colorectal myoelectrical activity in humans. *IEEE Trans. Biol. Med. Eng.* **23**, 101–110 (1976).
93. R. J. Patton and D. A. Linkens, A conversational program for analytical modelling of action potentials in nerve and muscle. *Computer Prog. Biomed.* **5**, 142–152 (1975).
94. T. Endo and S. Mori, Mode analysis of a multimode ladder oscillator. *IEEE Trans. Cct. Syst.* **23**, 100–113 (1976).
95. N. E. Diamant, K. Rose and E. J. Davison, Computer simulation of intestinal frequency gradient. *Amer. J. Physiol.* **219**, 1684–1690 (1970).
96. S. K. Sarna, E. E. Daniel and Y. J. Kingma, Simulation of slow-wave electrical activity of the small intestine. *Amer. J. Physiol.* **221**, 166–175 (1971).
97. Van der Pol, A theory of the amplitude of free and forced triode vibrations. *Tijdchrift Ned. Radiogenoot* **1**, 3–31 (1920).
98. W. Nijenhuis, A note on a generalized Van der Pol equation. *Philips Res. Rept.* **4**, 401–406 (1949).
99. R. Rosen, Some comments on activation and inhibition. *Bull. Math. Biol.* **41**, 427–446 (1979).
100. J. Higgins, The theory of oscillating reactions. *Ind. Eng. Chem.* **59**, 18–62 (1967).
101. R. Rosen, *Dynamical Systems Theory in Biology*. Wiley, New York (1970).
102. M. Sugita, Functional analysis of chemical systems *in vitro* using a logical circuit equivalent. *J. Theor. Biol.* **1**, 414–430 (1961).
103. I. C. Baianu, A molecular-set-variable model of structural and regulatory activities in metabolic and genetic systems. *Fed. Proceed. Amer. Soc. Experim. Biol.* **43**, 917 (1984).
104. M. W. Warner, Lattices and lattice-valued relations in biology. *Bull. Math. Biol.* **45**, 193–208 (1983).
105. J. Grasman, The mathematical modeling of entrained biological oscillators. *Bull. Math. Biol.* **46**, 407–422 (1984).
106. J. P. Gollub *et al.*, Periodicity and chaos in coupled nonlinear oscillators. *Science* **200**, 48–50 (1978).
107. J. F. G. Auchmuty and G. Nicolis, Bifurcation analysis of reaction diffusion equations—III. Chemical oscillations. *Bull. Math. Biol.* **38**, 325–350 (1976).
108. J. Grasman and M. J. W. Jansen, Mutually synchronized relaxation oscillators as prototypes of oscillating systems in biology. *J. Math. Biol.* **7**, 171–197 (1979).
109. G. B. Ermentrout, n:m phase-locking of weakly coupled oscillators. *J. Math. Biol.* **12**, 327–342 (1981).
110. L. Glass and M. C. Mackey, A simple model for phase locking of biological oscillators. *J. Math. Biol.* **7**, 339–352 (1979).
111. L. Glass and R. Perez, Fine structure of phase locking. *Phys. Rev. Lett.* **48**, 1772–1775 (1982).
112. M. R. Guevara, L. Glass and A. Shrier, Phase locking, period-doubling bifurcation and irregular dynamics in periodically stimulated cardiac cells. *Science* **214**, 1350–1353.
113. Van Meerwijk, G. de Bruin, A. C. G. van Ginneken, J. van Hartevelts, A. J. Jongsma, S. S. Scott and D. L. Ypey, Phase resetting properties of cardiac pacemaker cells, preprint, University of Amsterdam (1983) (cited by J. Grasman Ref. [105]).
114. D. L. Ypey, W. P. M. van Meerwijk, E. Ince and G. Gross, Mutual entrainment of two pacemaker cells. A study with an electronic parallel conductance model. *J. Theor. Biol.* **86**, 731–755 (1980).
115. D. L. Ypey and G. de Bruin, Suppression of pacemaker activity by rapid repetitive phase delay. *Biol. Cybernet.* **45**, 177–184 (1982).
116. G. A. Petrillo, L. Glass and T. Trippenbach, Phase locking of the respiratory rhythm in cats to a mechanical ventilator. *Can. J. Physiol. Pharmacol.* **61**, 599–607 (1983).

117. T. Allen, On the arithmetic of phase locking: Coupled neurons as a lattice on R^2. *Physica* **6D**, 305–320 (1983).
118. J. Kreifeldt, Ensemble entrainment of self-sustaining oscillations: a possible application to neural signals. *Math. Biosci.* **8**, 425–436 (1970).
119. F. H. Lopes da Silva, A. van Rotterdam, B. Parts, E. van Heusden and W. Burr, Models of neuronal populations: the basic mechanisms of rhythmicity, in *Progress in Brain Research* (Edited by D. Swaab and M. E. Corner), Vol. 45, pp. 281–308. Biomedical Press, Amsterdam (1976).
120. P. E. Phillipson, P. Schuster and F. Kemler, Dynamical machinery of a biochemical clock. *Bull. Math. Biol.* **46**, 339–356 (1984).
121. M. Eigen and P. Schuster, *The Hypercycle*. Springer-Verlag, Berlin (1979).
122. A. L. Hodgkin and A. F. Huxley, A quantitative description of membrane current and its application to conduction and excitation in nerve. *J. Physiol.* **117**, 500–544 (1952).
123. R. E. Plant, The analysis of models for excitable membranes: An introduction, in *Some Mathematical Questions in Biology-Neurobiology* (Edited by R. M. Miura), *Lectures on Mathematics in the Life Sciences*, Vol. 15, pp. 27–54. American Mathematical Society, Providence, RI (1982).
124. F. Strumwasser, Types of information stored in single neurons, in *Invertebrate Nervous Systems* (Edited by C. A. G. Wiersma), pp. 291–230 (1967).
125. P. A. Mathiew and F. A. Roberge, Characteristics of pacemaker oscillations in Aplysia neurons. *Can. J. Physiol. Pharmacol.* **49**, 787–795 (1971).
126. D. Junge and C. L. Stephens, Cyclic variation of potassium conductance in a burst-generating neuron in Aplysia. *J. Physiol.* **235**, 155–181 (1973).
127. R. E. Plant, The effects of calcium $^{++}$ on bursting neurons: a modeling study. *Biophys. J.* **21**, 217–237 (1978).
128. R. E. Plant, Mathematical description of a bursting pacemaker neuron by a modification of the Hodgkin–Huxley equations. *Biophys. J.* **16**, 227–244 (1976).
129. B. D. Hassard, Bifurcation of periodic solutions of the Hodgkin–Huxley model for the squid giant axon. *J. Theor. Biol.* **84**, 401–420 (1978).
130. J. Rinzel, On repetitive activity in nerve. *Fed. Proc. Amer. Soc. Exp. Biol.* **37**, 2793–2802 (1978).
131. R. W. Meech, Intracellular calcium injection causes increased potassium conductance in Aplysia nerve cells. *Comp. Biochem. Physiol.* **42A**, 493–499 (1972).
132. A. C. Scott, Nerve pulse interactions, in *Some Mathematical Questions in Biology-Neurobiology* (Edited by R. M. Miura), *Lectures on Mathematics in the Life Sciences*, Vol. 15, pp. 27–45. American Mathematical Society, Providence, RI (1982).
133. S. G. Waxman, Regional differentiation of the axon: a review with special reference to the concept of a multiplex neuron. *Brain Res.* **47**, 269–288 (1972).
134. M. E. Scheibel and A. B. Scheibel, *Intern. J. Neurosci.* **6**, 195 (1973) (Abstract).
135. N. Rashevsky, *Mathematical Biophysics*, 3rd Rev. Ed. Dover, New York (1960).
136. N. Rashevsky, Neurocybernetics as a particular case of general regulating mechanisms in biological and social organisms. *Concepts de l'Age de la Science* **3**, 243–258 (1968).
137. A. V. Holden, Stochastic processes in neurophysiology: Transformation from point to continuous processes. *Bull. Math. Biol.* **45**, 443–465 (1983).
138. I. Aleksander, Random logic nets: Stability and adaptation. *Int. J. Man-Mach. Stud.* **5**, 115–131 (1973).
139. I. C. Baianu, Energetic considerations in the interpretation of electroencephalograms. *Ann. Univ. Bucharest (Phys.)* **21**, 61–67 (1972).
140. S. E. Fienberg, Stochastic models for single neuron firing trains: A survey. *Biometrics* **30**, 399–427 (1974).
141. A. V. Holden, Models of the stochastic activities of neurons, in *Lecture Notes in Biomathematics*, Vol. 12. Springer-Verlag, Berlin (1976).
142. G. Sampath and S. K. Srinivasan, Stochastic models for spike trains of single neurons. *Lecture Notes in Biomathematics*, Vol. 16. Springer-Verlag, Berlin (1980).
143. A. C. Scott, The electrophysics of a nerve fiber. *Rev. Mod. Phys.* **4**, 487–533 (1975).
144. S. Amari, A mathematical approach to neural systems, in *Systems Neuroscience* (Edited by J. Metzler), pp. 67–117. Academic Press, New York (1974).
145. K. G. Kirby and M. Conrad, The enzymatic neuron as a reaction-diffusion network of cyclic nucleotides. *Bull. Math. Biol.* **46**, 765–783 (1984).
146. R. R. Kampfner and M. Conrad, Computational modeling of evolutionary learning processes in the brain. *Bull. Math. Biol.* **45**, 931–968 (1983).
147. R. Rosen, *Dynamical Systems Theory in Biology*. Wiley, New York (1970).
148. P. Greengard, *Cyclic Nucleotides, Phosphorylated Proteins and Neuronal Function*. Raven Press, New York (1978).
149. G. I. Drummon, Cyclic nucleotides in the nervous system, in *Cyclic Nucleotide Research* (Edited by P. Greengard and G. A. Robinson), Vol. 15, pp. 373–494. Raven Press, New York (1978).
150. R. Rosen, The representation of biological systems from the standpoint of the theory of categories. *Bull. Math. Biophys.* **20**, 317–341 (1958).
151. R. Rosen, Abstract biological systems as sequential machines—III. *Bull. Math. Biophys.* **26**, 141–148 (1966).
152. M. A. Arbib, Categories of (M, R)-systems. *Bull. Math. Biophys.* **28**, 511–517 (1966).
153. I. C. Baianu, Some algebraic properties of (M, R)-systems. *Bull. Math. Biol.* **35**, 213–217 (1973).
154. M. W. Warner, Representations of (M, R)-systems by categories of automata. *Bull. Math. Biol.* **44**, 661–668 (1982).

155. M. A. Arbib, *The Algebraic Theory of Machines, Languages and Semigroups*. Academic, New York (1968).
156. N. Rashevsky, *Mathematical Biophysics: Physicomathematical Foundations of Biology*. University of Chicago Press, Chicago (1938).
157. R. Rosen, Pattern generation in networks, in *Progress in Theoretical Biology* (Edited by R. Rosen), Vol. 6, pp. 497–525. Academic Press, New York (1981).
158. W. Pitts, The linear theory of neuron networks. *Bull. Math. Biophys.* **5**, 23–31 (1943).
159. H. D. Landahl, W. S. McCulloch and W. Pitts, Statistical firing in neuron networks. *Bull. Math. Biophys.* **5**, 135–137 (1943).
160. S. A. Kauffman, Metabolic stability and epigenesis in randomly constructed genetic nets. *J. Theor. Biol.* **22**, 437–467 (1969).
161. S. A. Kauffman, Homeostasis and differentiation in random genetic networks. *Nature* **224**, 177–178 (1969).
162. S. A. Kauffman, Behavior of randomly constructed genetic nets: Binary element nets, in *Towards a Theoretical Biology* (Edited by C. H. Waddington), Vol. 3, pp. 18–37. Edinburgh U. P., Edinburgh (1970).
163. S. A. Kauffman, Gene regulation networks: A theory of their global structure and behaviour. *Curr. Topics Dev. Biol.* **6**, 145–182 (1971).
164. S. A. Kauffman, Assessing probable regulatory structures and dynamics of the Metazoan genome. Kinetic logic, in *Lecture Notes in Biomathematics* (Edited by A. A. Moscona and A. Monnoy), Vol. 29, pp. 30–61. Springer-Verlag, Berlin (1979).
165. J. S. Griffith, *Mathematical Neurobiology*. Academic, London (1971).
166. M. A. Arbib, *The Metaphorical Brain*. Wiley, New York (1972).
167. J. Szentágothai and M. A. Arbib, Conceptual models of neural organization. *NRP Bull.* **12**, 305–510 (1974).
168. M. A. Arbib, *Theories of Abstract Automata*. Prentice-Hall, New York (1969).
169. A. Muir and M. W. Warner, The dynamics of symmetric nets. *Bull. Math. Biol.* **45**, 781–792 (1983).
170. E. M. Harth, T. J. Csermely, B. Beck, and R. D. Lindsay, Brain functions and neural dynamics. *J. Theor. Biol.* **26**, 93–120 (1970).
171. A. Van Rotterdam, F. H. Lopes da Silva, J. van der Ende, M. A. Viergerer and A. J. Hermans, A Model of the spatial-temporal characteristics of the alpha-rhythm. *Bull. Math. Biol.* **44**, 283–305 (1982).
172. H. K. Hartline and F. Ratcliff, Inhibitory interaction in the retina of Limulus, in *Handbook of Sensory Physiology*, (Edited by M. G. F. Fortes), Vol. VII/2, pp. 381–447. Springer, Berlin (1972).
173. R. A. Sherlock, Analysis of the behavior of Kauffman binary networks—I. State space description and the distribution of limit cycle lengths. *Bull. Math. Biol.* **41**, 687–706 (1979).
174. H. von Foerster, Memory without record, in *The Anatomy of Memory* (Edited by D. P. Kimble), pp. 388–433. Science and Behavior Books, Palo Alto, CA (1967).
175. D. F. Stubbs, Perceptual learning machines and the brain. *Stochastics* **1**, 301–314 (1975).
176. N. Wiener and A. Rosenblueth, The mathematical formulation of conduction of impulses in a network of connected excitable elements, specifically in cardiac muscle. *Arch. Inst. Cardiology Mexic* **XVI**, 205–265 (1946).
177. A. E. Gelfand and C. C. Walker, *Network Modeling Techniques: Inferrence from Small Scale Properties to Large Scale Systems*. Dekker, New York (1984).
178. A. E. Gelfand, A behavioral summary for completely random nets. *Bull. Math. Biol.* **44**, 309–320 (1982).
179. F. Fogelman-Soulié, E. Goles-Chacc and G. Weisbuch, Roles of the different Boolean mappings in random networks. *Bull. Math. Biol.* **44**, 715–730 (1982).
180. H. Atlan, F. Fogelman-Soulié, J. Salomon and G. Weisbuch, Random Boolean networks. *Cybernet. Syst.* **12**, 103–121 (1981).
181. R. Thomas, Kinetic logic—A Boolean approach to the analysis of complex regulatory systems, in *Lecture Notes in Biomathematics* (Edited by R. Thomas), Vol. 29. Springer-Verlag, Berlin (1979).
182. A. Shimbel, An analysis of theoretical systems of differentiating nervous tissue. *Bull. Math. Biophys.* **10**, 131–143 (1948).
183. A. Rapoport, Cycle distribution in random nets. *Bull. Math. Biophys.* **10**, 145–157 (1948).
184. R. Solomonoff and A. Rapoport, Connectivity of random nets. *Bull. Math. Biophys.* **13**, 107–117 (1951).
185. M. R. Gardner and W. R. Ashby, Connectance of large dynamic (cybernetic) systems: Critical values for stability. *Nature* **228**, 784 (1970).
186. D. F. Stubbs and P. I. Good, Connectivity in random networks. *Bull. Math. Biol.* **38**, 295–304 (1976).
187. R. J. Wilson, *Introduction to Graph Theory*. Bell and Bain, Glasgow (1972).
188. R. Warwick and P. Williams, *Anatomy*. Longman, London (1973).
189. J. N. Hunt and D. F. Stubbs, Economy in the brain. *Lancet*, May 5, *24* 997 (1973).
190. J. R. Griffith, On the stability of brain-like structures. *Biophys. J.* **3**, 299–308 (1963).
191. L. D. Harmon, Problems in neural modeling, in *Neural Theory and Modeling* (Edited by R. F. Reiss), pp. 9–30. Stanford U. P., Stanford, CA (1964).
192. H. G. Landau, On some problems of random nets. *Bull. Math. Biophys.* **14**, 203–212 (1952).
193. R. E. McMurtrie, Determinants of stability of large randomly connected Systems. *J. Theor. Biol.* **50**, 1–11 (1975).
194. S. A. Newman, A source of stability in metabolic networks. *J. Theor. Biol.* **35**, 227–232 (1972).
195. D. J. M. Park, Local stability in metabolic networks with conserved moieties and steady state subnetworks. *J. Theor. Biol.* **49**, 431–437 (1975).
196. R. L. Somorjai and D. N. Gogwami, Relationship between stability and connectedness in non-linear systems. *Nature* **236**, 466 (1972).
197. P. Doreian, On the connectivity of social networks. *J. Math. Sociol.* **3**, 245–258 (1974).

198. J. D. Cowan, Spontaneous symmetry-breaking in large scale nervous activity. *Int. J. Quantum Chem.* **22**, 1059–1082 (1982).
199. G. B. Ermentrout and J. D. Cowan, Secondary bifurcation in neuronal nets. *SIAM J. Appl. Math.* **39**, 323–340 (1980).
200. D. H. Sattinger, Group representation theory, bifurcation theory and pattern formation. *J. Funct. Anal.* **28**, 50–101 (1978).
201. A. Muir and M. W. Warner, The dynamics of symmetric nets. *Bull. Math. Biol.* **45**, 781–792 (1983).
202. H. R. Wilson and J. D. Cowan, Excitatory and inhibitory interactions in localized populations of model neurons. *Biophys. J.* **12**, 1–24 (1972).
203. A. Muir, The construction of homogeneous nets. *Bull. Math. Biol.* **43**, 415–426 (1981).
204. L. Zadeh, Fuzzy sets. *Inf. Control* **8**, 338–353 (1965).
205. M. W. Warner, Lattices and lattice-valued relations in biology. *Bull. Math. Biol.* **45**, 415–426 (1981).
206. C. C. Walker, Beyond the binary case in random nets. *Bull. Math. Biol.* **46**, 845–858 (1984).
207. J. R. Clay and N. S. Goel, Diffusion models for firing a neuron with varying threshold. *J. Theor. Biol.* **39**, 633–644 (1973).
208. J. P. Changeux and A. Danchin, Selective stabilization of developing synapses—a mechanism for the specification of neuronal networks. *Nature (London)* **264**, 705–712 (1976).
209. L. M. Ricciardi, *Diffusion Processes and Related Topics in Biology*. Springer-Verlag, Berlin (1977).
210. Z. Schuss, *Theory and Applications of Stochastic Differential Equations*. Wiley, New York (1976).
211. A. Friedman, *Stochastic Differential Equations and Applications*, Vols. I and II. Academic, New York (1976).
212. R. N. Bhattacharya, Criteria for recurrence and existence of invariant measures for multidimensional diffusions. *Ann. Probab.* **6**, 541–553 (1978).
213. R. Z. Hasminskii, *Stochastic Stability of Differential Equations*. Sijthoff and Noordoff, Alphen aar den Rijn (1980).
214. H. Kesten and Y. Ogura, Recurrence properties of Lotka–Volterra models with random fluctuations. *J. Math. Soc. Japan* **32**, 335–366 (1981).
215. W. Kliemann, Qualitative theory of stochastic dynamical systems—Applications to life sciences. *Bull. Math. Biol.* **45**, 483–506 (1983).
216. W. Kliemann and W. Rümelin, On the growth of linear systems parametrically disturbed by a diffusion process. Rept. #27, Forschungsschwerpunk Dynamische Systeme, University of Bremen (1981).
217. L. Arnold and W. Kliemann, Qualitative theory of stochastic systems, in *Probabilistic Analysis and Related Topics* (Edited by A. T. Barucha-Reid), Vol. 3. Academic, New York (1983).
218. L. Arnold, W. Horsthemke and J. Stucki, The influence of external, real and white noise on the Lotka–Volterra model. *Biomed. J.* **21**, 451–471 (1979).
219. M. Conrad and O. Rössler, Example of a system which is computation universal but not effectively programmable. *Bull. Math. Biol.* **44**, 443–448 (1982).
220. O. Rössler, Chaos and strange attractors in chemical kinetics, in Synthetics—Far from Equilibrium (Edited by A. Pacault and C. Vidal), pp. 107–113. Springer-Verlag, Heidelberg (1979).
221. R. Rosen, On analogous systems. *Bull. Math. Biophys.* **30**, 481–492 (1968).
222. J. M. Day, Expository lectures on topological semigroups, in *Algebraic Theory of Machines, Languages and Semigroups* (Edited by M. A. Arbib), pp. 147–189. Academic Press, New York (1969).
223. M. Witten, Some generalized conjugacy Theorems and the concepts of fitness and survival in logistic growth models. *Bull. Math. Biol.* **42**, 507–528 (1980).
224. I. C. Baianu and D. Scripcariu, On adjoint dynamical systems. *Bull. Math. Biol.* **35**, 475–486 (1973).
225. F. Jacob and J. Monod, On the regulation of gene activity, in *Cold Spring Harbor Symposium on Quantitative Biology* (Edited by Leonora Frisch), Cold Spring Harbor Lab., New York Vol. 26, pp. 193–211 (1961).
226. I. C. Baianu, A logical model of genetic activities in Łukasiewicz algebras: The non-linear theory. *Bull. Math. Biol.* **39**, 249–258 (1977).
227. G. Georgescu and C. Vraciu, On the characterization of Łukasiewicz algebras. *J. Algebra* **16**(4), 486–495 (1970).
228. J. M. Varley, H. M. MacGregor and H. P. Erba, Satellite DNA is transcribed on lampbrush chromosomes. *Nature (London)* **283**, 686–688 (1980).
229. E. M. Johnson, G. R. Cambell and V. G. Allfrey, Different nucleosome structures on transcribing and nontranscribing ribosomal gene sequences. *Science* **206**, 1192–1193 (1979).
230. A. Ginzburg, Algebraic Theory of Automata. Academic Press, New York (1968).
231. K. Krohn and J. L. Rhodes, Algebraic theory of machines, I: The decomposition results. *Trans. Amer. Math. Soc.* **CXVI**, 450–464 (1965).
232. K. Krohn, J. L. Rhodes and B. R. Tilson, The prime decomposition theorem of the algebraic theory of machines, in *The Algebraic Theory of Machines* (Edited by M. A. Arbib), pp. 81–125. Academic, New York (1968).
233. *The Algebraic Theory of Machines, Languages and Semigroups* (Edited by M. A. Arbib). Academic, New York (1968).
234. A. R. Smith, Simple computation-universal cellular spaces and self-reproduction. Conf. Record., *IEEE 9th Ann. Symp. Switching and Automata Theory*, pp. 269–277 (1968).
235. E. G. Wagner, An approach to modular computers, I: Spider automata and embedded automata. *IBM Res. Rept.* RC-1107 (1964).

236. M. A. Arbib, Automata theory and development: Part I. *J. Theor. Biol.* **14**, 131–156 (1967).
237. R. Rosen, Som realizations of (M, R)-systems and their interpretation. *Bull. Math. Biophys.* **33**, 303–319 (1971).
238. I. C. Baianu and M. Marinescu, A functional construction of (M, R)-systems. *Rev. Roum. Math. Pure Appl.* **19**, 389–391 (1974).
239. N. Rashevsky, *Organsimic Sets*. William Clowes & Sons, London, Beccles and Colchester (1972).
240. A. F. Bartholomay, Molecular set theory. III: The wide sense kinetics of molecular sets. *Bull. Math. Biophys.* **33**, 355–372 (1971).
241. I. C. Baianu, Natural transformations of organismic structures. *Bull. Math. Biol.* **42**, 431–446 (1980).
242. I. C. Baianu, Natural transformation models in molecular biology. SIAM Natl. Meeting, Denver, Colorado (1983).
243. C. A. Leguizamon, Concept of energy in biological systems. *Bull. Math. Biol.* **35**, 565–572 (1975).
244. S. Eilenberg and S. MacLane, General theory of natural equivalences. *Trans. Am. Math. Soc.* **58**, 231–294 (1945).
245. N. Popescu, *The Theory of Categories with Applications to Rings and Modules*. Academic Press, New York (1971).
246. O. M. Olson and K. Gausing, Post-transcriptional control of coordinated ribosomal protein synthesis in *Escherichia coli*. *Nature* **283**, 599–600 (1980).
247. A. M. DiBerardino and N. Hoffner, Origin of chromosomal abnormalities in nuclear transplants—A reevaluation of nuclear differentiation and nuclear equivalence in amphibians. *Develop. Biol.* **23**(2), 185–209 (1970).
248. D. M. Kan, Adjoint functors. *Trans. Am. Math. Soc.* **87**, 294–330 (1968).
249. Zs. Schwarz and H. Kossel, The primary structure of 16s rDNA from *Zea mays* chloroplast is homologous to *E. coli* 16s rRNA. *Nature* **283**, 739–742 (1980).
250. A. F. Bartholomay, Some mathematical aspects of the medical diagnostic process. I. A general mathematical model. *Bull. Math. Biophys.* **33**, 413–424 (1971).
251. J. Argémi, H. Chagneux, C. Ducreux and M. Gola, Qualitative study of a dynamical system for metrazol-induced paroxysmal depolarization shifts. *Bull. Math. Biol.* **46**, 903–922 (1984).